“Relevance of transcription to topoisomerase II-mediated cancer treatments”

Dissertation

submitted to attain the academic degree

“Doctor of Natural Sciences”

(Dr. rer. nat.)

at the department of Biology

of the Johannes Gutenberg University Mainz

Piyush More

born on **25.04.1992** in **Dehuroad, Maharashtra, India**

Mainz, 22.03.2019

Dean:

1. Reviewer:

2. Reviewer:

Day of the oral examination: 03.05.2019

Table of Contents

Lists of figures

List of tables

List of abbreviations

Abbreviation	Explanation
AML	Acute Myeloid Leukemia
CI	Combination Index
CLUE	CMAP and LINCS Unified Environment
CMap	Connectivity Map
DAVID	Database for Annotation, Visualization, and Integrated Discovery
DMEM	Dulbecco's Modified Eagle's Medium
DMSO	Dimethyl Sulfoxide
FDR	False Discovery Rate
FITC	Fluorescein isothiocyanate
GEC	Gene Expression Changes
GEL	Gene Expression Levels
GEO	Gene Expression Omnibus
GEPIA	Gene Expression Profiling Interactive Analysis
GTEx	The Genotype-Tissue Expression
HDAC	Histone Deacetylase
IC50	Inhibitory Concentration 50
IPA	Ingenuity Pathway Analysis
MLL	Mixed Lineage Leukemia
mTOR	Mechanistic Target of Rapamycin
MTT	3-(4,5-Dimethylthiazol-2-Yl)-2,5-Diphenyltetrazolium Bromide
PAch	Project Achilles
PBS	Phosphate-Buffered Saline
PI	Propidium Iodide
ROS	Reactive Oxygen Species
shRNA	short hairpin RNA
siRNA	small interfering RNA
TCGA	The Cancer Genome Atlas
TET	Tetracycline
TOP2	Topoisomerase II
TOP2A	Topoisomerase II alpha
TOP2B	Topoisomerase II beta
TPM	Transcripts per million
WGCNA	Weighted gene co-expression analysis
WST	[2-(2-methoxy-4-nitrophenyl)-3-(4-nitrophenyl)-5-(2,4-disulfophenyl)-2H-tetrazolium, monosodium salt

1 Summary

Cancer treatments with classic cytotoxic drugs are constrained by the resistance of cancer cells and indiscriminate toxicity towards normal cells. They are gradually being replaced by the drugs and molecules targeting cancer-specific molecules and processes. However, only a few of such targeted drugs provide clinical benefits compared to cost-effective classical drugs. Herein, I investigated an unexplored approach of improving the efficacy of the classical anti-cancer drug etoposide. I hypothesized that the response to etoposide, a widely used topoisomerase II poison, can be safely enhanced by considering treatment-evoked gene expression changes. To this end, I analyzed the basal transcriptomes and etoposide-evoked transcriptional changes in fibrosarcoma and acute myeloid leukemia (AML) cell lines. Using two parallel approaches of co-regulation within gene expression networks and essentiality for cancer cell survival, I identified and validated druggable drivers of etoposide cytotoxicity. Drivers with pre-treatment expression modulating the etoposide cytotoxicity (e.g. BIRC5 and PARP9) synergized with etoposide. Drivers essential for cancer cell survival and repressed after etoposide treatment (e.g. PFKP and PLK1) contributed to its cytotoxicity by evoking cell death. Drivers with etoposide-like gene expression changes (e.g. ANLN and MYC) synergized with etoposide as well as exhibited standalone cytotoxicity. Altogether, both pre-treatment gene expression levels and treatment-evoked gene expression changes drive the etoposide cytotoxicity. These drivers could be targeted to potentially replace etoposide or to enhance its efficacy. This approach can further be used to identify replacements and rational combination partners of other classical anti-cancer drugs interfering with gene expression.

2 Zusammenfassung

Die Wirksamkeit von Krebsbehandlungen mit klassischen Zytostatika wird durch Resistenzen und Toxizitäten eingeschränkt. Die klassischen Zytostatika werden daher nach und nach durch Medikamente ersetzt, die auf krebsspezifische Moleküle und Prozesse abzielen. Im Vergleich zu kostengünstigen klassischen Medikamenten bieten jedoch nur wenige dieser zielgerichteten Arzneimittel klinische Vorteile. Im Verlauf dieser Arbeit versuchte ich, die Wirksamkeit des klassischen Antikrebsmedikaments Etoposid zu verbessern. Ich stellte die Hypothese auf, dass die Antwort auf Etoposid, ein weit verbreitetes Topoisomerase-II-Gift, gesteigert werden kann, wenn die durch die Behandlung hervorgerufenen Genexpressionsänderungen berücksichtigt werden. Zu diesem Zweck analysierte ich die basalen Transkriptome sowie die durch Etoposid hervorgerufenen transkriptionellen Veränderungen in Zelllinien des Fibrosarkoms und der akuten myeloischen Leukämie (AML). Mit zwei parallelen Ansätzen, d.h. der Ko-Regulation innerhalb von Genexpressionsnetzwerken und der essenziellen Bedeutung für das Überleben von Krebszellen, identifizierte und validierte ich therapeutische Zielmoleküle welche die Etoposid-Zytotoxizität verstärken. „Drivers“, deren Expression vor der Behandlung die Etoposid-Zytotoxizität beeinflussten (z. B. BIRC5 und PARP9), wirkten mit Etoposid synergistisch. „Drivers“, die für das Überleben von Krebszellen essentiell waren und nach einer Etoposid-Behandlung reprimiert wurden (z. B. PFKP und PLK1), verstärkten dessen Zytotoxizität durch Zelltod. „Drivers“, die Etoposid-ähnliche Genexpressionsänderungen hervorriefen (z. B. ANLN und MYC) wirkten synergistisch mit Etoposid und zeigten eigenständige Zytotoxizität. Zusammengefasst steuern sowohl die Genexpressionsniveaus vor der Behandlung als auch die durch die Behandlung hervorgerufenen Genexpressionsänderungen die Zytotoxizität von Etoposid. Diese „Drivers“ könnten gezielt genutzt werden, um Etoposid zu ersetzen oder seine

Wirksamkeit zu steigern. Darüber hinaus könnten mit dieser Herangehensweise Alternativen sowie Kombinationen für andere klassischen Krebsmedikamente identifiziert werden, die die Genexpression beeinflussen.

3 Introduction

Most classic anticancer drugs are indiscriminately toxic towards both cancerous and normal dividing cells due to the interference with the fundamental cellular processes of DNA metabolism or mitosis. They are therefore gradually being replaced by drugs targeting molecules and processes more specific to cancer cells. For example, the identification of the bcr-abl fusion protein expressed exclusively in chronic monomyelocytic leukemia led to the development of the well-tolerated inhibitor imatinib (An, Tiwari et al. 2010). The development of this and of many other new anticancer drugs has been driven by advances in the understanding of tumor biology. In coming years, the cancer chemotherapy is most likely to be tailored to individual patients. However, development and approval of drugs targeting such individual targets will take several years. Even more, such targeted drugs often confer rather modest clinical benefits and they remain out-of-reach to most patients because of high cost (Schilsky and Schnipper 2018).

An alternative approach of finding and targeting cancer-specific effectors of cytotoxic drugs has not been explored. Cytotoxic drugs display a remarkable sensitivity towards particular cancer entities (e.g. cis-platinum is effective against solid tumors like NSCLC, testicular cancer or ovarian cancer, but not against hematological cancers). This work explores the sensitivity-relevant transcriptional drivers of clinically used cytotoxic drugs to understand the basis of selective sensitivity and to further enhance it.

3.1 Cancer chemotherapy

Cancer remains one of the major health concerns worldwide. It is second-leading cause of death with 18.1 million new cases and 9.6 million deaths in 2018 globally (Bray, Jacques et al. 2018, Siegel, Miller et al. 2018). Several factors contribute to increased cancer prevalence, including

aging population, as well as environmental and lifestyle changes. This is especially evident in rapidly developing countries which display a shift from poverty-associated cancers to lifestyle-associated cancers (Kanavos 2006).

The complexity of cancer in terms of genetic constitution, combined with variability in response to chemotherapeutic drugs, make treating them particularly challenging (Hanahan and Weinberg 2011). These variabilities are often observed within a single cancer entity. Cancer treatment strategies include surgery, radiotherapy, chemotherapy, and immunotherapy. Surgery is the ideal treatment for solid tumors detected at an early stage. For large tumors the radiotherapy provides an alternative for surgery (Urruticoechea, Alemany et al. 2010). However, both of these approaches are employed for local therapies. Chemotherapy is the preferred treatment for advanced solid tumors and for hematological malignancies.

There are various classes of clinically used anticancer drugs including alkylating agents, antibiotics and antimetabolites, topoisomerase inhibitors, and mitosis inhibitors. Unlike local treatments, chemotherapy is not restricted to particular site, but rather targets proliferating cells. Hence, chemotherapeutic drugs are indiscriminately toxic towards cancer cells as well as normal dividing cells including hair follicles, gastrointestinal epithelial cells, and bone marrow cells. This results in numerous side effects, including, among others, hair loss, stomach ulcers, and anemia, in the patients receiving chemotherapy, restricting their applicability.

There are numerous of drugs approved for each cancer type, which are either cytotoxic or targeted towards specific cancer entities (**Table 3.1.1**) (Sun, Wei et al. 2017).

Table 3.1.1: Overview of the number of drugs approved for each cancer type (Sun, Wei et al. 2017).

Cancer	Number of cytotoxic drugs	Number of targeted drugs	Total number of drugs
Leukemia	24	16	40
Lymphoma	14	14	28
Breast cancer	13	14	27
Lung cancer	10	7	17
Prostate cancer	3	12	15
Ovarian cancer	10	2	12
Melanoma	1	10	11
Colorectal cancer	5	5	10
Kidney cancer	2	8	10
Stomach cancer	5	5	10
Brain cancer	6	2	8
Multiple myeloma	3	5	8
Pancreatic cancer	5	3	8
Testicular cancer	6	0	6
Head and neck cancer	3	2	5
Sarcoma	3	2	5
Bladder cancer	4	0	4
Thyroid cancer	1	3	4
Bone cancer	2	1	3
Basal cell carcinoma	0	2	2
Cervical cancer	2	0	2
Gestational trophoblastic disease	2	0	2
Adrenal cortical carcinoma	1	0	1
Choriocarcinoma	1	0	1
Esophageal cancer	0	1	1
Gastroenteropancreatic neuroendocrine tumor	0	1	1
Kaposi’s sarcoma	0	1	1
Liver cancer	0	1	1
Mesothelioma	1	0	1
Myelofibrosis	0	1	1
Penile cancer	1	0	1
Retinoblastoma	1	0	1
Vulvar cancer	1	0	1

Even with current advancements and availability of number of drugs (**Table 3.1.1**), most patients with advanced cancers still exhibit poor prognosis, mostly because of residual cancer cells. And hence there is great need to improve the standard treatment regimen. Hence, there is ever-growing research to identify new potent drugs as well as to utilize alternative strategies such as immunotherapy (Zhang and Chen 2018). However, there are not many efforts addressing the efficacy and safety of existing chemotherapeutic drugs which are very potent despite lacking the cancer cell specificity. This is especially crucial considering increasing number of targeted drugs which are applicable to ever smaller cohort of patients (Arbiser 2007, Widakowich, de Castro et al. 2007). There are two ways of addressing this. First, replace these non-specific drugs with drugs targeting molecules and processes more specific to cancer cells. Second, combine existing chemotherapeutic drugs with synergistic partners to reduce their dosage and, hence, side-effects.

3.2 Topoisomerase II as cancer targets

Topoisomerase II (TOP2) poisons constitute one of the widely used and successful classes of anti-cancer drugs (Nitiss 2009). Unfortunately, due to the involvement of TOP2 in such fundamental cellular processes as DNA replication and transcription, its poisoning affects both cancerous and normal cells, including non-dividing ones. Thus, in addition to the transient bone marrow toxicity, TOP2 poisons cause irreversible side-effects such as secondary leukemia due to chromosomal rearrangements (Pendleton, Lindsey et al. 2014), and cardiotoxicity (McGowan, Chung et al. 2017).

DNA topoisomerases are the essential enzymes involved in the processes such as replication and transcription. Human DNA topoisomerases consist of three types including type IA (*TOP3A* and *TOP3B*), type IB (*TOP1* and *TOP1MT*), and type IIA (*TOP2A* and *TOP2B*). Monomeric type I enzymes catalyze DNA single-stand breaks, while dimeric type II enzymes catalyze DNA-double

strand breaks to relieve the topological strain (Pommier 2013). These enzymes resolve higher order DNA structure through two trans-esterification steps. The first trans-esterification step creates an DNA adduct, which generates TOP2-DNA cleavable complex causing the topological change. The second trans-esterification step re-seals the break. This process has extensively been exploited in cancer chemotherapy. TOP2 poisoning has been utilized in the clinic for more than 50 years as first-line therapy for blood as well as solid cancers (Marinello, Delcuratolo et al. 2018). Topoisomerase II (TOP2) poisons constitute one of the widely used and successful classes of anti-cancer drugs (Nitiss 2009, Pommier, Sun et al. 2016). The main TOP2 poison classes include anthracyclines, camptothecins, and epipodophyllotoxins. TOP2 poisons, such as epipodophyllotoxin etoposide, target the short-lived TOP2-DNA cleavable complex and prevent the re-ligation of transient DSBs. This generates high number of TOP2-associated DSBs, which trigger apoptosis (Nitiss 2009, Pommier, Leo et al. 2010). The process of TOP2 poisoning by etoposide is depicted in **Fig. 3.2.1**.

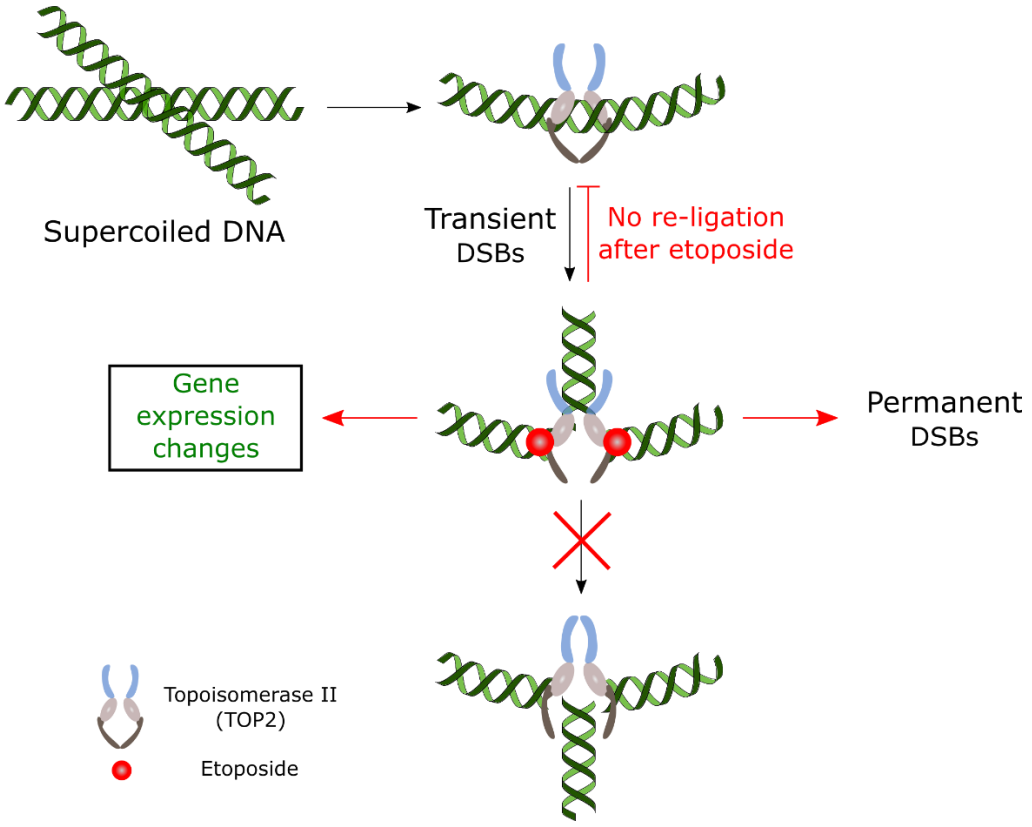

Fig. 3.2.1: Pictorial representation of topoisomerase II (TOP2) poisoning by etoposide and its consequences.

TOP2 poisons constitute one of the most important anti-cancer drugs. They are used in managing almost all types of chemotherapy-responsive cancers. Clinically used and approved TOP2 poisons are listed in the **Table 3.1.1**.

Table 3.2.1: Overview of the topoisomerase II (TOP2) poisons used in clinic (Cowell and Austin 2012, Chemocare 2019).

Class	Drug	Use
Acridine	Amsacrine	Acute adult leukemia, Lymphoma
Benzo[c]phenanthridine alkaloid	NK314	Adult T-cell leukemia-lymphoma
Anthracenedione	Mitoxantrone	Breast cancer, Leukemia, Non-Hodgkin lymphoma
Anthracyclines	Daunorubicin	Acute myeloid leukemia, Acute lymphoblastic leukemia, Acute promyelocytic leukemia
	Doxorubicin	Acute lymphoblastic leukemia, Acute myeloid leukemia, Bone sarcoma, Breast cancer, Endometrial cancer, Gastric cancer, Head and neck cancer, Hodgkin and non-Hodgkin lymphoma, Liver cancer, Kidney cancer, Multiple myeloma, Neuroblastoma, Ovarian cancer, Small cell lung cancer, Soft tissue sarcoma, Thyomas, Thyroid cancer, Transitional cell bladder cancer, Uterine sarcoma, Wilms' tumor, Waldenstrom macroglobulinemia
	Epirubicin	Breast cancer
	Idarubicin	Acute lymphoblastic leukemia, Acute myeloid leukemia, Chronic myelogenous leukemia
Camptothecins	Irinotecan	Metastatic colon or rectal cancer
	Topotecan	Lung cancer, Ovarian cancer
Epipodophyllotoxins	Etoposide	Acute myeloid leukemia, Bladder cancer, Hodgkin's and non-Hodgkin's lymphoma, Kaposi's sarcoma, Lung cancer, Prostate cancer, Stomach cancer, Testicular cancer, Uterine cancer, Wilm's tumor
	Teniposide	Acute lymphocytic leukemia (in children)
Quinolones	Voreloxin	Acute myeloid leukemia

Clearly, doxorubicin and etoposide are the TOP2 poisons most widely used against cancers, especially against hematological ones. The anti-cancer activity of doxorubicin is additionally contributed to by DNA intercalation and generation of reactive oxygen species, and hence not limited to TOP2 poisoning (Thorn, Oshiro et al. 2011). Because of wide applicability to a number of cancer types and specificity for TOP2, I have focused on etoposide.

Etoposide is synthesized from podophyllotoxin isolated from *Podophyllum peltatum* rhizome. It targets the type IIA topoisomerases TOP2A and TOP2B. Its clinical use is limited by the

indiscriminate toxicity towards normal cells. Etoposide causes secondary leukemia due to chromosomal rearrangements (Pendleton, Lindsey et al. 2014), usually a translocation of the mixed lineage leukemia (MLL) gene on the chromosome 11q23. Clearly, there is a need to optimize etoposide-regimens to reduce such chromosomal rearrangements.

3.3 Gene expression and drug response

Ever-decreasing cost of genomic profiling has allowed for high-throughput profiling of cancer cells. This has elevated our understanding of tumor growth, progression, and response and driven the development of many targeted therapeutics. During the last decade, there have been several efforts to associate the base line transcriptomic levels and mutation profiles with the response to cytotoxic drugs (Whyte and Holbeck 2006, Zhang, Wang et al. 2015, Vural, Simon et al. 2018). The basal expression of some genes has been linked to the drug resistance (Robert, Vekris et al. 2004). A well-characterized explanation of etoposide resistance is the overexpression of MRP1 (encoded by *ABCC1*) (Legrand, Zittoun et al. 1999, Benyahia, Huguet et al. 2004). However, this and other identified targets have failed to make significant clinical impact.

Considering the dynamic nature of the cells, there have been few efforts addressing the transcriptomic profiles generated by drug treatments. Recently, drug-evoked gene expression changes (GEC) have been investigated using network analysis of cellular perturbation profiles (Rees, Seashore-Ludlow et al. 2016). Further, drug-evoked GEC, have been utilized to investigate mechanism and downstream pathways of drug treatments (Iorio, Tagliaferri et al. 2009, Woo, Shimoni et al. 2015). Currently, there are a few ongoing big-data initiatives generating transcriptomic changes caused by drug treatments, including Connectivity Map (CMap) from the Broad Institute. Such resources could be implemented in drug discovery pipelines to facilitate target identification based on drug-evoked GEC.

Considering the role of TOP2A in transcription, I hypothesized that TOP2 poisoning with etoposide could evoke *specific* GEC across various cancer cell lines. I planned to investigate such TOP2A-dependent GEC using an engineered fibrosarcoma cell line (HTETOP) with inducible repression of TOP2A. I next planned to explore the etoposide-evoked GEC for treatment optimization in the cancer entity AML, described in following section.

3.4 Acute Myeloid Leukemia

Acute myeloid leukemia (AML) is a type of blood neoplasm characterized by numerous genomic alterations (such as FLT3, NPM1, RUNX1, and IDH1 & 2). AML accounts for 80% of leukemia cases in adult patients with 5-year survival rate of 24% (De Kouchkovsky and Abdul-Hay 2016, Pearsall, Lincz et al. 2018). Chemotherapy is the main form AML management (Dombret and Gardin 2016). Cytarabine and daunorubicin, or idarubicin or mitoxantrone, or sometimes cladribine are preferentially utilized for the induction therapy to destroy most of the bone marrow cells. However, such intensive therapy is not tolerable to older patients (Ossenkoppele and Lowenberg 2015). Furthermore, treatment strategies for relapsed AML are not yet clearly defined. MEC regimen (mitoxantrone in combination with etoposide and cytarabine) is one of the common regimens used for relapsed AML. However, it is associated with increased side-effects in AML patients (Ramos, Mo et al. 2015, Thol, Schlenk et al. 2015). Hence, there is a need to improve efficacy and reduce the toxicity of these treatment regimens. To this end, the classical chemotherapeutics in AML are gradually being supplemented by drugs targeting molecules and processes more specific to cancer cells. For example, midostaurin and enasidenib can be nowadays added to standard chemotherapeutic regimens (Stein, DiNardo et al. 2017, Stone, Mandrekar et al. 2017). However, this option is reserved for patients carrying specific mutations in the protein targets of these drugs, FLT3 and IDH2, respectively.

I chose AML as a cancer model, since it is frequently treated with etoposide, especially for relapsed AML (Dombret and Gardin 2016). This work explores the alternative and largely untested approach of fine-tuning approved etoposide-based therapies by combining them with already approved or experimental drugs. I reasoned that,

- etoposide-driven changes in the expression and activity of specific proteins mediate, at least in part, etoposide's cell killing effects and
- drugs targeting some of these mediators will be already available for testing as combination treatments.

Apoptosis resulting from etoposide-driven DNA damage is accompanied by considerable gene expression changes of unexplored consequences (E. Jeong et al., 2018; Troester, Hoadley, Parker, & Perou, 2004). I assessed etoposide-driven gene expression changes by comparing pre-and post-treatment cell transcriptomes. I also considered the impact of prior-to-treatment gene expression levels on the response to etoposide across AML cell lines. Here, I reasoned that, in addition to expression *changes*, the response to etoposide is likely to be affected by *pre-existing* levels of proteins modulating its effects. I intended to enrich for *drivers* as opposed by *bystanders* of etoposide cytotoxicity using two parallel approaches. Firstly, I focused on genes co-regulated within networks and additionally correlating with etoposide cytotoxicity. Genes involved in such networks are more likely to be involved in etoposide response compared to genes taken individually (Langfelder and Horvath 2008, Li, Zhou et al. 2018). Secondly, I focused on individual, but *essential* genes, i.e. on those reducing the survival of each of the AML cell lines investigated when knocked down using shRNA (Tsherniak, Vazquez et al. 2017). Here I considered that tumor growth and metastasis are driven only by a fraction of the accompanying molecular changes and assumed a similar relationship for etoposide response and gene expression

levels. Among drivers thus identified, I differentiated between *modulators*, *mediators*, and *emulators* of etoposide response. Etoposide modulators are genes, whose expression correlates with etoposide cytotoxicity, but remains unchanged upon treatment. Etoposide mediators are genes that convey cytotoxicity via etoposide-driven changes in their expression levels. Etoposide emulators are upstream gene modulations and other drugs that evoke gene expression profiles resembling those evoked by etoposide.

To distinguish between cytotoxicity drives from bystanders, I developed two parallel approaches. Firstly, I considered the network of genes co-regulated across AML cell lines. The reason was such genes are more likely to be enriched for etoposide-relevant biological processes compared to individual genes (Langfelder and Horvath 2008, Li, Zhou et al. 2018). Secondly, to distinguish between mediators and bystanders of etoposide cytotoxicity among etoposide-evoked GEC, I considered each gene's essentiality (Tsherniak et al., 2017) for cell survival in each individual AML cell line. Because of unavailability of HTETOP essentiality data, another approach, considering high pre-treatment expression, involvement in cancer-related processes, and comparative high expression in cancer tissues, was developed to define essentiality. I hypothesized that the modulators could be targeted to enhance the efficacy of etoposide, while effectors could be investigated for their involvement in the cytotoxicity.

4 Materials and methods

4.1 Cell culture and drugs

HTETOP cell line was kindly provided by Dr. Andy Porter (Imperial College London, UK). It was cultured in DMEM media (Sigma Aldrich, Germany) supplemented with 10% FCS, 20 mM HEPES buffer, 1 mM sodium pyruvate, and antibiotics as reported before (Carpenter and Porter 2004). HTETOP cells were maintained at 37°C and 10% CO_2. Tetracycline (TET) at 1 µg/ml was added to cells resulting in >95% TOP2A mRNA and protein repression (Yan, Deng et al. 2009). Acute Myeloid Leukemia (AML) cell lines HL-60, MOLM-13, MONO-MAC-6, MV-4-11, NB-4, NOMO-1, OCI-AML3, and THP-1 were obtained from Dr. Thomas Kindler, University Medical Center, Mainz. Three additional AML cell lines (F-36P, KASUMI-1, and OCI-AML2) were purchased from Deutsche Sammlung von Mikroorganismen und Zellkulturen (DSMZ, Germany). Cell lines were maintained at 37° C and 5% CO_2 in appropriate media (**Table 5.7.1**). 293T cells were cultured in DMEM (Gibco, Germany) along with 10% FBS (Biochrom, Germany). Cell lines were routinely verified for mycoplasma contamination using Venor®GeM Mycoplasma Detection Kit (Sigma-Aldrich, Germany). Cell lines were authenticated by Multiplexion, Germany. The inhibitors were purchased from Abcam (UK), Biozol (Germany), and Santa Cruz Biotechnology (US).

4.2 Cell viability assay

1800 cells (in 100 µL media) were seeded in 96 well plates and incubated overnight at 37° C in 10% CO_2 incubator, followed by tetracycline treatment (2 µg/mL in 100 µL media) and incubated for 24 hours to knock down the TOP2A expression. Media was then replaced, and the cells were treated with different concentrations of etoposide and doxorubicin for 24 and 48 hours. After the

treatment, 20 µL MTT were added and cells were incubated for 4 hours at 37° C followed by addition of solubilization buffer and then incubated overnight in dark. Absorbance was measured at 570 nm. Cell viability in response to drug treatment was calculated considering the absorbance of DMSO treated cells as 100% cell viability.

The viability of AML cell lines in response to etoposide treatment was monitored using WST-8 cell viability kit (PromoKine, German). All AML cell lines were seeded (1 X 10^4 cells per well) in a 96-well plate and incubated overnight. Cells were then treated for 24 hours with various concentrations of etoposide (0.02, 0.05, 0.1, 0.2, 0.37, 0.78, 1.56, 3.13, 6.25, 12.5, 25, 50 µM)., after the treatment with etoposide, 10% WST-8 reagent was added to the cells. After 1-4 hours incubation in the dark at room temperature, absorbance was measured at 450 nm using Spectramax iD3 (Molecular Devices, US) spectrometer. Absorbance from the DMSO-treated cells (vehicle control) was considered as 100% cell viability and used to calculate percentage cell viability after etoposide treatment.

4.3 Annexin V apoptosis assay

The flow cytometry-based apoptosis detection was performed using FITC Annexin V apoptosis detection kit I (BD Biosciences). 2 X 10^5 cells/mL were seeded in a 6-well plate and incubated overnight. Cells were then treated with cell line-specific etoposide IC_{50} concentrations, derived from the cell viability assay, for 24 hours, washed twice with ice-cold PBS, and resuspended in binding buffer (1 X 10^6 cells/ml). Thereafter, 100 µL of cell suspension (1 X 10^5 cells) was transferred to a new tube, followed by addition of 5 µL each of Annexin V and PI staining solution (FITC Annexin V apoptosis detection kit I, BD Biosciences). Cells were then gently vortexed and incubated in dark for 15 minutes at room temperature. 400 µL of binding buffer was then added to the cells and analyzed using BD Accuri C6 flow cytometer (BD Biosciences, US).

4.4 RNA-Seq: RNA extraction and library preparation

The gene expression profiles in untreated and etoposide-treated AML and HTETOP cell lines were determined by RNA sequencing. 1 X 10^6 cells per well were seeded in a 6 well plate containing 5 mL of the media. Cells were incubated overnight and then treated for 24 hours with etoposide at cell line-specific IC_{50} concentrations (for AML cell lines) or at 20 µM concentration (for HTETOP cell line). HTETOP cell line was separately treated with doxorubicin at 1 µM concentration for 24 hours in presence and absence of TOP2A. For HTETOP cell line, only one biological replicate was generated. AML cells from 3 wells were then pooled together and total RNA was isolated using TriFast, peqGOLD total RNA kit and DNase I Digest kit (VWR PEQLAB GmbH, Germany) according to manufacturer's instructions. The quality and integrity of the extracted RNA was examined using a 2100 Bioanalyzer (Agilent technologies). Samples were sequenced by Illumina HiSeq 2000 using TruSeq stranded mRNA HT sample prep kit. RNA quality analysis, library preparation and sequencing was performed by the Genomics Core Facility at the Institute of Molecular Biology (IMB, Mainz, Germany). The targeted sequencing depth was 30 million reads (for AML) or 50 million reads (for HTETOP). HTETOP samples were generated and sequenced at the Star Seq GmbH (Germany) by Dr. Shiwei Deng (University Medical Center, Mainz).

4.5 RNA-Seq: Analysis

The quality of raw sequencing reads was assessed using FastQC (Babraham Bioinformatics, Cambridge, UK). These reads were then mapped to the human reference genome (gencode release 25 GRCh38.p7) using the STAR aligner (v2.5.3a) (Dobin, Davis et al. 2013), with the option "--quantMode GeneCounts" to count the number of reads mapped per gene. Quality of the expression data was assessed using NOISeq (v2.20.0) (Tarazona, Furio-Tari et al. 2015) R package (R Core Team 2014). The differential gene expression analysis was then performed using edgeR (v3.20.1)

(Robinson, McCarthy et al. 2010). Genes with fold-change higher than 2 and false discovery rate (FDR) below 0.05 were considered as differentially expressed. The R script used in this analysis is appended.

4.6 Weighted gene co-expression network analysis (WGCNA)

To identify modulators and mediators of etoposide sensitivity, weighted gene co-expression network analysis (WGCNA) was performed using basal gene expression in AML cell lines prior and after etoposide treatment. The resulting co-regulated networks were compared to identify genes (a) co-regulated only before treatment, (b) co-regulated only after treatment, and (c) unaffected by treatment. Gene Ontology analysis was performed for identified networks using the Database for Annotation, Visualization and Integrated Discovery (DAVID, https://david.ncifcrf.gov/). Cell line specific expression levels of co-regulated genes unaffected by treatment were correlated with cell-specific etoposide IC_{50} concentrations by Pearson correlation statistics using the WGCNA package in R (Langfelder and Horvath 2008). The co-regulated genes with positive and negative correlation with etoposide IC_{50} were selected for Gene Ontology analysis using DAVID.

4.7 Identification of mediators among etoposide-evoked gene expression changes

The Project Achilles (PAch) (Cowley, Weir et al. 2014) dataset was utilized to retrieve genes most likely to be essential for AML cell survival. PAch investigated the effect of more than 11k shRNA-mediated individual gene knockdowns on cell survival in 501 cancer cell lines, including all AML cell lines used in the present study. Genes with negative DEMETER scores (defined in a previous study (Tsherniak, Vazquez et al. 2017)) were considered essential for cancer cell survival. Genes essential for 6 or more AML cell lines as well as differentially expressed after etoposide treatment were considered potential essential mediators and validated experimentally. To identify mediators

of etoposide cytotoxicity in HTETOP cell line different approach was utilized because of unavailability of essentiality data from PAch. The genes highly expressed in HTETOP and repressed after etoposide treatment were selected. Gene Ontology analysis was performed using Ingenuity Pathway Analysis (IPA, Qiagen Inc., https://www.qiagenbioinformatics.com/products/ingenuitypathway-analysis) to restrict the repressing GEC to the pathways involved in cancer and cell proliferation. For quantifying the gene expression in normal tissues, transcript per million (TPM) data was downloaded for 33 normal tissues from GTEx. For cancer tissues, fragments per kilobase million (FPKM) data was retrieved for 29 cancer tissues from The Cancer Genome Atlas (TCGA). FPKM was then converted to TPM and the average expression was compared to normal tissues using R. The genes with high expression in cancer tissues were selected and were further screened for their etoposide-evoked repression in other cancer cell lines obtained from Gene Expression Omnibus (GEO). Furthermore, the putative upstream regulators of etoposide-evoked GEC in HTETOP were identified using IPA and Connectivity Map (CMap).

4.8 Prediction of etoposide emulators

Emulators, i.e. gene modulations and compounds that evoke GEC similar to those following etoposides, were identified using the CMap (Subramanian, Narayan et al. 2017). CMap provides changes in the expression of 1000 genes following gene perturbations and treatments with numerous small-molecule compounds. These genes and drugs were identified by uploading the top 300 overlapping etoposide-evoked GEC (150 up- and 150 down-regulated) from AML and HTETOP cell lines to CMap via the CLUE platform (CMap and LINCS Unified Environment).

4.9 Driver validation using inhibitors

The inhibitors against the selected drivers were identified using the GeneCards (Ben-Ari Fuchs, Lieder et al. 2016), IUPHAR/BPS guide to pharmacology (Alexander, Fabbro et al. 2017), and CMap (Subramanian, Narayan et al. 2017) resources. These drivers were then validated using WST-8 cell viability assay. AML cell lines were treated for 24 hours with 1 nM, 100 nM, and 10 µM of each inhibitor alone, as well as in combinations with cell-specific IC_{25} concentrations of etoposide, followed by WST-8 cell viability assay. Percentage cell viability compared to vehicle-treated cells, taken as 100%, was calculated for single and combination treatments. For combination treatment screening, the synergy was defined as per-response additivity approach (Foucquier and Guedj 2015). The combination index (CI) was calculated as $\mathrm{CI} = \frac{E_A + E_B}{E_{AB}}$, where E_A is the effect of inhibitor A, E_B is the effect of etoposide and E_{AB} is the effect of combination of inhibitor A and etoposide. CI < 1 was considered as synergy with etoposide, while CI > 1 was considered as antagonism, and CI = 1 was considered as additive effect.

4.10 Driver validation using sh/siRNA-mediated gene knockdown

siRNA sequences targeting the gene of interest in HTETOP cells were selected using Project Achilles (PAch) database. The shRNA target sequences with highest consistency scores and lowest p-value were selected. The targets of these sequences were verified using online siRNA-Check tool developed by Genomics and Bioinformatics Group, LMP, CCR, National Cancer Institute. siRNAs were then synthesized using Sigma custom oligo service. HTETOP cells were then transfected with 10 nM siRNA for 24 hours using JetPrime transfection reagent. WST-8-based cell viability assay was performed 24 hours after transfection to evaluate the effect of gene knockdown on cell viability. The gene knockdown was monitored using SYBR green qPCR. Primers used in this work are listed in **Appendix table 2**.

To investigate the effect of individual gene knockdowns on AML cell survival, Viral Shah (University Medical Center Mainz) cloned shRNA targeting *BCL2A1*, *IGFIR*, and *ROCK1* into Tet-pLKO.1-puro vector (kindly provided by Dimitri Wiederschain, Novartis Institutes for BioMedical Research, Cambridge, MA). shRNA sequences were obtained from the PAch resource and were synthesized by Sigma-Aldrich, along with RHS4743 expressing scrambled shRNA (supplementary data S1 Table 2). Lentiviral particles were generated by co-transfecting psPAX2, pMD2.G along with previously generated shRNA expressing vectors into 293T cells. Transfection was carried out using TransIT (Mirus) as per the manufacturer's instructions. To achieve stable transduction, AML cell lines were seeded 1 X 10^6 in a 6-well plate, with each virus supernatant in presence of 5 µg/mL polybrene and spin-infected at 2500 rpm at 32°C for 1 and 45 hours. Following 16 hours incubation at 37°C, cells were supplemented with 1-2 µg/mL puromycin (Sigma-Aldrich, Germany). Furthermore, to induce knockdown of the indicated drivers, 5 X 10^5 cells per well were seeded in 6-well cell culture plates. The knockdown was then induced by treating the cells with doxycycline (200 ng/mL) and cell viability was measured after 24, 48, and 72 hours using the WST-8 assay. The effect of shRNA-mediated gene knockdown on cell viability was calculated by comparing doxycycline-untreated and -treated cells.

4.11 DNA damage measurement using flow cytometry

To compare the amount of DNA damage caused by etoposide alone and in combination with other drugs, the levels of phosphorylated H2A.X in HL-60 cells were measured using flow cytometry. The fixed HL-60 cells were stained using the H2A.X phosphorylation assay kit (Merck, Germany) according to manufacturer's instructions. In short, 5 X 10^5 HL-60 cells were seeded per well in a 6-well plate and incubated overnight. Cells were treated for 24 hours with IC_{25} concentration of etoposide alone and in combination with other drugs. Next, cells were harvested and washed with

PBS followed by fixation. Cells were then stained with either FITC-conjugated anti-phospho-Histone H2A.X (Ser139) or with the negative control mouse IgG-FITC conjugate for 20 minutes on ice. The amount of H2A.X was then measured using BD Accuri flow cytometer. The data was then analyzed using FlowJo software (v10).

4.12 TCGA survival analysis

The raw gene expression counts for 151 AML patients were retrieved from TCGA through the Broad GDAC Firehose, along with the clinical data, using the R package RTCGAToolbox (v2.8.0) (Samur 2014). Univariate survival analysis compared the groups with high expression (above median) and low expression (below median) of selected drivers. p-values for Kaplan-Meier plots were calculated using Log-rank test. The comparison between gene expression in AML patients and normal blood samples was performed using Gene Expression Profiling Interactive Analysis (GEPIA) web server (Tang, Li et al. 2017).

4.13 Statistical analysis

Unless otherwise specified, the experiments reflect 3 biological replicates. Data was analyzed using R language packages and GraphPad Prism software (v7). Graphs were plotted as mean ± SD. The etoposide IC_{50} concentrations were calculated using GraphPad Prism software by fitting the dose response curve by non-linear regression. Shapiro-Wilk test was performed to determine normal distribution for parametric tests. Two-way ANOVA with Benjamini and Hochberg FDR correction was performed to identify inhibitors with significant cytotoxicity (Benjamini and Hochberg 1995). Mann-Whitney test was performed to identify significant expression change between resistant and sensitive AML cell lines.

5 Results

5.1 Etoposide-mediated cytotoxicity in HTETOP is TOP2A-dependent

To investigate the dependency of TOP2A for etoposide-evoked GEC, it was crucial to examine TOP2A-specific cytotoxicity of etoposide. To this end, HTETOP cells were treated with different concentrations of etoposide and doxorubicin for 24 and 48 hours, in the presence and absence of TOP2A. The cell viability was measured using MTT assay. As seen in **Fig. 5.1.1,** both etoposide and doxorubicin exhibited dose-dependent cytotoxicity in HTETOP cell line in the presence of TOP2A. However, TOP2A knockdown by tetracycline (TET) treatment inhibited etoposide-mediated cytotoxicity (**Fig. 5.1.1A** and **B**). On the other hand, TOP2A knockdown had no effect on doxorubicin-mediated cytotoxicity (**Fig. 5.1.1C** and **D**). This is consistent with the known mechanism of action of these two drugs, where doxorubicin, in addition to TOP2 poisoning, exerts its cytotoxic potential through direct intercalation with the DNA, as well as through damage to the mitochondria by means of oxidative stress (ROS generation), and on the other side etoposide being solely dependent on TOP2 poisoning. The results demonstrate that, in absence of TOP2A, etoposide is very little cytotoxic. Its remaining cytotoxicity most likely results from TOP2B poisoning.

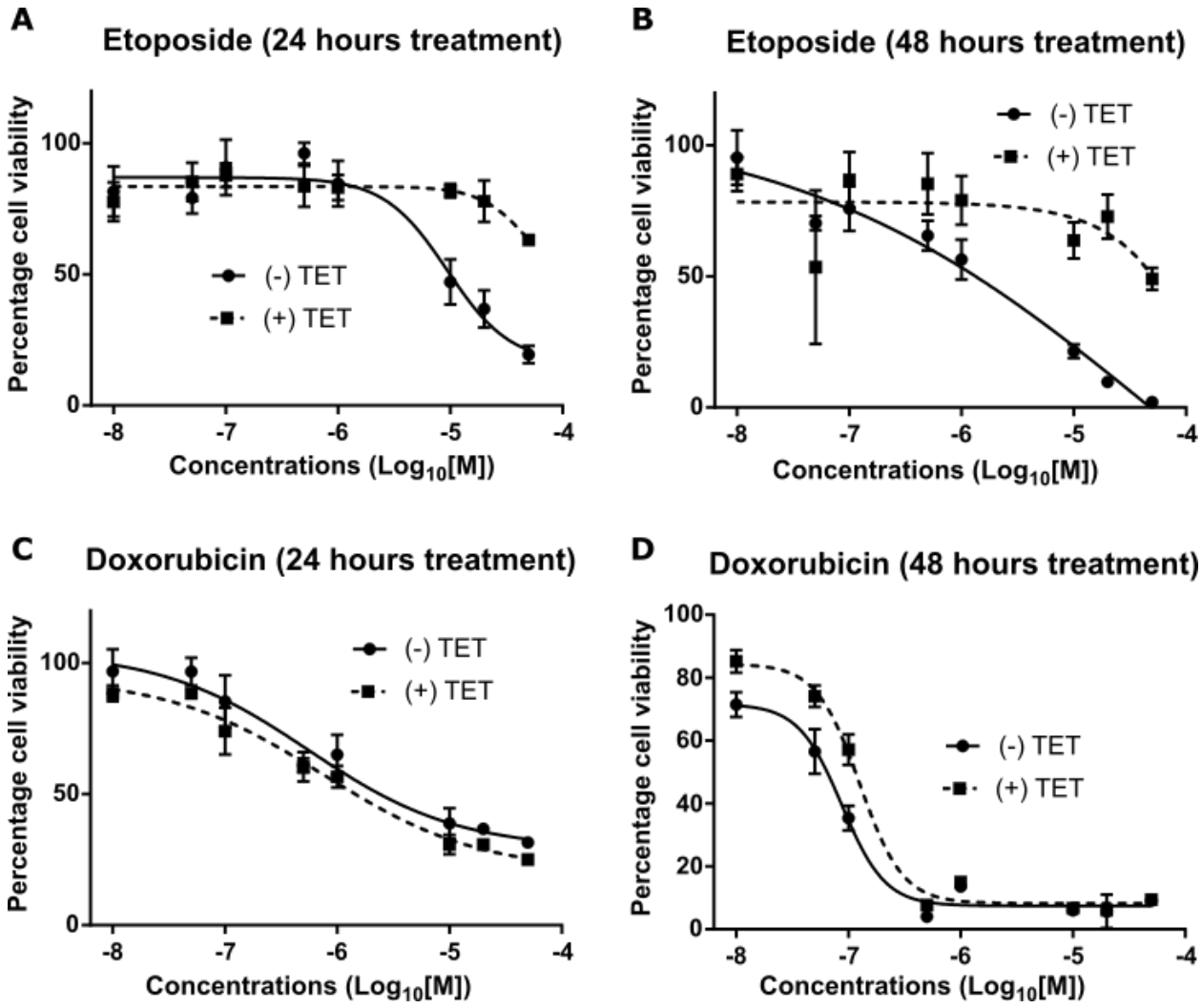

Fig. 5.1.1: **HTETOP cell viability in response to TOP2 poisons**. MTT-based cell viability assay in HTETOP cell line after treatment with topoisomerase-II (TOP2) poisons etoposide (A and B) and doxorubicin (C and D) after 24 and 48 hours. Data are represented as mean values ± SD.

5.2 Etoposide-evoked specific gene repressions in HTETOP cell line

HTETOP cell line was sequenced by mRNA sequencing before and after 20 µM etoposide or 1 µM doxorubicin treatment by Dr. Shiwei Deng (University Medical Center, Mainz). After processing for the quality control step using FastQC, the paired-end sequencing data was mapped to reference genome (hg38) using HISAT2 (version 2.0.4). The count for mapped reads were generated using htseq-count (version 0.6.1) and then DESeq2 was used to identify gene expression changes following the etoposide treatment. As shown in **Fig. 5.2.1**, etoposide-evoked gene

repressions accounted for 65% of all GEC. On the other hand, doxorubicin-evoked gene inductions accounted for 57% of all GEC (**Fig. 5.2.2**). Furthermore, doxorubicin evoked more GEC (4861) compared to etoposide (859) (**Fig. 5.2.3A**).

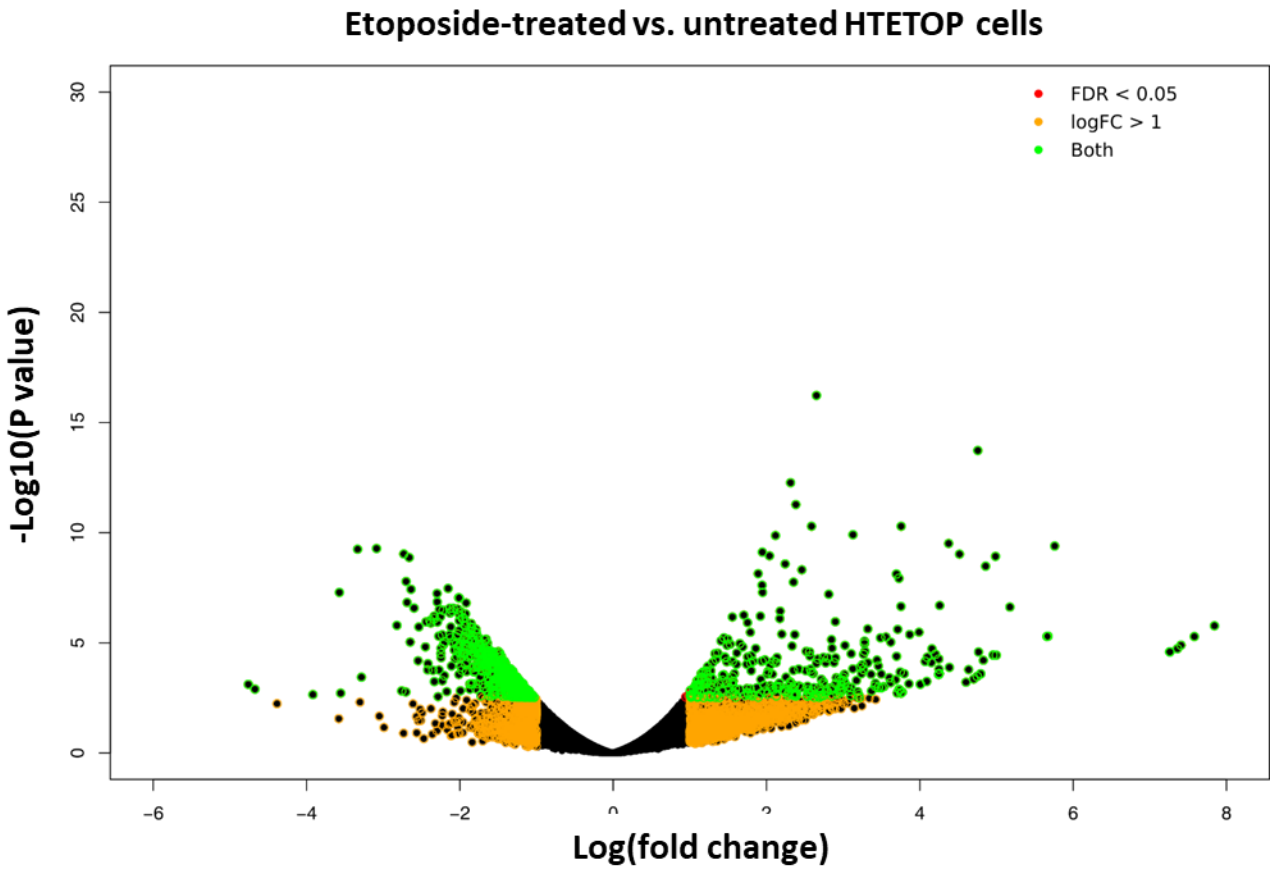

Fig. 5.2.1: **Effect of etoposide on gene expression in HTETOP cells**. Volcano plot representing gene expression changes (GEC) in HTETOP cells following etoposide treatment (20 µM) for 24 hours.

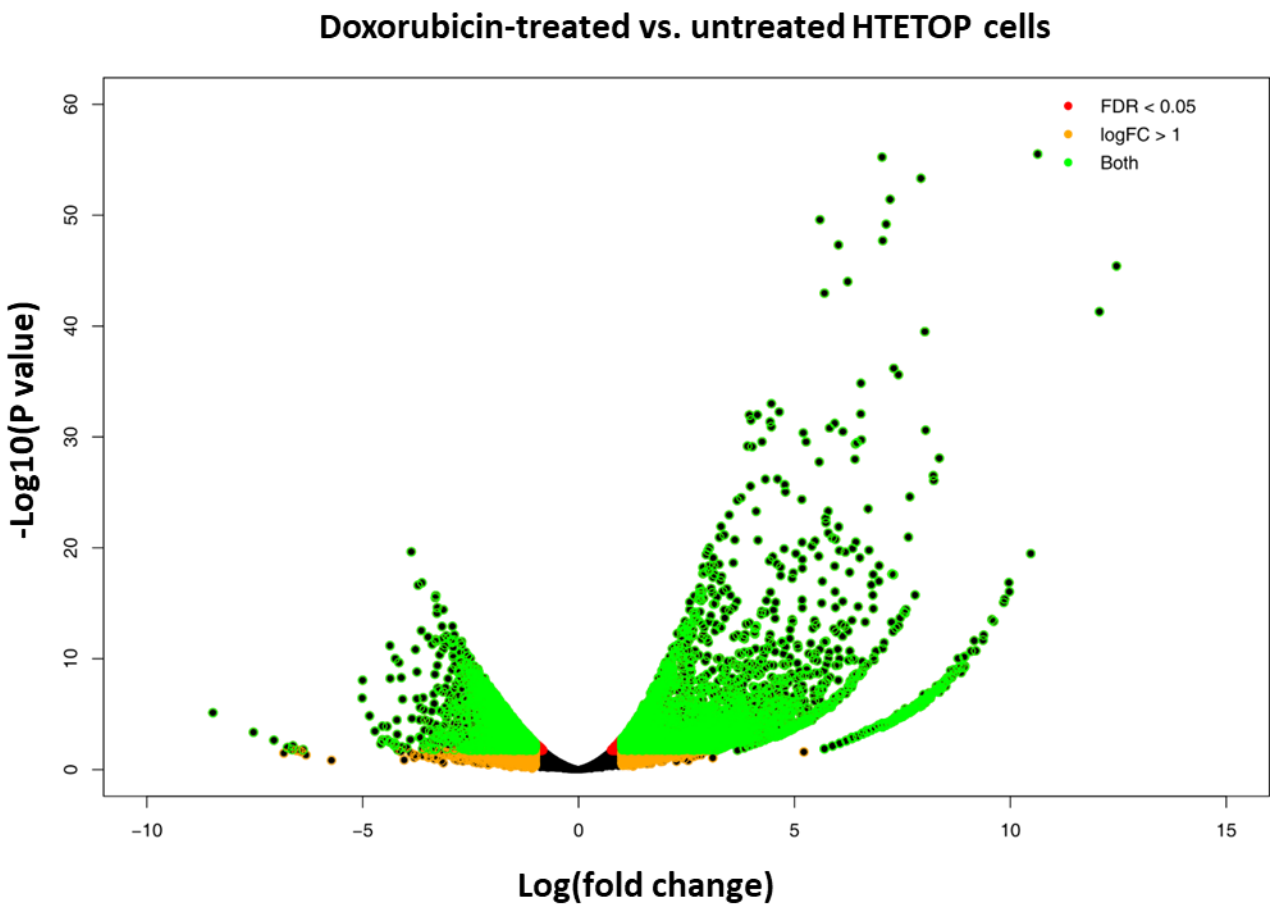

Fig. 5.2.2: **Effect of doxorubicin on gene expression in HTETOP cells**. Volcano plot representing gene expression changes (GEC) in HTETOP cells following doxorubicin treatment (1µM) for 24 hours.

I further compared the effect of TOP2A availability on GEC evoked by etoposide and doxorubicin. As observed with the cytotoxicity (**Fig. 5.1.1**), etoposide-evoked GEC were TOP2A dependent, while absence of TOP2A did not have high impact on doxorubicin-evoked GEC. In the absence of TOP2A, etoposide-evoked GEC reduced from 859 to 91 (**Fig. 5.2.3C**). There were 425 TOP2A-dependent GEC evoked by etoposide and 112 evoked by doxorubicin (**Fig. 5.2.3D**). This reflects that, unlike with doxorubicin, a majority of etoposide-evoked GEC are mediated by TOP2A poisoning.

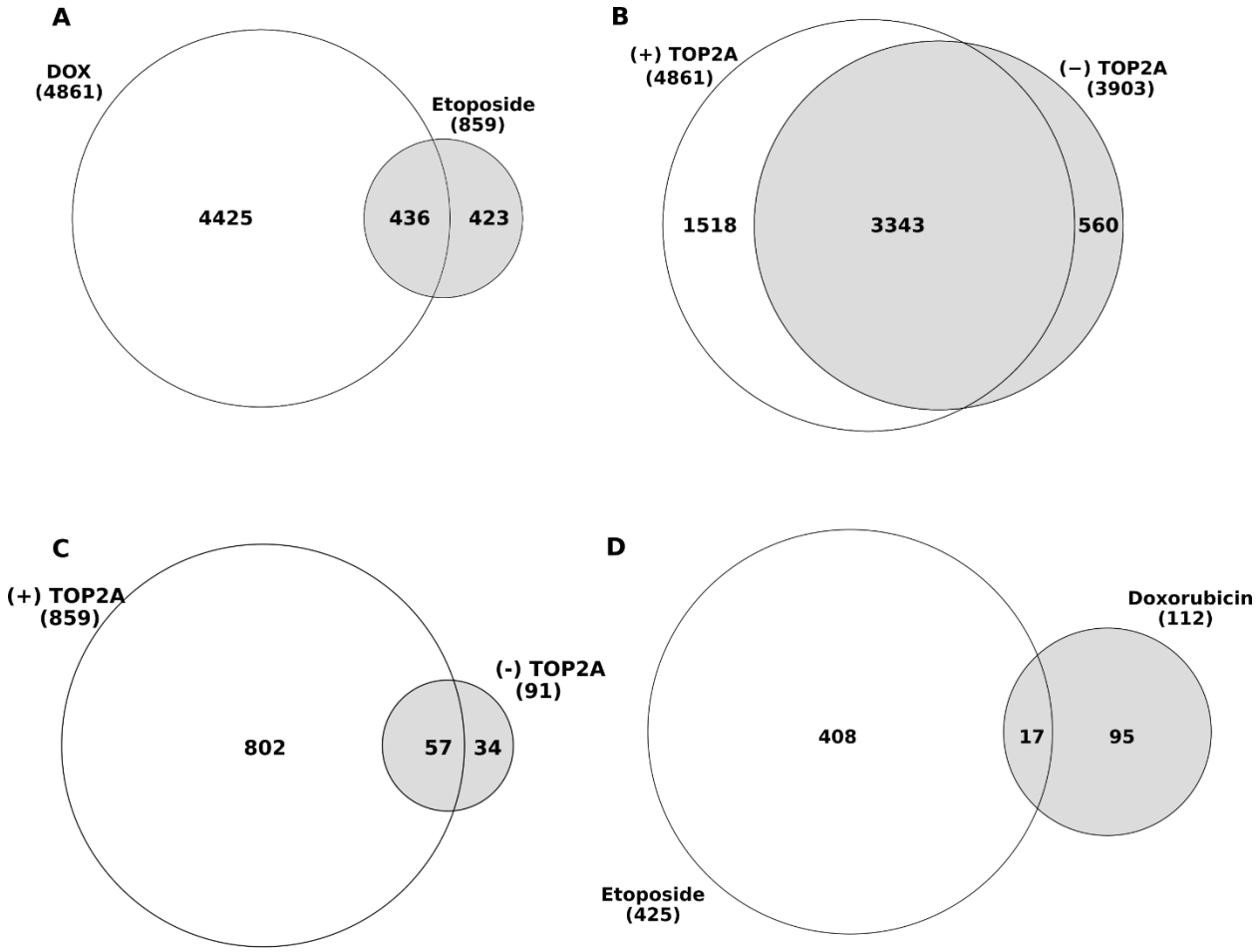

Fig. 5.2.3: **TOP2A-dependent gene expression changes after etoposide and doxorubicin treatments of HTETOP cells**. (A) Comparison of gene expression changes (GEC) after doxorubicin and etoposide treatment, (B) and (C) represent the numbers of GEC after doxorubicin and etoposide treatment respectively, in presence and absence of TOP2A, (D) comparison of TOP2A-dependent GEC after doxorubicin and etoposide treatments.

5.3 Etoposide predominantly represses the high-expressing genes in HTETOP cell line

To understand the mechanism of etoposide-evoked TOP2A-dependent gene repression, the basal gene expression level (GEL) in HTETOP cells was investigated. I quantified transcripts per million (TPM) from mapped RNA-Seq counts. To correlate TOP2 poisoning-related GEC as a function of GEL, I divided all expressed genes into 3 categories according to their TPM values. Next, a density graph of all TPM values was plotted to define expressed genes. Then quantile approach was

followed to define low, average and high expressing genes. Considering the role of TOP2A in transcriptional regulation, I compared etoposide-evoked GEC of high and low expressing genes as a function of TOP2A enrichment. High expressing genes were preferentially repressed after both doxorubicin and etoposide treatment. When considered at the entire transcriptome level, 22% (1067) of genes with high basal GEL were repressed after doxorubicin treatment (**Fig. 5.3.1A**) compared to 0.6% (28) of genes with low basal GEL (**Fig. 5.3.1B**) in the presence of TOP2A. The absence of TOP2A did not have significant impact on doxorubicin-mediated repression of genes with high basal GEL. Similarly, 6% (289) of genes with high basal GEL were repressed after etoposide treatment (**Fig. 5.3.1C**) compared to 0.15% (7) of genes with low basal GEL (**Fig. 5.3.1D**) in presence of TOP2A. As expected, the absence of TOP2A reduced etoposide-mediated repression of the genes with high basal GEL from 6% (289) to 0.15% (7).

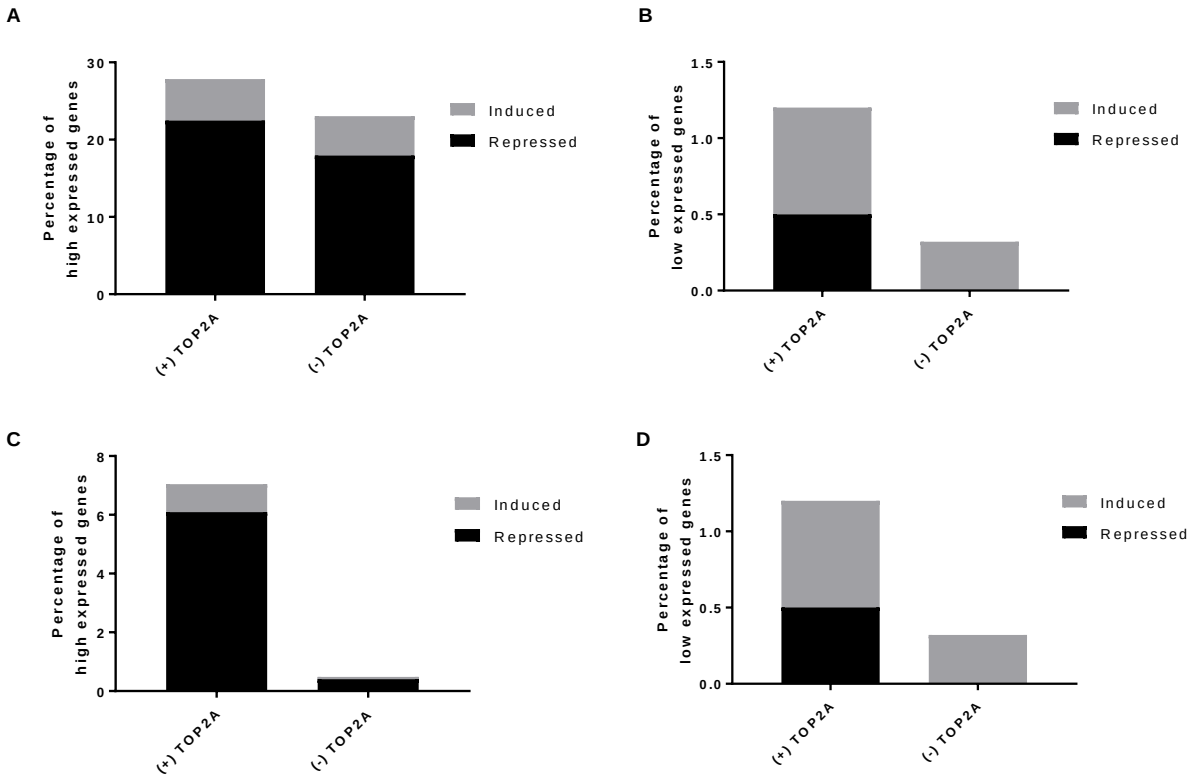

Fig. 5.3.1: **Predominance of gene repression after treatment with etoposide and doxorubicin in HTETOP cells**. Percentage of high (A) and low (B) expressing genes from HTETOP cells differentially expressed after doxorubicin treatment in presence and absence of TOP2A. Percentage of high (C) and low (D) expressing genes differentially expressed after etoposide treatment in presence and absence of TOP2A.

The predominance of gene repressions among high expressing genes is in agreement with the role of TOP2A in transcription. Some of the repressing GEC could contribute to cell killing effect of etoposide, especially repressions in genes essential for survival.

5.4 Etoposide evokes specific GEC in other cancer entities

To validate the findings from HTETOP cell line in other cancer entities, I obtained etoposide-evoked GEC from GEO and CMap. There were 14 cell lines representing 8 cancer types (**Table 5.4.1**). Out of these 14 cell lines, 6 cell lines exhibited predominance of etoposide-evoked repressing GEC, which could contribute in cell killing. However, all these cell lines had been treated with different etoposide concentrations for different timepoints.

Table 5.4.1: **Effect of etoposide on gene expression in various cancer cell lines**. Overview of etoposide-evoked gene expression changes (GEC) in the cell lines representing different cancer entities obtained from GEO and connectivity Map (CMap).

Cancer type	Cell line	Source	Accession number	Etoposide concentration (µM)	Treatment time (hours)	Numbers of induced genes (%)	Numbers of repressed genes (%)
AML	HL-60	Connectivity Map	-	7	6	185 (59%)	127 (41%)
B cell lymphoma	OCI-Ly3	GEO	GSE60408	IC_{20}	24	56 (1%)	5478 (99%)
	OCI-Ly7	GEO	GSE60409	IC_{20}	24	351 (64%)	198 (36%)
	U-2932	GEO	GSE60410	IC_{20}	24	280 (49%)	291 (51%)
Breast cancer	HME-CC	GEO	GSE1647	10	12	439 (54%)	380 (46%)
	MCF-7	GEO	GSE1648	40	12	56 (43%)	74 (57%)
	ME-16-C	GEO	GSE1649	20	12	101 (49%)	107 (51%)
	ZR-75-1	GEO	GSE1650	30	12	308 (31%)	681 (69%)
Burkitt's lymphoma	Ramos	GEO	GSE23169	20	6	624 (34%)	1218 (66%)
Colorectal cancer	HCT-116	GEO	GSE71980	20	-	3016 (51%)	2844 (49%)
	SW-620	GEO	GSE33624	60	2	897 (58%)	661 (42%)
Fibrosarcoma	HT-1080	GEO	GSE59368	3	24	245 (47%)	281 (53%)
Histiocytic lymphoma	U-937	GEO	GSE66660	0.4	48	359 (76%)	115 (24%)
Melanoma	MelJuSo	GEO	GSE33624	60	2	516 (78%)	144 (22%)
Prostate cancer	PC-3	Connectivity Map	-	7	6	14 (56%)	11 (44%)

After comparing the etoposide-evoked GEC from all cancer cell lines obtained from GEO, CMap, and from my experiment in HTETOP, I identified overlapping GEC among these cell lines. *BTG2* (NGF-inducible anti-proliferative protein PC3) was induced in 8, while *PLK1* (polo-like kinase 1) was repressed in 10 cancer cell lines after etoposide treatment (

Table 5.4.2A and **B**).

Table 5.4.2: **Overview of the etoposide-evoked gene expression changes (GEC) overlapping in 5 or more cancer cell lines**. (A) Etoposide-evoked inducing GEC (B) Etoposide-evoked repressing GEC (top 22 shown).

A

Etoposide-induced genes	Number of cell lines
BTG2	8
ATF3	7
CDKN1A	7
CD86	6
GDXR	6
GDF15	6
IFI6	6
RETSAT	6
SESN1	6
SLAMF7	6
TP53I3	6
ACTA2	5
ANKRA2	5
CEACAM1	5
CYFIP2	5
FAS	5
FUCA1	5
GAA	5
GADD45A	5
JUN	5
SFN	5
TP53INP1	5

B

Etoposide-repressed genes	Number of cell lines
PLK1	10
CDC20	9
CENPE	9
PSRC1	8
ASPM	7
BUB1	7
CCNB1	7
CENPF	7
DLGAP5	7
HMMR	7
MKI67	7
STAG1	7
SYNCRIP	7
TOP2A	7
AURKA	6
BIRC5	6
BUB1B	6
CCNB2	6
CCNF	6
DIAPH3	6
DPYD	6
KIF4A	6

5.5 Prediction and validation of mediators of etoposide cytotoxicity in HTETOP cell line

I restricted the prediction to the etoposide-evoked genes repressions because of their predominance in HTETOP cell line. To define essential gene repressions, I first selected the genes with high basal GEL and subsequent repression after etoposide treatment (289 genes). These genes were then restricted to 53 genes based on pathways involved in cancer and cell proliferation, using IPA. Then, the GEC from other cancer cell lines was used to select genes which are repressed in multiple cancer cell lines. Finally, gene expression for selected genes were compared in normal and cancer tissues to select essential gene repressions. **Fig. 5.5.1** represents an example of *DLGAP5* expression across normal and cancer tissues. *DLGAP5* and other selected genes had higher average expression in cancer tissues compared to normal tissues.

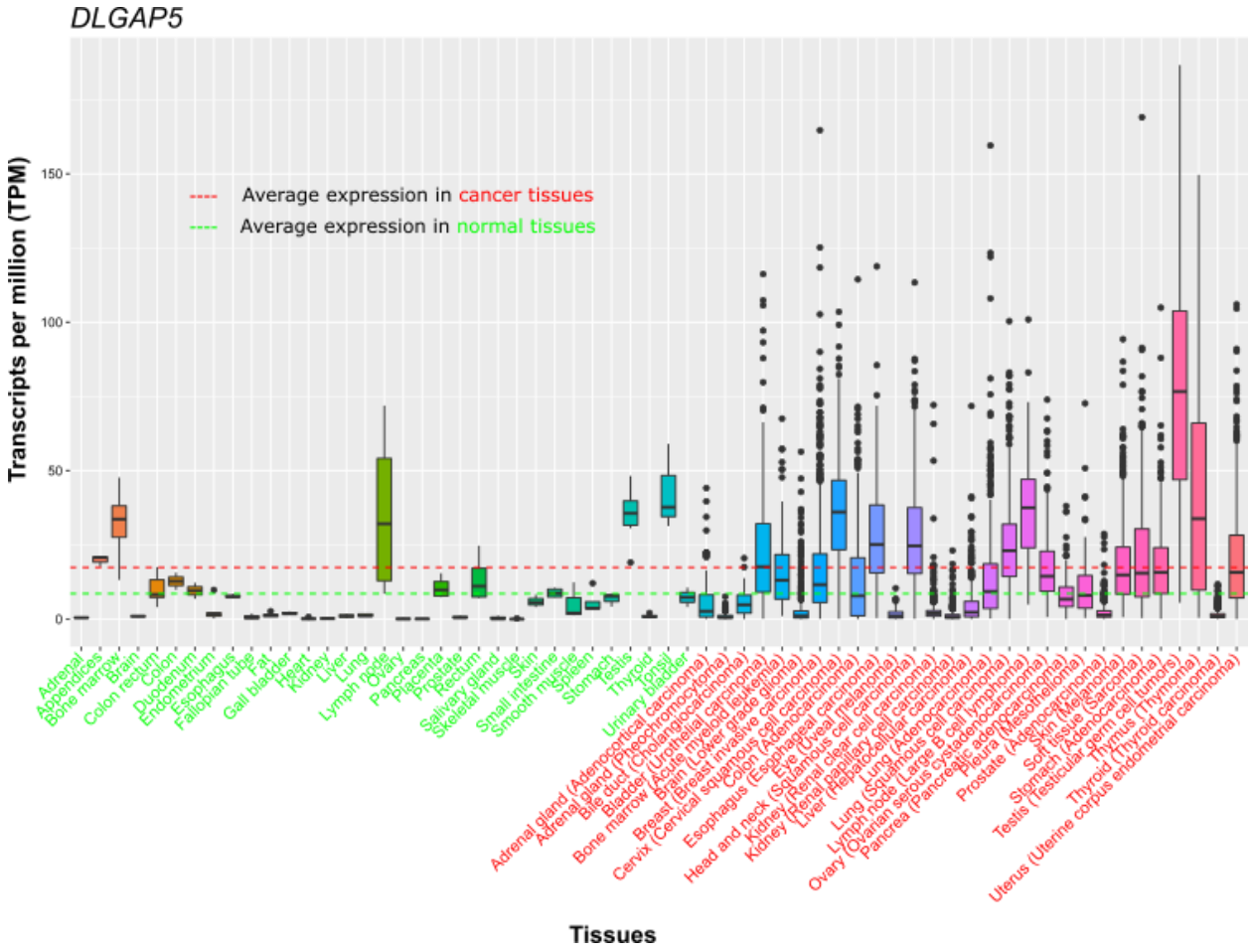

Fig. 5.5.1: **Expression of etoposide-mediator in cancer tissues**. Boxplot representing average DLGAP5 expression across 33 normal tissues obtained from GTEx and 29 cancer tissues obtained from TCGA.

IPA and CLUE resources provided the putative upstream regulators modulating etoposide-evoked GEC in HTETOP cell line. Altogether, I selected 14 predicted essential repressing GEC and 6 putative upstream regulators from IPA and CLUE (**Table 5.5.1**). All the identified targets were knocked down using siRNA-mediated transfection. The siRNA sequences are listed in **Appendix table 1**. The knockdown was confirmed by SYBR green qPCR using target specific primers.

Table 5.5.1: **Selected mediators among etoposide-evoked gene expression changes (GEC) and putative upstream regulators in HTETOP cell line**. Log2FC represents fold change from RNA-Seq experiments after the etoposide treatment. Comparison with other cancer cell lines is based obtained from gene expression omnibus (GEO) and connectivity map (CMap).

Gene symbol	Log2FC (HTETOP)	Number of cancer cell lines gene repressed in	Cancer cell lines gene repressed in
Etoposide-repressed genes with high expression in HTETOP			
CDC20	-1.6	9	HCT-116, HL-60, HT-1080, HTETOP, MCF-7, OCI-Ly3, Ramos, U-2932, ZR-75-1
CDK6	-1.7	3	HME-CC, HTETOP, OCI-Ly3
CENPF	-1.6	7	HCT-116, HL-60, HT-1080, HTETOP, MCF-7, OCI-Ly3, ZR-75-1
DLGAP5	-1.2	7	HCT116, HL-60, HT-1080, HTETOP, MCF-7, OCI-Ly-3, ZR-75-1
FOSL1	-1.2	2	HTETOP, Ramos
HMGA2	-1.6	1	HTETOP
IGF2BP 1	-1.1	2	HTETOP, OCI-Ly3
KIF20A	-1.2	5	HCT-116, HL-60, HTETOP, MCF-7, OCI-Ly3
MCM6	-1.2	6	HCT-116, HT-1080, HTETOP, MelJuSo, OCI-Ly3, ZR-75-1
NCAPD2	-1.4	4	HCT-116, HTETOP, OCI-Ly3, ZR-75-1
PFKP	-1.2	2	HTETOP, OCI-Ly3
PLAU	-1.4	2	HME-CC, HTETOP
SLC7A5	-1.3	3	HME-CC, HTETOP, OCI-Ly3
TPX2	-1.1	6	HCT-116, HT-1080, HTETOP, MCF-7, OCI-Ly3, ZR-75-1
Upstream regulators (Ingenuity)			
ANLN	-1.3	5	HCT-116, HT-1080, HTETOP, OCI-Ly3, ZR-75-1
FOXM1	-1.4	3	HCT-116, HT-1080, HTETOP
Gene knockdowns evoking etoposide-like GEC (emulators)			
MED1	-	1	ZR-75-1
RPA2	-	1	HCT-116
TOPBP1	-	1	HCT-116
YWHAH	-	2	ZR-75-1

To achieve optimal gene knockdown, I optimized the cell seeding density and siRNA concentration. I selected the density of 5000 cells in as 96-well plate and 10nM siRNA concentration, as these parameters show minimum effect of scrambled sequence transfection on cell viability (**Fig. 5.5.2**).

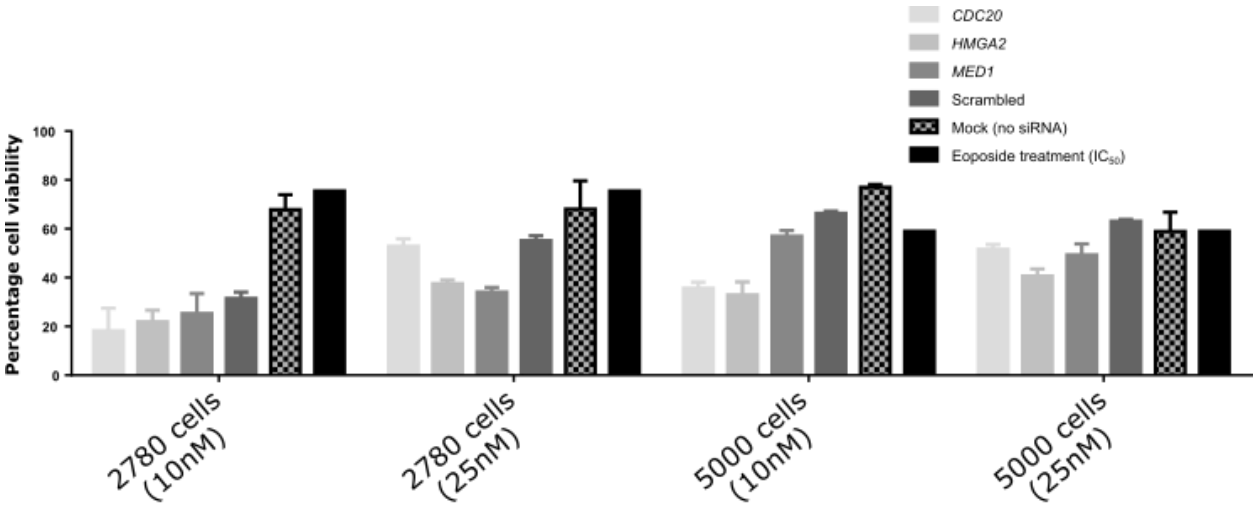

Fig. 5.5.2: **Optimization of cell numbers and siRNA concentration for knockdown in HTETOP cell line.**

Next, I measured the percentage of viable cells after knocking down all the selected targets using siRNA. In addition, I also investigated the effects of knockdown on etoposide sensitization by etoposide treatment at IC_{50} concentration for 24 hours after the siRNA transfection for 24 hours. As shown in **Fig. 5.5.3**, the knockdown of the predicted essential GEC *PFKP* and *PLAU* and of the putative upstream regulator *ANLN* exerted cytotoxic response in HTETOP cell line. However, no target sensitized cells to etoposide treatment.

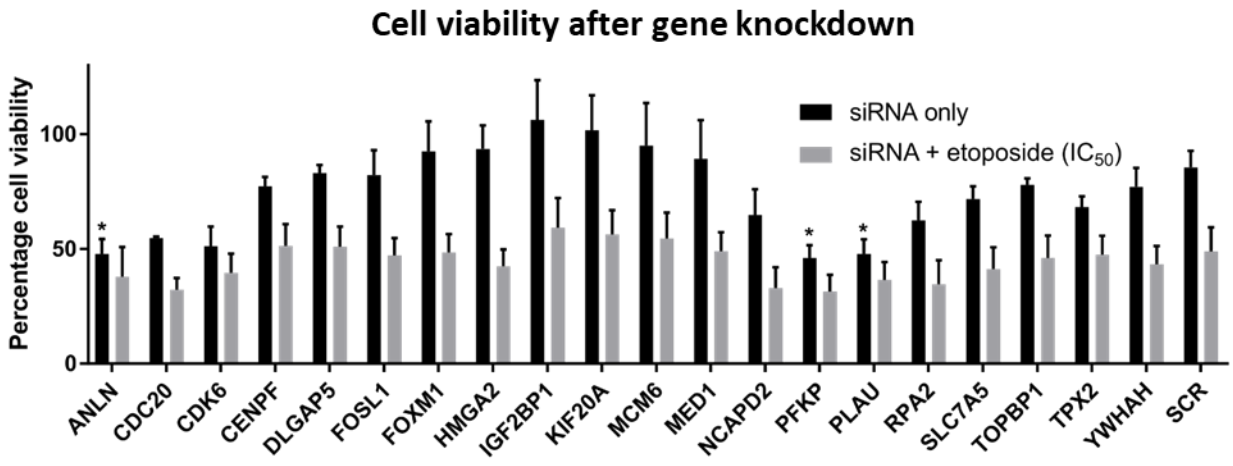

Fig. 5.5.3: **Effect of knockdown of the mediators of etoposide cytotoxicity on cell viability and etoposide sensitization using WST-8 cell viability assay.** Predicted mediators of etoposide cytotoxicity were knocked down using siRNA for 24 hours. Percentage cell viability compared to untransfected cells, taken as 100%, was calculated and Mann-Whitney statistical test was performed using GraphPad Prism software (v7) to identify significant gene knockdowns compared to scrambled (SCR) sequence. (*q value < 0.05).

5.6 Identifying transcriptional modulators and effectors of etoposide in AML: Pipeline overview

To identify drugs that could supplement or replace etoposide, I determined, analyzed, and functionally verified gene expression profiles prior and after etoposide treatment (**Fig. 5.6.1**). Since multiple AML cell lines were available in contrast to HTETOP, an approach different from the one described for HTETOP cell line was developed to facilitate identification of etoposide cytotoxicity drivers. Two parallel approaches were followed. First, I identified networks of co-expressing genes (step 1). Genes derived from co-expressing networks, whose co-regulation was unaffected by etoposide and whose expression correlated with etoposide IC_{50} were defined as potential modulators of etoposide cytotoxicity (step 2). Second, among the etoposide-evoked GEC (step 3), the essential genes were identified by applying PAch-derived survival essentiality filter (step 4). Putative etoposide emulators, i.e. gene modulations and drugs that cause GEC either similar or contrary to those evoked by etoposide, were identified using CMap (step 5). Putative

modulators, effectors and emulators thus identified were further scrutinized regarding biological function, relevance to a majority of AML cell lines, inhibitor availability, and subjected to functional validation.

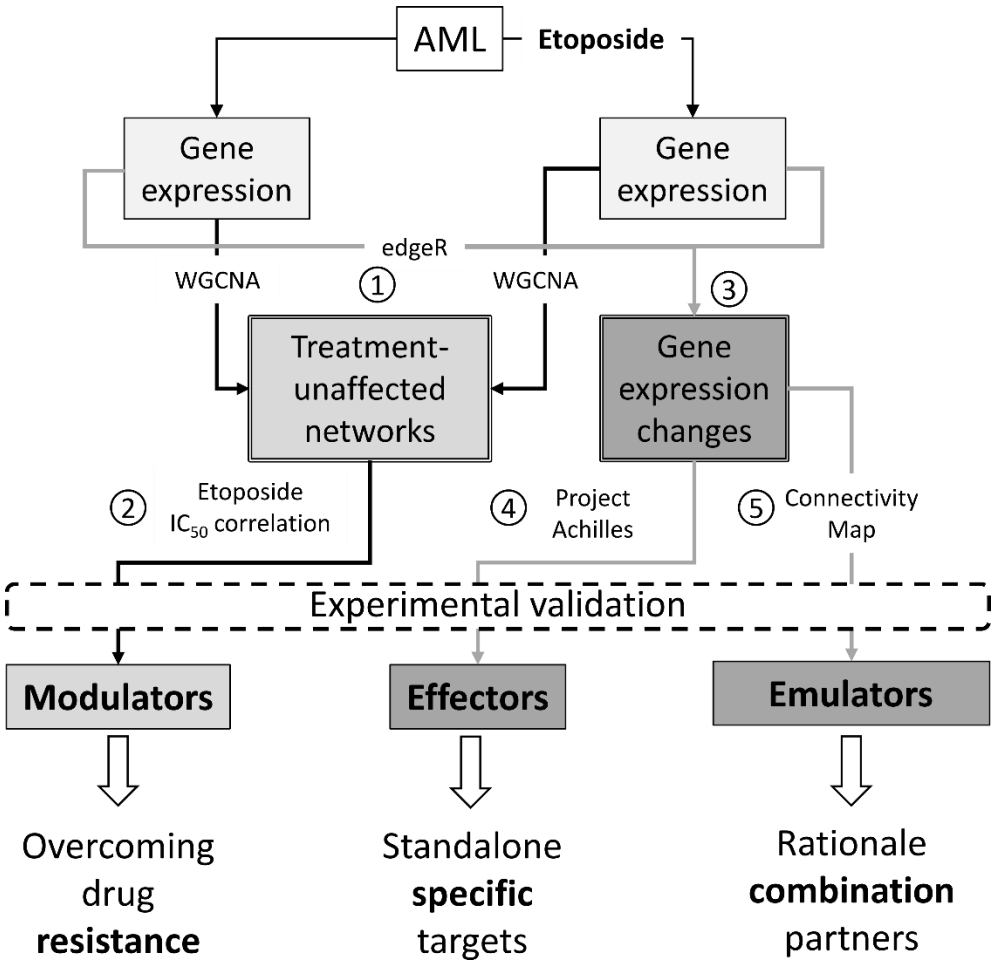

Fig. 5.6.1: **Pipeline to identify transcriptional drivers of etoposide in AML**. Step 1 and 2 represent quantification of genome-wide gene expression levels (GEL) prior and after etoposide treatment respectively, followed by co-expression network construction in step 3 and 4. Step 5 corresponds to comparison of co-expressing gene clusters before and after treatment to identify differentially co-expressed genes (DCG). Gene expression changes (GEC) from step 6 were utilized to identify GEC essential for survival (step 7) and etoposide-like or -contrary transcriptional drivers (step 8).

5.7 AML cell lines are differentially sensitive to etoposide treatment

Cell lines	RRID	AML classification	Growth medium	Fetal calf serum (heat inactivated)	Supplements	Growth condition
F-36P	CVCL_2037	AML M6	RPMI 1640	20%	10 ng/ml granulocyte-macrophhage colony stimulating factor	37° C, 5% CO2
HL-60	CVCL_0002	AML M3		10%	-	
KASUMI-1	CVCL_0589	AML M2		20%	-	
MOLM-13	CVCL_2119	AML M5		10%	-	
MONO-MAC-6	CVCL_1426	AML M5		10%	MEM Non-essential amino-acid solution, 100mM Na-pyruvate, 10µg/mL human insulin	
MV-4-11	CVCL_0064	AML M5		10%	-	
NB-4	CVCL_0005	AML M3		10%	-	
NOMO-1	CVCL_1609	AML M5		10%	-	
OCI-AML2	CVCL_1619	AML M4	alpha-MEM	20%	-	
OCI-AML3	CVCL_1844	AML M4		20%	-	
THP-1	CVCL_0006	AML M5	RPMI 1640	10%	-	

I investigated the response of 11 AML cell lines to 6 or 24 hours of etoposide treatment (0.02 – 50 µM) using WST-8 cell viability assay. Most of the cell lines did not respond sufficiently to 6-hour etoposide treatment (**Fig. 5.7.1**). Hence, the experiment was proceeded with 24 hours treatment, which revealed differential response by AML cell lines (**Fig. 5.7.2**). The IC_{50} concentrations varied from 0.3 µM, for the most sensitive cell line OCI-AML2, to 99 µM, for the most resistant cell line F-36P (

Table 5.7.1).

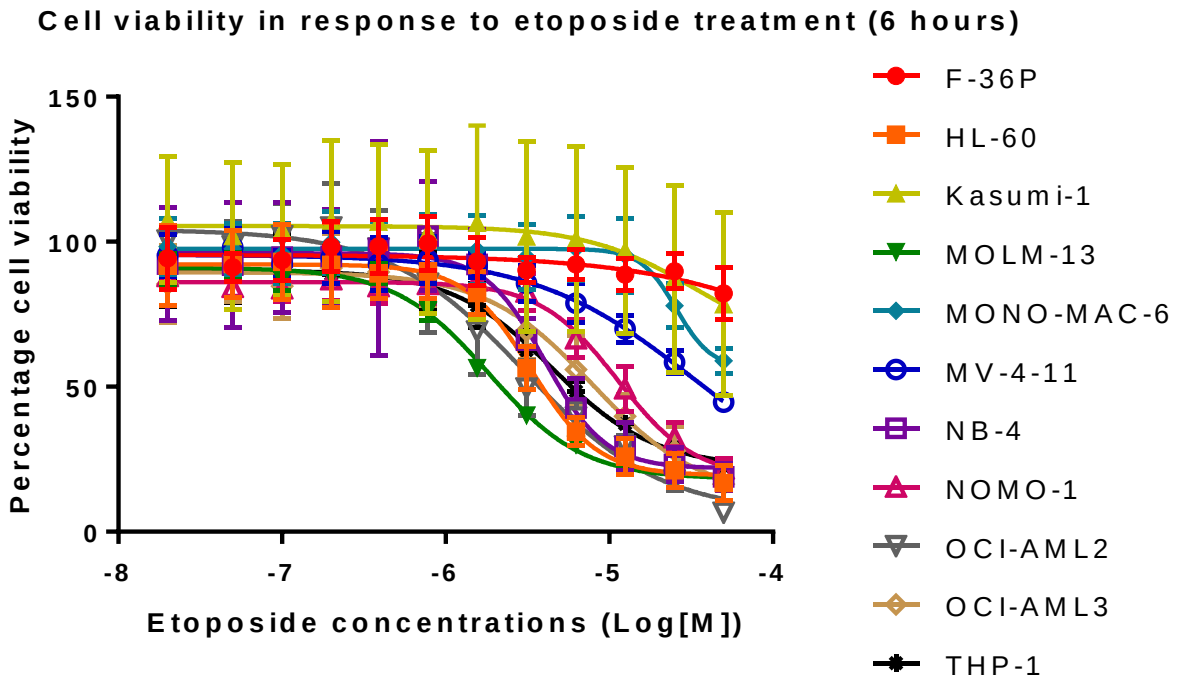

Fig. 5.7.1: **WST8-based concentration dependent effect of etoposide on survival of AML cell lines after 6 hours treatment.** Percentage cell viability compared to vehicle-treated cells, taken as 100%, was calculated. Dose response curve was generated by fitting the data by non-linear regression using GraphPad Prism software (v7). Values represent mean ± SD from 3 biological replicates.

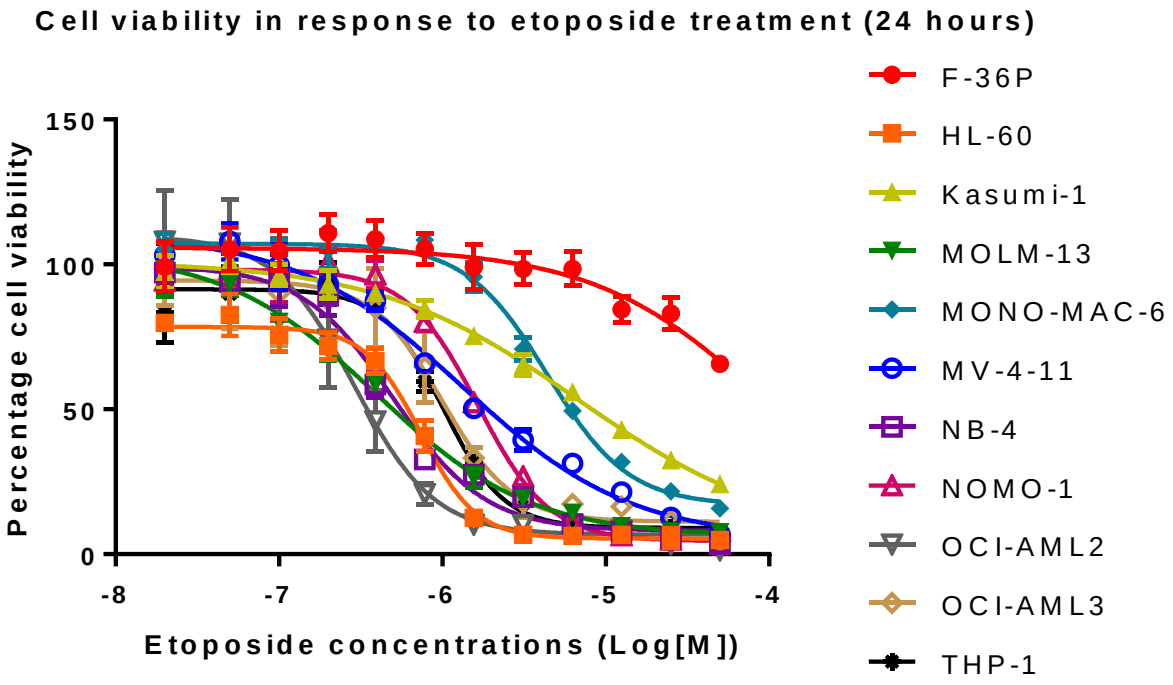

Fig. 5.7.2: **WST8-based concentration dependent effect of etoposide on survival of AML cell lines after 24 hours treatment.** Percentage cell viability compared to vehicle-treated cells, taken as 100%, was calculated. Dose response curve was generated by fitting the data by non-linear regression using GraphPad Prism software (v7). Values represent mean ± SD from 3 biological replicates.

Table 5.7.1: **Culture conditions and etoposide response by all investigated AML cell lines.** Etoposide IC_{50} and IC_{25} concentrations were derived using GraphPad Prism software (v7) by fitting the dose response curve by non-linear regression. RRID of the cell lines were obtained from the Resource Identification Portal.

Cell lines	RRID	AML classification	Growth medium	Fetal calf serum (heat inactivated)	Supplements	Growth condition	Etoposide IC_{50} (µM)	Etoposide IC_{25} (µM)
F-36P	CVCL_2037	AML M6	RPMI 1640	20%	10 ng/ml granulocyte-macrophhage colony stimulating factor	37° C, 5% CO_2	98.81	25.96
HL-60	CVCL_0002	AML M3		10%	-		0.74	0.48
KASUMI-1	CVCL_0589	AML M2		20%	-		6.80	1.43
MOLM-13	CVCL_2119	AML M5		10%	-		0.39	0.12
MONO-MAC-6	CVCL_1426	AML M5		10%	MEM Non-essential amino-acid solution, 100mM Na-pyruvate, 10µg/mL human insulin		4.39	2.34
MV-4-11	CVCL_0064	AML M5		10%	-		1.33	0.36
NB-4	CVCL_0005	AML M3		10%	-		0.50	0.25
NOMO-1	CVCL_1609	AML M5		10%	-		1.65	0.95
OCI-AML2	CVCL_1619	AML M4	alpha-MEM	20%	-		0.29	0.16
OCI-AML3	CVCL_1844	AML M4		20%	-		1.00	0.58
THP-1	CVCL_0006	AML M5	RPMI 1640	10%	-		1.01	0.63

These IC_{50} concentrations were derived from WST8-based cell viability assay, which measures the metabolic activity of cells. Cellular dehydrogenases reduce WST-8 to water soluble formazan, whose level corresponds to viability of cells. This approach might leave out the metabolically inactive, but live cells. Hence, WST-derived IC_{50} concentrations were validated for apoptosis using flow cytometric measurements of Annexin V-FITC stained AML cell lines treated with cell-specific IC_{50} concentrations of etoposide. I expected 50% apoptosis with etoposide treatment at cell-specific IC_{50} concentrations. I observed 19 – 51% apoptosis after etoposide treatment (**Fig. 5.7.3**).

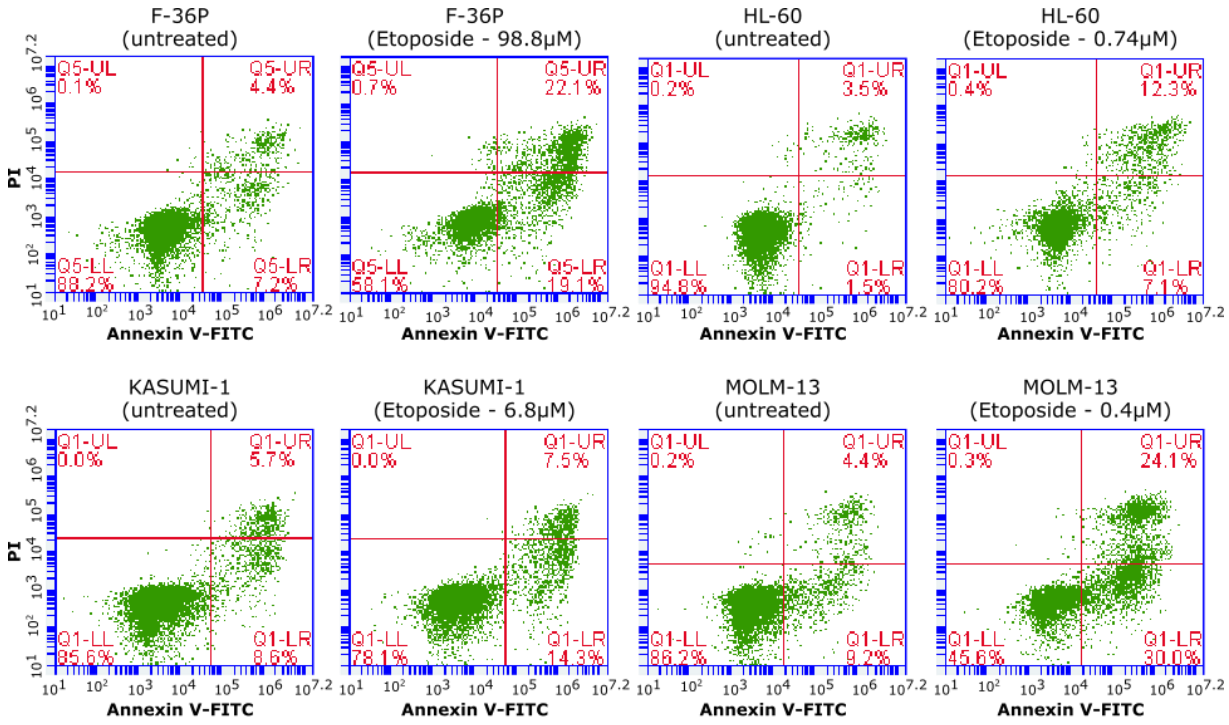

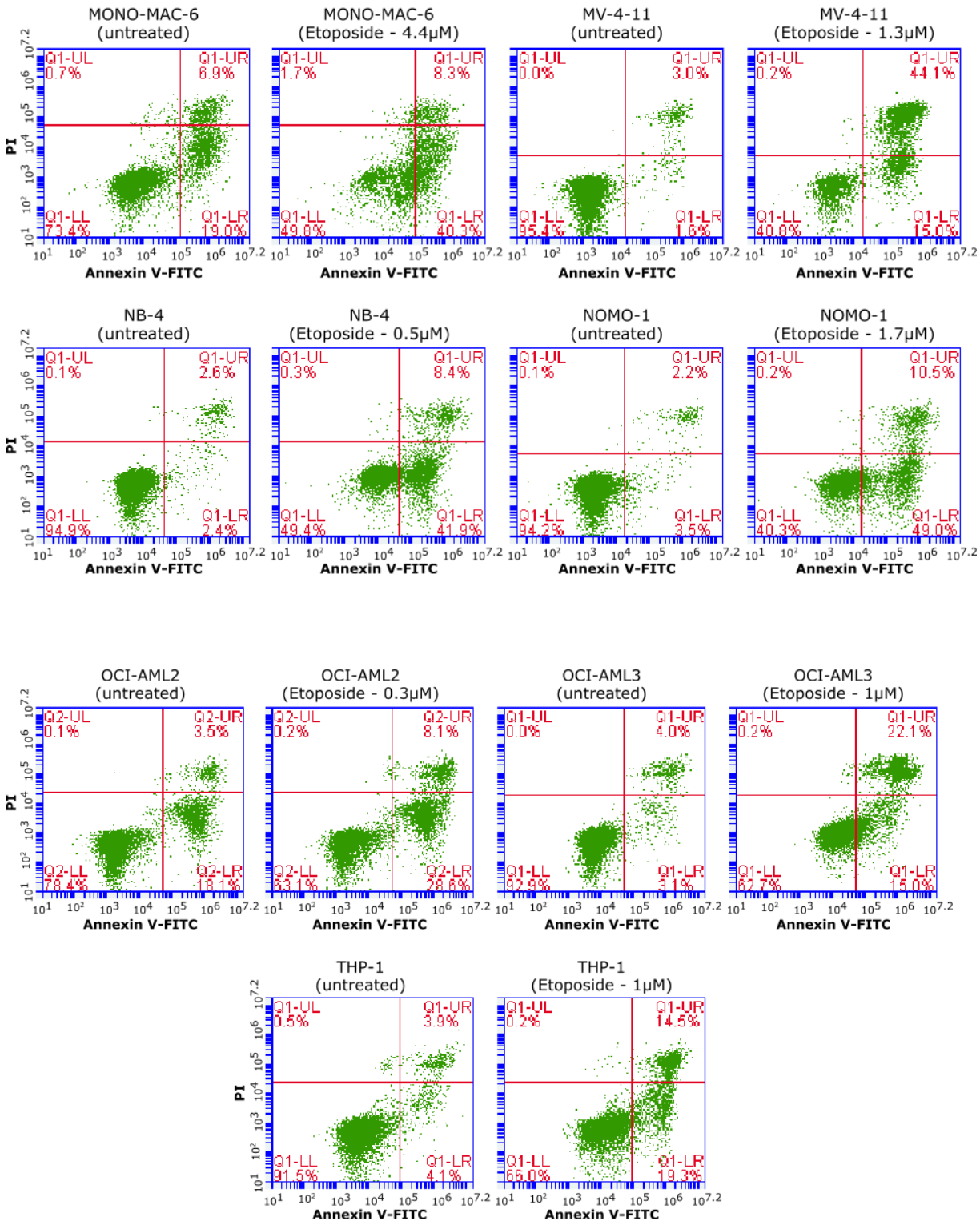

Fig. 5.7.3: **Percentage of apoptotic AML cells in response to etoposide treatment.** Different AML cell lines were treated with IC25 concentrations of etoposide for 24 hours, followed by Annexin-FITC and PI staining and detection by flow cytometry. Quadrant LL represents healthy cells, LR represents early apoptotic cells, and UR represents late apoptotic cells.

5.8 Modulators of etoposide synergize AML cell lines to drug

To identify modulators of etoposide whose expression correlate with etoposide response, all AML cell lines were treated with cell-specific IC_{50} concentrations of etoposide for 24 hours to obtain similar cytotoxicity levels. The RNA-Seq data from etoposide-treated OCI-AML2 cells was discarded, because it failed in the quality control of raw RNA sequences. Using WGCNA, I identified genes co-regulated in all 11 untreated AML cell lines, as well as in the remaining 10 etoposide-treated cell lines. I identified the genes co-regulated in untreated cell lines as well as in etoposide-treated AML cell lines. The co-regulated genes found only in untreated cells comprise cell proliferation, transcription, apoptosis, and others (**Table 5.8.1**). The genes co-regulated only in networks newly formed after etoposide treatment regulate, among others, transcription, response to DNA damage, and DNA repair (**Table 5.8.2**).

Table 5.8.1: **Pathways corresponding to co-expressing gene clusters in untreated AML cell lines.** WGCNA analysis was performed to identify gene clusters co-regulated in untreated AML cell lines. These clusters were annotated for biological processes using DAVID. Modules from last column (color names) represent identified clusters. Terms highlighted in bold type are etoposide-treatment related processes.

Term	Counts	PValue	Module names
GO:0006351~transcription, DNA-templated	19	0.01	darkolivegreen
GO:0000122~negative regulation of transcription from RNA polymerase II promoter	12	0.01	orange
GO:0000122~negative regulation of transcription from RNA polymerase II promoter	11	0.00	darkolivegreen
GO:0045892~negative regulation of transcription, DNA-templated	10	0.01	orange
GO:0051301~cell division	9	0.03	salmon
GO:0006915~apoptotic process	**8**	**0.02**	**darkolivegreen**
GO:0008380~RNA splicing	8	0.00	orange
GO:0000398~mRNA splicing, via spliceosome	8	0.00	orange
GO:0007067~mitotic nuclear division	8	0.02	salmon
GO:0016032~viral process	8	0.04	salmon
GO:0000086~G2/M transition of mitotic cell cycle	7	0.00	orange
GO:0043123~positive regulation of I-kappaB kinase/NF-kappaB signaling	7	0.01	salmon
GO:0015031~protein transport	7	0.02	steelblue
GO:0008285~negative regulation of cell proliferation	**6**	**0.04**	**darkolivegreen**
GO:0006406~mRNA export from nucleus	6	0.00	orange
GO:0051092~positive regulation of NF-kappaB transcription factor activity	6	0.01	salmon
GO:0007050~cell cycle arrest	6	0.02	salmon
GO:0050852~T cell receptor signaling pathway	6	0.02	salmon
GO:0098609~cell-cell adhesion	5	0.04	darkolivegreen
GO:0010629~negative regulation of gene expression	5	0.02	orange
GO:0006888~ER to Golgi vesicle-mediated transport	5	0.03	orange
GO:0090090~negative regulation of canonical Wnt signaling pathway	5	0.03	orange
GO:0006397~mRNA processing	5	0.04	orange
GO:0018105~peptidyl-serine phosphorylation	5	0.04	salmon
GO:0010629~negative regulation of gene expression	5	0.00	skyblue3
GO:0006890~retrograde vesicle-mediated transport, Golgi to ER	5	0.00	steelblue
GO:0031124~mRNA 3'-end processing	4	0.01	orange
GO:0006405~RNA export from nucleus	4	0.01	orange
GO:0032091~negative regulation of protein binding	4	0.01	orange
GO:0006369~termination of RNA polymerase II transcription	4	0.01	orange
GO:0016569~covalent chromatin modification	4	0.04	orange

GO:0070507~regulation of microtubule cytoskeleton organization	4	0.00	salmon
GO:0007249~I-kappaB kinase/NF-kappaB signaling	4	0.03	salmon
GO:0071456~cellular response to hypoxia	4	0.01	skyblue3
GO:0018105~peptidyl-serine phosphorylation	4	0.02	skyblue3
GO:0042787~protein ubiquitination involved in ubiquitin-dependent protein catabolic process	4	0.05	steelblue
GO:0048593~camera-type eye morphogenesis	3	0.00	darkolivegreen
GO:0007052~mitotic spindle organization	3	0.02	orange
GO:0000381~regulation of alternative mRNA splicing, via spliceosome	3	0.03	orange
GO:0010501~RNA secondary structure unwinding	3	0.04	orange
GO:0014067~negative regulation of phosphatidylinositol 3-kinase signaling	3	0.00	salmon
GO:0032006~regulation of TOR signaling	3	0.01	salmon
GO:0030214~hyaluronan catabolic process	3	0.01	salmon
GO:0021542~dentate gyrus development	3	0.01	salmon
GO:0070423~nucleotide-binding oligomerization domain containing signaling pathway	3	0.03	salmon
GO:2001238~positive regulation of extrinsic apoptotic signaling pathway	3	0.03	salmon
GO:0046627~negative regulation of insulin receptor signaling pathway	3	0.04	salmon
GO:0010803~regulation of tumor necrosis factor-mediated signaling pathway	3	0.04	salmon
GO:0032480~negative regulation of type I interferon production	3	0.04	salmon
GO:0070555~response to interleukin-1	3	0.05	salmon
GO:0051321~meiotic cell cycle	3	0.05	salmon
GO:0007018~microtubule-based movement	3	0.04	skyblue3
GO:0045931~positive regulation of mitotic cell cycle	3	0.01	steelblue
GO:0007595~lactation	3	0.02	steelblue
GO:0060337~type I interferon signaling pathway	3	0.05	steelblue
GO:0061484~hematopoietic stem cell homeostasis	2	0.02	Dark olivegreen
GO:0071929~alpha-tubulin acetylation	2	0.02	salmon
GO:0090140~regulation of mitochondrial fission	2	0.03	steelblue
GO:0019885~antigen processing and presentation of endogenous peptide antigen via MHC class I	2	0.04	steelblue
GO:0051988~regulation of attachment of spindle microtubules to kinetochore	2	0.04	steelblue

Table 5.8.2: **Pathways corresponding to co-expressing gene clusters in etoposide-treated AML cell lines.** WGCNA analysis was performed to identify gene clusters co-regulated in etoposide-treated AML cell lines. These clusters were annotated for biological processes using DAVID. Modules from last column (color names) represent identified clusters. Terms highlighted in bold type are etoposide-treatment related processes.

Term	Count	PValue	Modules
GO:0006351~transcription, DNA-templated	61	0.00	tan
GO:0006355~regulation of transcription, DNA-templated	52	0.00	tan
GO:0006351~transcription, DNA-templated	40	0.05	magenta
GO:0006355~regulation of transcription, DNA-templated	32	0.05	magenta
GO:0006351~transcription, DNA-templated	23	0.02	royalblue
GO:0000122~negative regulation of transcription from RNA polymerase II promoter	22	0.00	magenta
GO:0006364~rRNA processing	20	0.00	magenta
GO:0051301~cell division	19	0.00	tan
GO:0006260~DNA replication	17	0.00	tan
GO:0007067~mitotic nuclear division	17	0.00	tan
GO:0051301~cell division	14	0.00	magenta
GO:0006281~DNA repair	**13**	**0.00**	**tan**
GO:0006468~protein phosphorylation	12	0.00	Light yellow
GO:0007062~sister chromatid cohesion	11	0.00	tan
GO:0000398~mRNA splicing, via spliceosome	11	0.00	tan
GO:0042384~cilium assembly	9	0.00	magenta
GO:0060271~cilium morphogenesis	9	0.00	magenta
GO:0000722~telomere maintenance via recombination	9	0.00	tan
GO:0000082~G1/S transition of mitotic cell cycle	9	0.00	tan
GO:0006974~cellular response to DNA damage stimulus	**9**	**0.02**	**tan**
GO:0006281~DNA repair	**8**	**0.00**	**Royal blue**
GO:0006888~ER to Golgi vesicle-mediated transport	8	0.01	tan
GO:0098609~cell-cell adhesion	7	0.01	Dark red
GO:0010501~RNA secondary structure unwinding	7	0.00	magenta
GO:0070126~mitochondrial translational termination	7	0.00	magenta
GO:0016569~covalent chromatin modification	7	0.00	royalblue
GO:0008380~RNA splicing	7	0.00	royalblue
GO:0051301~cell division	7	0.04	royalblue
GO:0007059~chromosome segregation	7	0.00	tan
GO:0000724~double-strand break repair via homologous recombination	**7**	**0.00**	**tan**
GO:1901796~regulation of signal transduction by p53 class mediator	**7**	**0.01**	**tan**
GO:0000086~G2/M transition of mitotic cell cycle	7	0.02	tan
GO:0006888~ER to Golgi vesicle-mediated transport	6	0.00	darkred
GO:0070125~mitochondrial translational elongation	6	0.00	ivory
GO:0070126~mitochondrial translational termination	6	0.00	ivory
GO:0070125~mitochondrial translational elongation	6	0.01	magenta
GO:0090263~positive regulation of canonical Wnt signaling pathway	6	0.04	magenta

GO:0042787~protein ubiquitination involved in ubiquitin-dependent protein catabolic process	**6**	**0.00**	**royalblue**
GO:0007067~mitotic nuclear division	6	0.03	royalblue
GO:0006271~DNA strand elongation involved in DNA replication	**6**	**0.00**	**tan**
GO:0000731~DNA synthesis involved in DNA repair	**6**	**0.00**	**tan**
GO:0006302~double-strand break repair	**6**	**0.00**	**tan**
GO:0019886~antigen processing and presentation of exogenous peptide antigen via MHC class II	5	0.00	darkred
GO:0000209~protein polyubiquitination	5	0.04	darkred
GO:0001701~in utero embryonic development	5	0.04	darkred
GO:0006364~rRNA processing	5	0.00	ivory
GO:0006412~translation	5	0.01	ivory
GO:0038061~NIK/NF-kappaB signaling	5	0.02	magenta
GO:0051436~negative regulation of ubiquitin-protein ligase activity involved in mitotic cell cycle	5	0.02	magenta
GO:0051437~positive regulation of ubiquitin-protein ligase activity involved in regulation of mitotic cell cycle transition	5	0.03	magenta
GO:0031145~anaphase-promoting complex-dependent catabolic process	5	0.03	magenta
GO:0006368~transcription elongation from RNA polymerase II promoter	5	0.04	magenta
GO:0006364~rRNA processing	5	0.03	orange
GO:0007062~sister chromatid cohesion	5	0.01	royalblue
GO:0006511~ubiquitin-dependent protein catabolic process	5	0.04	royalblue
GO:0006270~DNA replication initiation	5	0.00	tan
GO:0042769~DNA damage response, detection of DNA damage	**5**	**0.00**	**tan**
GO:0019985~translesion synthesis	5	0.00	tan
GO:0034080~CENP-A containing nucleosome assembly	5	0.00	tan
GO:0043966~histone H3 acetylation	5	0.00	tan
GO:0030307~positive regulation of cell growth	5	0.04	tan
GO:0051436~negative regulation of ubiquitin-protein ligase activity involved in mitotic cell cycle	4	0.01	darkred
GO:0051437~positive regulation of ubiquitin-protein ligase activity involved in regulation of mitotic cell cycle transition	4	0.01	darkred
GO:0031145~anaphase-promoting complex-dependent catabolic process	4	0.02	darkred
GO:0030521~androgen receptor signaling pathway	4	0.00	lightyellow
GO:0006446~regulation of translational initiation	4	0.02	magenta
GO:0001541~ovarian follicle development	4	0.03	magenta
GO:0075733~intracellular transport of virus	4	0.04	magenta
GO:0006521~regulation of cellular amino acid metabolic process	4	0.04	magenta
GO:0030150~protein import into mitochondrial matrix	4	0.00	orange
GO:0032508~DNA duplex unwinding	4	0.00	royalblue

GO:0006310~DNA recombination	4	0.02	royalblue
GO:0006338~chromatin remodeling	4	0.02	royalblue
GO:0000083~regulation of transcription involved in G1/S transition of mitotic cell cycle	4	0.01	tan
GO:0000732~strand displacement	4	0.01	tan
GO:0006139~nucleobase-containing compound metabolic process	4	0.04	tan
GO:0009725~response to hormone	3	0.04	lightyellow
GO:0007566~embryo implantation	3	0.04	lightyellow
GO:0070936~protein K48-linked ubiquitination	3	0.05	lightyellow
GO:0001522~pseudouridine synthesis	3	0.02	magenta
GO:0030490~maturation of SSU-rRNA	3	0.02	magenta
GO:0000470~maturation of LSU-rRNA	3	0.02	magenta
GO:0042771~intrinsic apoptotic signaling pathway in response to DNA damage by p53 class mediator	**3**	**0.01**	**orange**
GO:0043124~negative regulation of I-kappaB kinase/NF-kappaB signaling	3	0.02	orange
GO:0031124~mRNA 3'-end processing	3	0.05	royalblue
GO:0046600~negative regulation of centriole replication	3	0.00	tan
GO:0006269~DNA replication, synthesis of RNA primer	3	0.00	tan
GO:0006884~cell volume homeostasis	3	0.01	tan
GO:0031571~mitotic G1 DNA damage checkpoint	**3**	**0.01**	**tan**
GO:0071732~cellular response to nitric oxide	3	0.02	tan
GO:0007099~centriole replication	3	0.02	tan
GO:0042276~error-prone translesion synthesis	3	0.03	tan
GO:0007091~metaphase/anaphase transition of mitotic cell cycle	2	0.03	darkred
GO:0031325~positive regulation of cellular metabolic process	2	0.03	darkred
GO:0032042~mitochondrial DNA metabolic process	2	0.03	lightyellow
GO:0009299~mRNA transcription	2	0.04	lightyellow
GO:0000472~endonucleolytic cleavage to generate mature 5'-end of SSU-rRNA from (SSU-rRNA, 5.8S rRNA, LSU-rRNA)	2	0.04	magenta
GO:0042347~negative regulation of NF-kappaB import into nucleus	2	0.06	orange
GO:0032877~positive regulation of DNA endoreduplication	2	0.03	tan
GO:0043009~chordate embryonic development	2	0.05	tan

By comparing pre- and post-treatment networks, I identified and analyzed genes with co-regulation unaffected by the treatment (**Fig. 5.8.1A** and **B**). In the figure, color names highlighted in bold type on y-axis are the clusters uniquely present in either untreated or etoposide-treated AML cell lines. I further analyzed the gene clusters unaffected by the treatment. The 24 treatment-unaffected

clusters comprised 5711 genes. The genes with expression levels correlating with etoposide response were involved in processes such as apoptosis, proteasomal catabolism, response to DNA damage, and DNA repair. The 71 genes correlating positively ($p < 0.05$, Pearson's $r > |0.5|$, S1 Table 5) with etoposide IC_{50} concentrations were considered putative *assisting modulators*; the 909 negatively correlating ones as putative *impeding modulators*. Among them, I identified the previously reported modulators *SLFN11* (Zoppoli, Regairaz et al. 2012, Rees, Seashore-Ludlow et al. 2016) and *SMARCA4* (Lee, Celik et al. 2018) whose expression correlated with etoposide sensitivity.

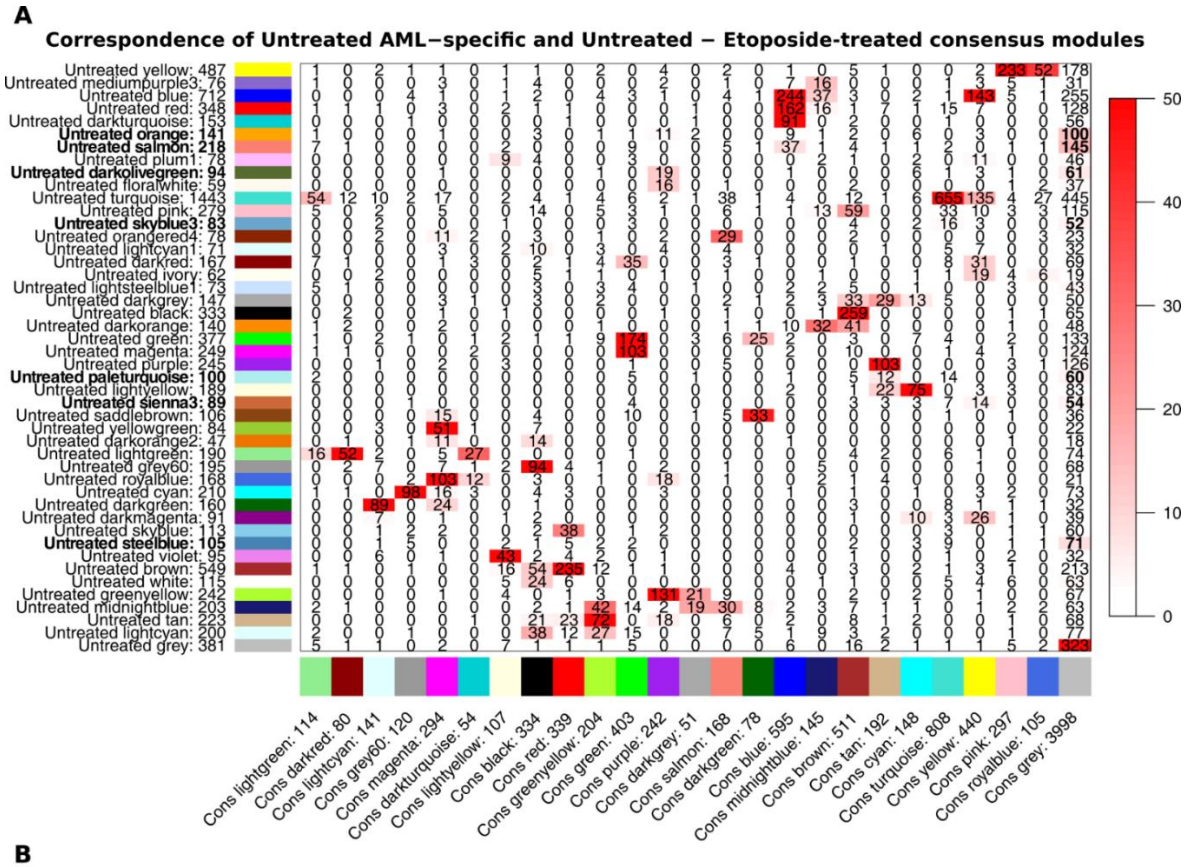
A
Correspondence of Untreated AML−specific and Untreated − Etoposide−treated consensus modules
Untreated yellow: 487
Untreated mediumpurple3: 76
Untreated blue: 712
Untreated red: 348
Untreated darkturquoise: 153
Untreated orange: 141
Untreated salmon: 218
Untreated plum1: 78
Untreated darkolivegreen: 94
Untreated floralwhite: 59
Untreated turquoise: 1443
Untreated pink: 279
Untreated skyblue3: 83
Untreated orangered4: 76
Untreated lightcyan1: 71
Untreated darkred: 167
Untreated ivory: 62
Untreated lightsteelblue1: 73
Untreated darkgrey: 147
Untreated black: 333
Untreated darkorange: 140
Untreated green: 377
Untreated magenta: 249
Untreated purple: 245
Untreated paleturquoise: 100
Untreated lightyellow: 189
Untreated sienna3: 89
Untreated saddlebrown: 106
Untreated yellowgreen: 84
Untreated darkorange2: 47
Untreated lightgreen: 190
Untreated grey60: 195
Untreated royalblue: 168
Untreated cyan: 210
Untreated darkgreen: 160
Untreated darkmagenta: 91
Untreated skyblue: 113
Untreated steelblue: 105
Untreated violet: 95
Untreated brown: 549
Untreated white: 115
Untreated greenyellow: 242
Untreated midnightblue: 203
Untreated tan: 223
Untreated lightcyan: 200
Untreated grey: 381
Cons lightgreen: 114
Cons darkred: 80
Cons lightcyan: 141
Cons grey60: 120
Cons magenta: 294
Cons darkturquoise: 54
Cons lightyellow: 107
Cons black: 334
Cons red: 339
Cons greenyellow: 204
Cons green: 403
Cons purple: 242
Cons darkgrey: 51
Cons salmon: 168
Cons darkgreen: 78
Cons blue: 595
Cons midnightblue: 145
Cons brown: 511
Cons tan: 192
Cons cyan: 148
Cons turquoise: 808
Cons yellow: 440
Cons pink: 297
Cons royalblue: 105
Cons grey: 3998
50
40
30
20
10
0
B
Correspondence of Etoposide−treated AML−specific and Untreated − Etoposide−treated consensus modules
Treated tan: 304
Treated lightsteelblue1: 76
Treated lightcyan1: 71
Treated salmon: 288
Treated darkorange2: 58
Treated skyblue: 104
Treated turquoise: 929
Treated black: 359
Treated darkred: 134
Treated white: 106
Treated saddlebrown: 98
Treated skyblue3: 85
Treated lightgreen: 167
Treated darkmagenta: 87
Treated darkgrey: 115
Treated magenta: 328
Treated purple: 318
Treated plum1: 79
Treated pink: 354
Treated bisque4: 49
Treated lightyellow: 150
Treated brown4: 57
Treated blue: 751
Treated red: 404
Treated royalblue: 141
Treated greenyellow: 317
Treated darkorange: 108
Treated darkolivegreen: 88
Treated orangered4: 79
Treated lightcyan: 183
Treated grey60: 171
Treated steelblue: 95
Treated yellow: 464
Treated floralwhite: 64
Treated darkgreen: 124
Treated midnightblue: 198
Treated yellowgreen: 85
Treated darkturquoise: 124
Treated green: 413
Treated violet: 90
Treated sienna3: 86
Treated brown: 538
Treated paleturquoise: 92
Treated orange: 113
Treated ivory: 67
Treated cyan: 256
Treated mediumpurple3: 77
Treated grey: 524
Cons lightgreen: 114
Cons darkred: 80
Cons lightcyan: 141
Cons grey60: 120
Cons magenta: 294
Cons darkturquoise: 54
Cons lightyellow: 107
Cons black: 334
Cons red: 339
Cons greenyellow: 204
Cons green: 403
Cons purple: 242
Cons darkgrey: 51
Cons salmon: 168
Cons darkgreen: 78
Cons blue: 595
Cons midnightblue: 145
Cons brown: 511
Cons tan: 192
Cons cyan: 148
Cons turquoise: 808
Cons yellow: 440
Cons pink: 297
Cons royalblue: 105
Cons grey: 3998
50
40
30
20
10
0

Fig. 5.8.1: **WGCNA consensus network analysis.** (A) Comparison of co-expression modules identified in untreated AML cell lines with consensus network (present in both untreated and etoposide-treated AML cell lines). (B) Comparison of co-expression modules identified in etoposide-treated AML cell lines with consensus network (present in both untreated and etoposide-treated AML cell lines). Color names on X- and Y-axis represent individual co-expressing modules and the number next to module represent total number of co-expressing genes identified in that particular module. Numbers in the heatmap represent number of genes common to consensus network on the X-axis, while the number of genes to extreme right (common to Cons grey module) are the co-expressing genes unique to untreated AML cells.

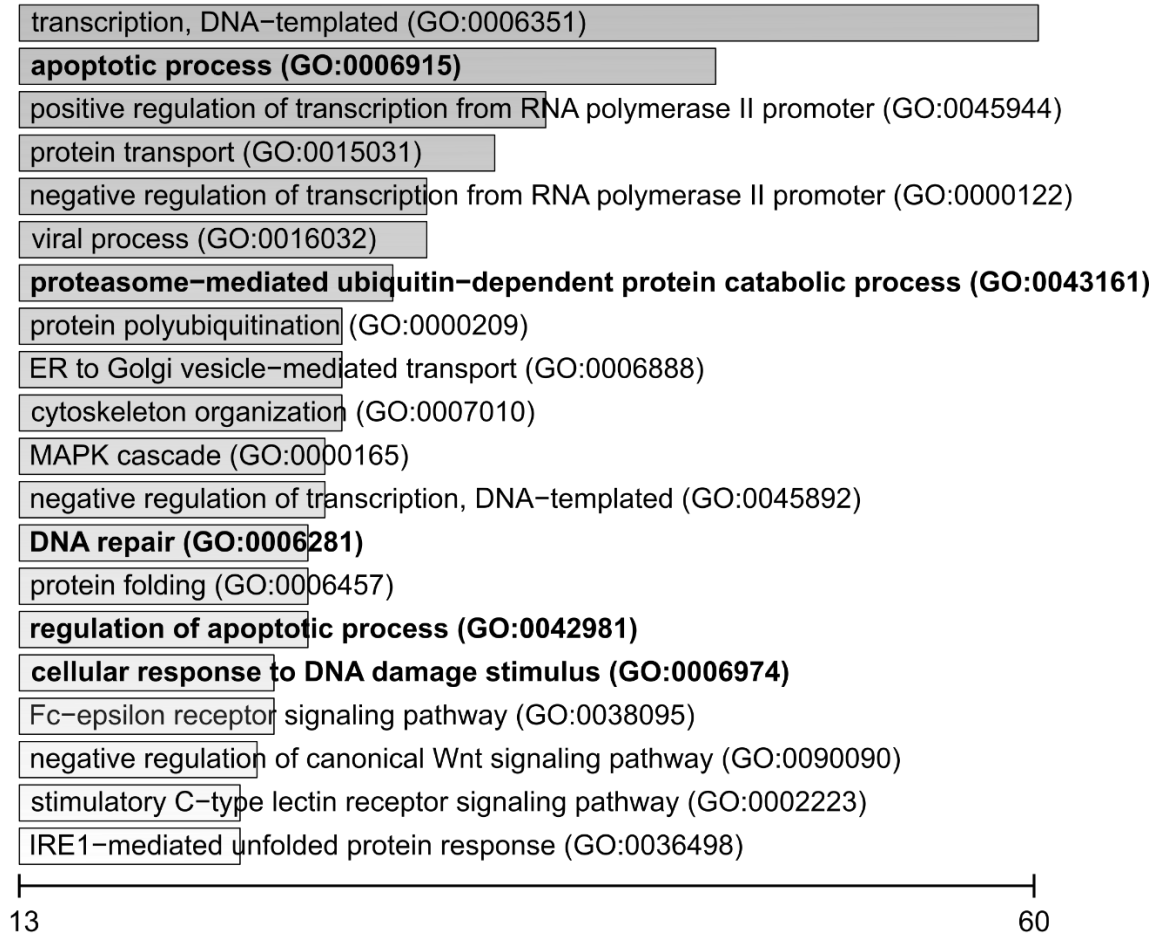

Fig. 5.8.2: Gene Ontology analysis for etoposide-modulators. Top 20 biological processes for the co-expressed genes from the consensus network negatively correlating with etoposide sensitivity. The scale represents number of genes enriched for individual biological processes. Processes previously linked to etoposide are shown in bold type.

The putative impeding modulators *BIRC5* and *PARP9* (correlation is shown in **Fig. 5.8.3**) were selected for experimental validation using chemical inhibitors against their protein products because of their involvement in apoptosis regulation and in double strand break repair, respectively. *NOTCH1* (**Fig. 5.8.3**) was selected for experimental validation to confirm its putative

etoposide-assisting activity. AML cell lines were treated for 24 hours with 3 concentrations (0.001 µM, 0.1 µM, and 10 µM) of chemical inhibitors alone, as well as in combination with cell line-specific IC_{25} concentrations of etoposide. The BIRC5 inhibitor GDC-0152 and the PARP inhibitor nicotinamide exhibited effects synergistic or additive to etoposide in 9 and 10 cell lines, respectively. The NOTCH1 inhibitor LY-3039478 antagonized with etoposide in 8 out of 11 AML cell lines (**Fig. 5.8.4**, **Table 5.8.3**, and **Appendix table 5**). Stand-alone cytotoxicity was observed in OCI-AML3 cells following BIRC5 inhibition and in two cell lines following NOTCH1 inhibition (**Table 5.8.3** and **Appendix table 4**). In summary, all putative modulators investigated were confirmed by chemical inhibitors.

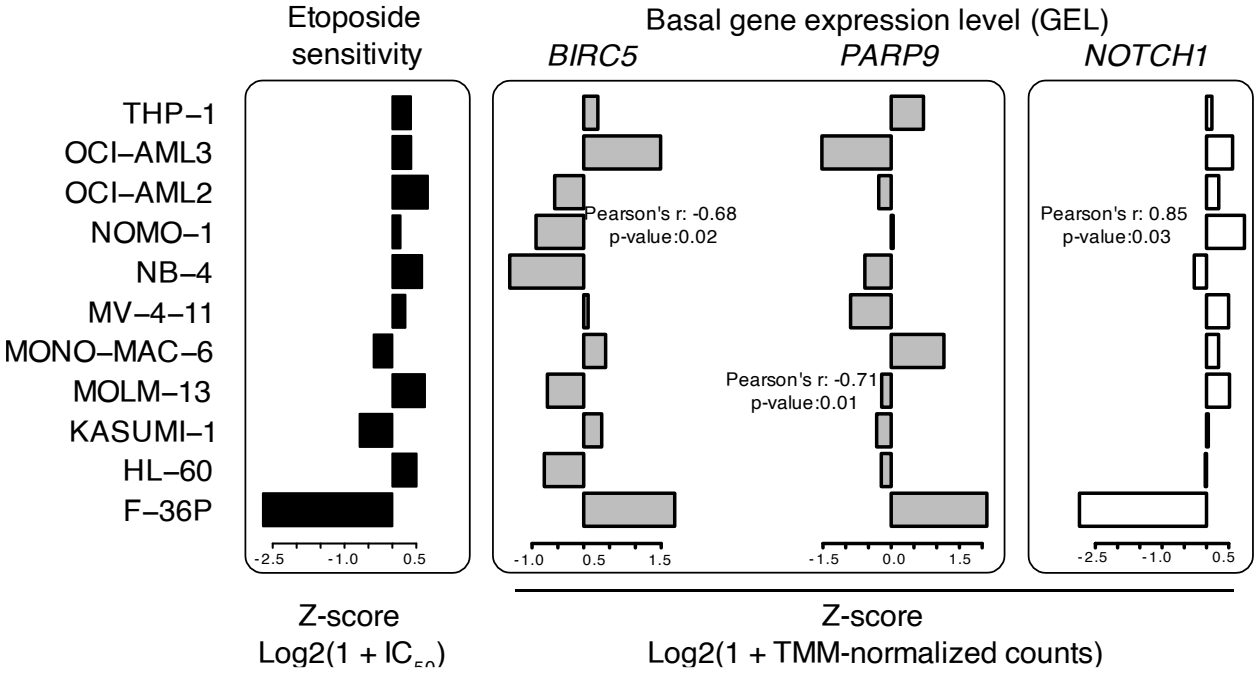

Fig. 5.8.3: Modulators gene expression correlation with etoposide sensitivity. Pearson correlations between the pre-treatment basal gene expression level of the impeding modulators *BIRC5* and *PARP9* and of the assisting modulator NOTCH1 with etoposide sensitivity across AML cell lines.

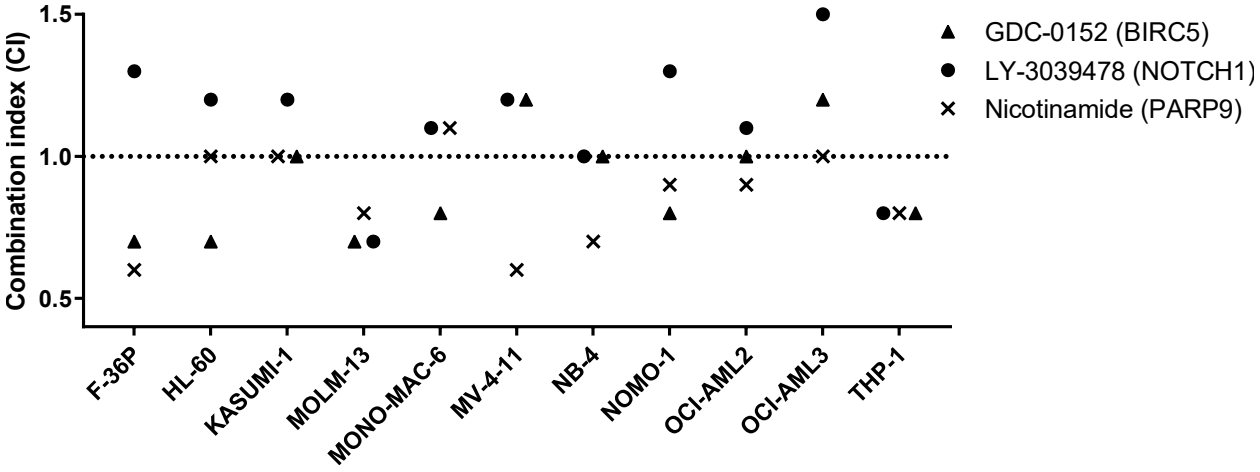

Fig. 5.8.4: **Synergy of modulators with etoposide in AML cells.** Combination index (CI; see Methods section 4.9 for details) for the cytotoxicity following treatment with IC_{25} concentrations of etoposide with inhibitors targeting the impeding modulators BIRC5 and PARP9 and the assisting modulator NOTCH1. CI < 1: synergism, CI = 1: additivity, and CI > 1: antagonism.

Driver type	Targets (inhibitors)	Stand-alone cytotoxicity (no. of cell lines)	Synergy/additivity with etoposide (no. of cell lines)
Modulators	NOTCH1 (LY-3039478)	2	2
	BIRC5 (GDC-0152)	1	**9**
	PARP9 (Nicotinamide)	0	**10**
Mediators	BCL2A1 (Sabutoclax)	**11**	1
	PRKCH (Sotrastaurin)	**7**	3
	PLK1 (Volasertib)	**11**	1
	IGF1R (GSK-1838705A)	**9**	2
Emulators	MYC (TWS-119)	**10**	2
	mTORi (Rapamycin)	**7**	**6**
	HDACi (Vorinostat)	**9**	**9**
	ROCK1 (Rockout)	3	**7**

Table 5.8.3: **Overview of the drivers of etoposide cytotoxicity in AML cells.** The drivers exhibiting stand-alone cytotoxicity in at least 6 AML cell lines are highlighted in light grey, drivers synergizing with etoposide in at least 6 AML cell lines in dark grey.

5.9 Etoposide-repressed essential genes contribute to cytotoxicity in AML lines

I next analyzed co-regulated genes correlating with the etoposide IC_{50} concentrations, but transcriptionally altered by etoposide treatment. The correlated genes *BRD4*, *MATL1*, and *MYC*

were involved in the clusters of genes co-regulated only in untreated AML cell lines; the correlated gene *SIRT1* was present in the co-expression network detected only after etoposide treatment. *BRD4* and *MYC* were transcriptionally repressed, while *MALT1* and *SIRT1* were transcriptionally induced by etoposide in the less responsive AML cell lines (supplementary Fig. 3). However, all of them, except *MYC*, were predicted to be essential in only 4 AML cell lines. Therefore, I next analyzed and functionally verified etoposide-driven GEC at the level of individual genes.

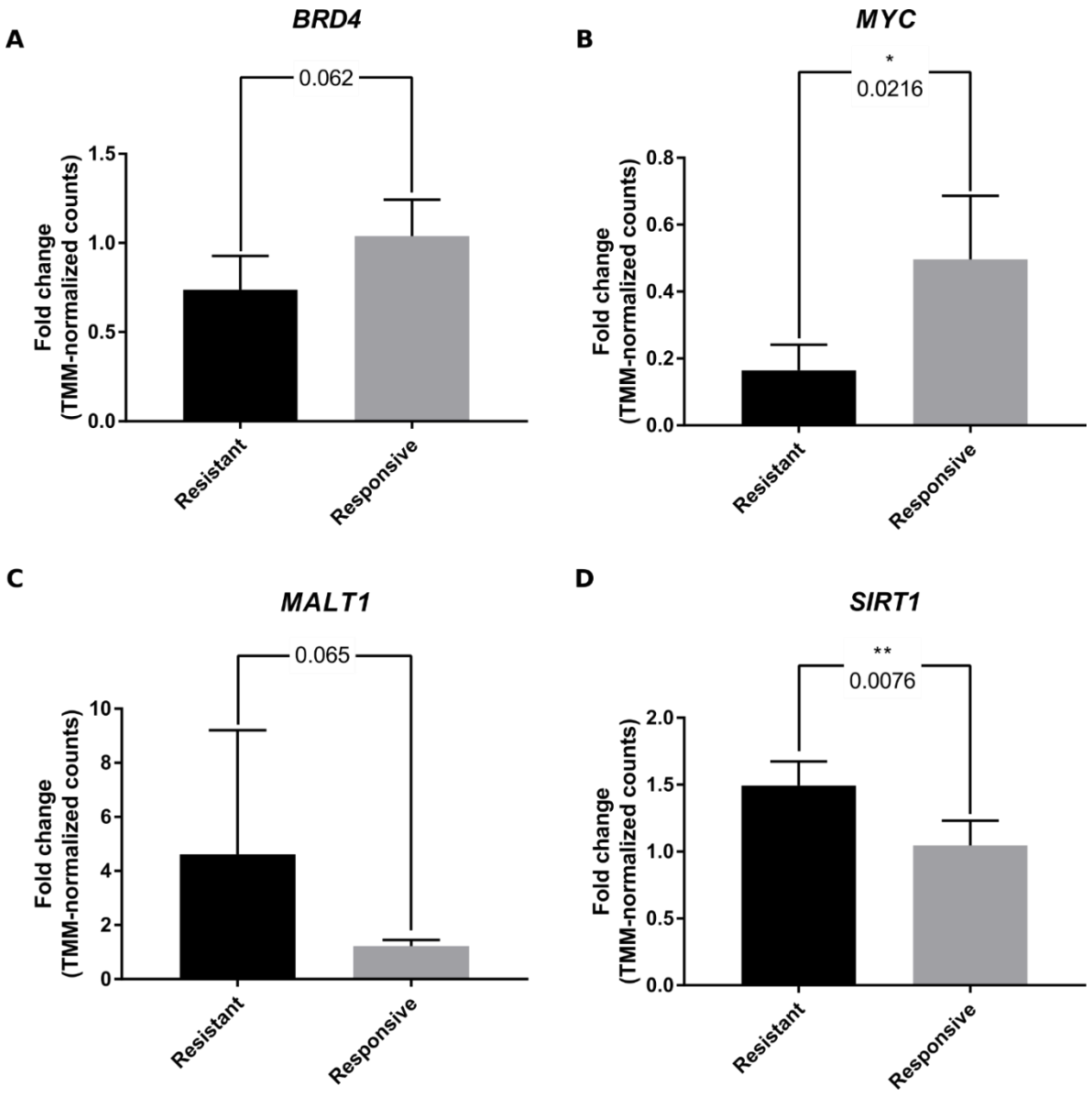

Fig. 5.9.1: Etoposide-evoked changes in the expression of co-regulating genes. Cell lines F-36P, KASUMI-1, and MONO-MAC-6 with highest etoposide IC_{50} concentrations were considered as resistant, while remaining AML cell lines were considered as etoposide-responsive. (A) and (B) targets BRD4 and MYC respectively repressed after etoposide treatment in resistant cell lines, (C) and (D) targets MALT1 and SIRT1 respectively induced after etoposide treatment in resistant cell lines. Fold change was calculated by comparing TMM-normalized counts after and before etoposide treatment for respective drivers. Mann-Whitney test was performed to identify significant fold change across two groups. (* and ** represents q value < 0.05 and 0.01 respectively).

The differential gene expression analysis using edgeR revealed that inductions accounted for the majority of etoposide treatment-driven changes in the gene expression (**Fig. 5.9.2** and **Table 5.9.1**).

On average, etoposide evoked 81% of gene inductions in AML cell lines after treatment with cell specific IC_{50} concentrations for 24 hours.

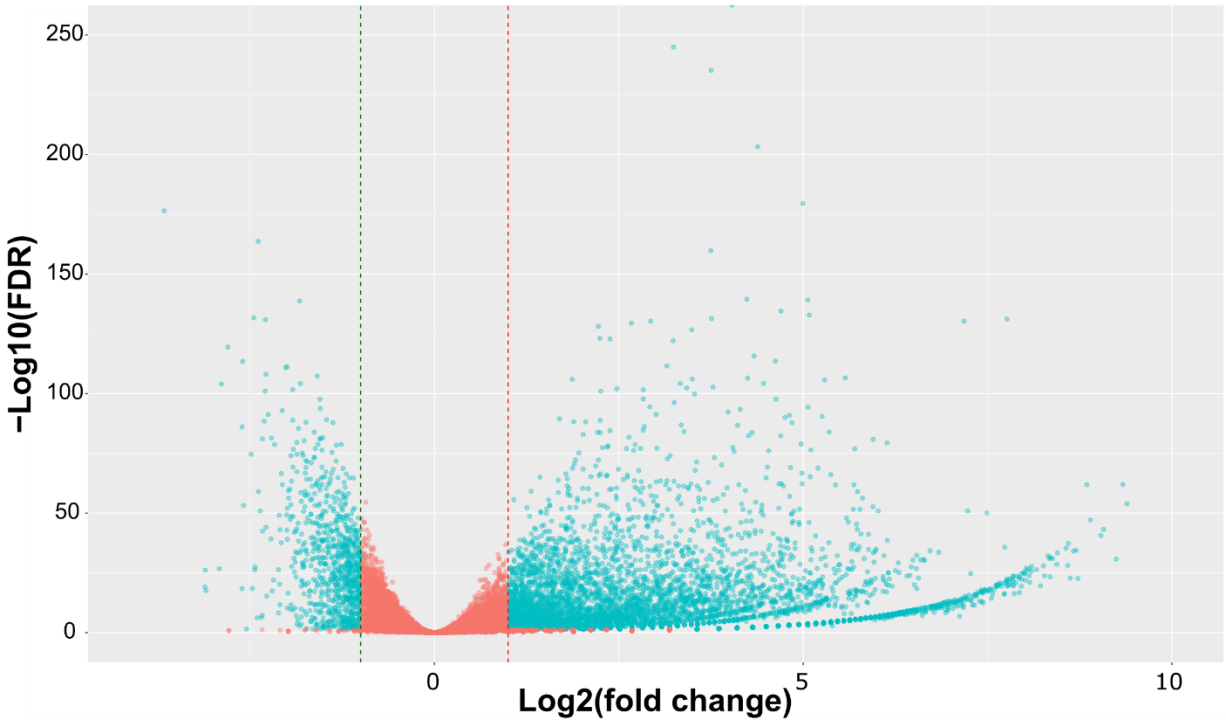

Fig. 5.9.2: Etoposide-evoked gene expression changes (GEC) in AML. Volcano plot representing (GEC) in F-36P cell line in response to etoposide treatment at IC_{50} concentration for 24 hours.

Table 5.9.1: **Numbers and percentages of etoposide-evoked inducing and repressing gene expression changes (GEC) in all investigated AML cell lines.** Differentially expressed genes were identify by comparing RNA-Seq gene counts from untreated and etoposide-treated AML cell lines using edgeR software.

Cell lines	Numbers of gene expression changes	Numbers of induced genes (%)	Numbers of repressed genes (%)
F36-P	4615	3882 (84.1)	733 (15.9)
HL-60	1007	875 (86.9)	132 (13.1)
KASUMI-1	3558	2874 (80.8)	684 (19.2)
MOLM-13	1643	1284 (78.2)	359 (21.9)
MONO-MAC-6	1788	1307 (73.1)	481 (26.9)
MV-4-11	2091	1883 (90.1)	208 (10.0)
NB-4	2383	1965 (82.5)	418 (17.5)
NOMO-1	1679	1177 (70.1)	502 (29.9)
OCI-AML3	1215	1028 (84.6)	187 (15.4)
THP-1	1278	1050 (82.2)	228 (17.8)

Essentiality analysis suggested that, on average, about 33% of etoposide-driven changes could have reduced AML cell survival (**Table 5.9.2**). An example of GEC grouped according to essentiality in F-36P cell line is shown in **Fig. 5.9.3**.

Table 5.9.2: Numbers and percentages of predicted essential genes using Project Achilles (PAch) among all etoposide-evoked gene expression changes (GEC).

Cell lines	Numbers of etoposide-evoked GEC	Number of predicted essential genes (%)	Etoposide-repressed predicted essential genes (%)	Etoposide-induced predicted essential genes (%)
F-36P	4615	1447 (31.3)	239 (16.5)	1208 (83.5)
HL-60	1007	348 (34.6)	45 (12.9)	303 (87.1)
KASUMI-1	3558	1234 (34.7)	227 (18.4)	1007 (81.6)
MOLM-13	1643	549 (33.4)	118 (21.5)	431 (78.5)
MONO-MAC-6	1788	602 (33.7)	144 (23.9)	458 (76.1)
MV-4-11	2091	702 (33.6)	63 (9)	639 (91)
NB-4	2383	762 (32)	128 (16.8)	634 (83.2)
NOMO-1	1679	580 (34.5)	156 (26.9)	424 (73.1)
OCI-AML3	1215	416 (34.2)	55 (13.2)	361 (86.8)
THP-1	1278	417 (32.6)	71 (17)	346 (83)

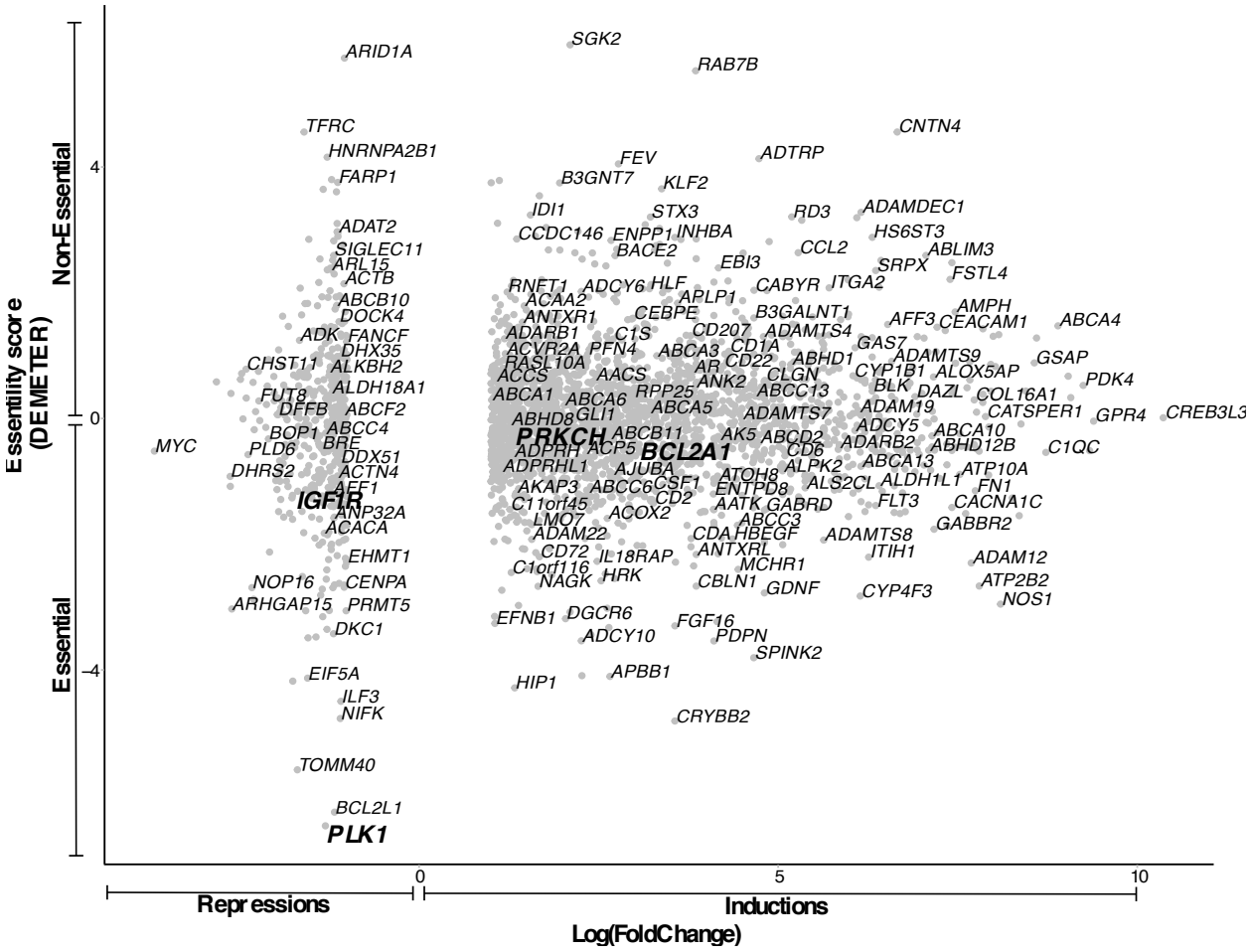

Fig. 5.9.3: **Scatterplot of etoposide-evoked differentially expressed genes in F-36P cell line, arranged according to essentiality for survival.** DEMETER score < 0 signifies essentiality. The genes essential for tumor cell survival and differentially expressed after etoposide treatment were considered as putative essential mediators. The mediators shortlisted for experimental validation (*BCL2A1*, *IGF1R*, *PLK1*, and *PRKCH*) are depicted in larger font. Other gene names are random examples taken from the entire gene set.

I selected *IGF1R* for experimental validation, since it was essential for 7 AML cell lines and repressed in 4 AML cell lines after etoposide treatment (**Fig. 5.9.4**). Likewise, *PLK1*, was essential as well as repressed in 4 AML cell lines (**Fig. 5.9.4**). I pursued *PLK1* because it exhibited highest essentiality for the least etoposide-sensitive F-36P cell line (**Fig. 5.9.3**). *BCL2A1* and *PRKCH* were selected because of their predicted essentiality for 6 AML cell lines each, and because they were induced by etoposide in 9 and 6 AML cell lines, respectively (**Fig. 5.9.4**).

I then treated all AML cell lines with the inhibitors of the protein products of these genes alone, as well as in combination with IC_{25} concentrations of etoposide. The inhibitors targeting the protein products of *BCL2A1* and *PLK1* exerted standalone cytotoxicity in all AML cell lines, while the IGF1R inhibitor and the PKC inhibitor exhibited cytotoxicity in 9 and 7 AML cell lines, respectively (**Fig. 5.9.4**, **Fig. 5.9.5**, and **Table 5.8.3**). Inhibition of BCL2A1 and PLK1 synergized with etoposide in MOLM-13 and NB-4 cell lines, respectively. Inhibition of PRKCH and IGF1R exhibited synergy with etoposide in 2 AML cell lines each (**Table 5.8.3** and **Appendix table 5**).

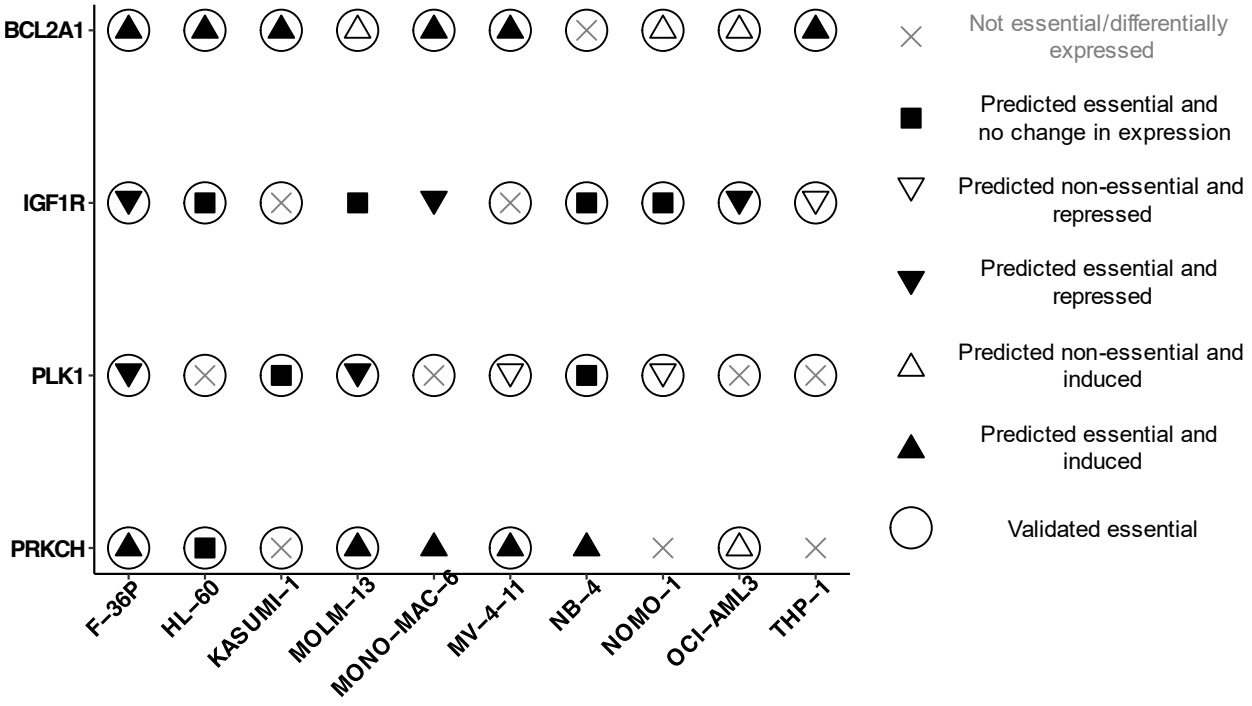

Fig. 5.9.4: **Experimental validation of putative essential mediators shortlisted in Fig. 5.9.3.** Cell viability was assessed by WST-8 assay after treatment with inhibitors targeting protein products of shortlisted drivers. Filled symbols represent predicted essentiality for survival in individual AML cell lines. Circles around the symbols represent experimentally confirmed cytotoxicity.

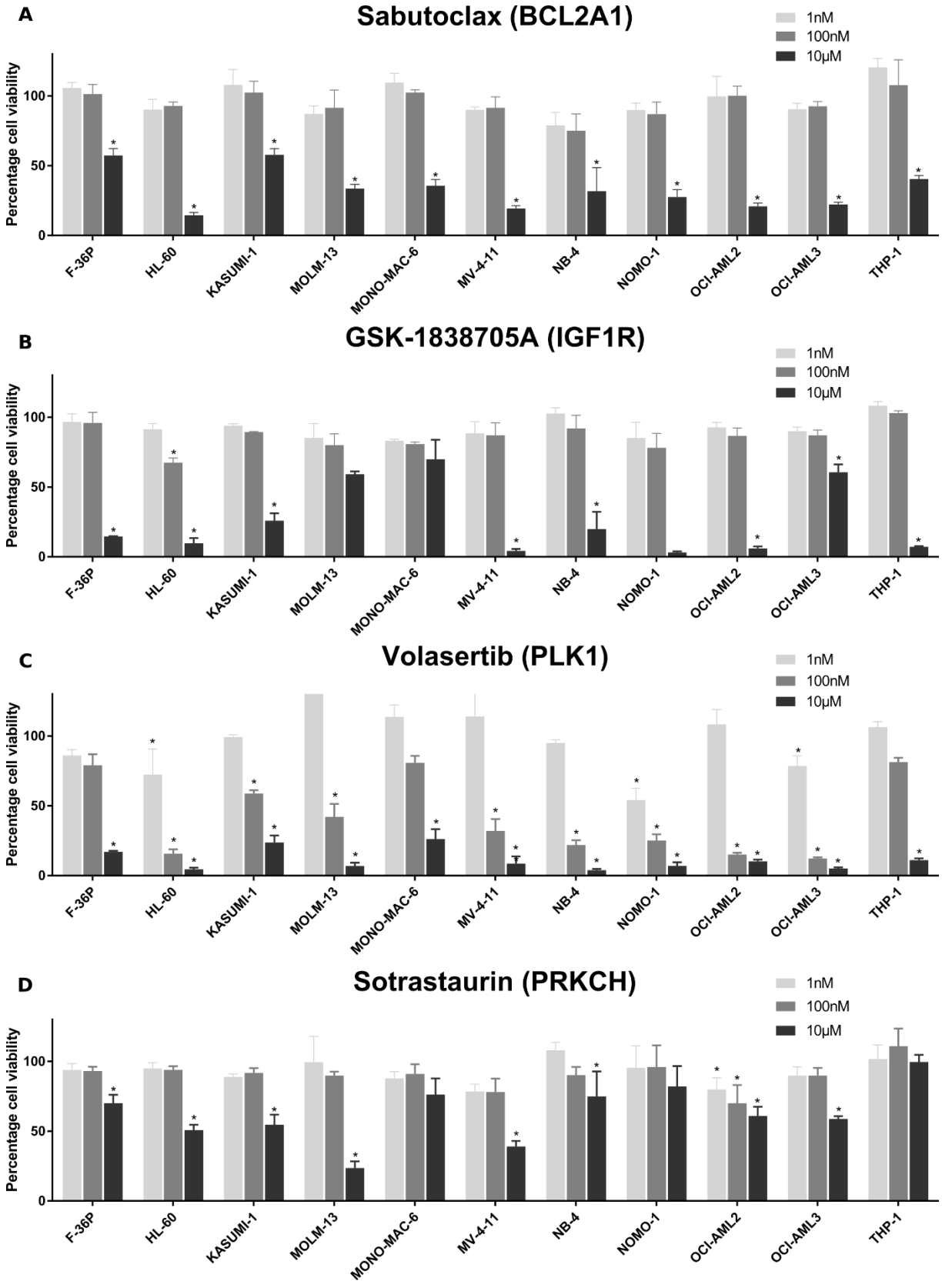
A
Sabutoclax (BCL2A1)
1nM
100nM
10μM
Percentage cell viability
0
50
100
F-36P
HL-60
KASUMI-1
MOLM-13
MONO-MAC-6
MV-4-11
NB-4
NOMO-1
OCI-AML2
OCI-AML3
THP-1
B
GSK-1838705A (IGF1R)
C
Volasertib (PLK1)
D
Sotrastaurin (PRKCH)

Fig. 5.9.5: **Contribution of mediators in AML cell killing using inhibitors.** Percentage cell viability in response to (A) sabutoclax (BCL2 inhibitor), (B) GSK-1838705A (IGF1R inhibitor), (C) volasertib (PLK1 inhibitor), and (D) sotrastaurin (PRKCH inhibitor) treatment respectively for 24 hours. Percentage cell viability compared to vehicle-treated control, taken as 100%, was calculated. Two-way ANOVA with Benjamini and Hochberg FDR test was performed to quantify significant difference. Data are represented as mean values ± SD and derived from 3 biological replicates. (* p-value < 0.05).

I additionally investigated, in HL-60 cells, the cytotoxic effects of the essential mediators BCL2A1 and IGF1R using shRNA-mediated knockdown. Knockdown of the mediator IGF1R was cytotoxic to HL-60 cells. (**Fig. 5.9.6**).

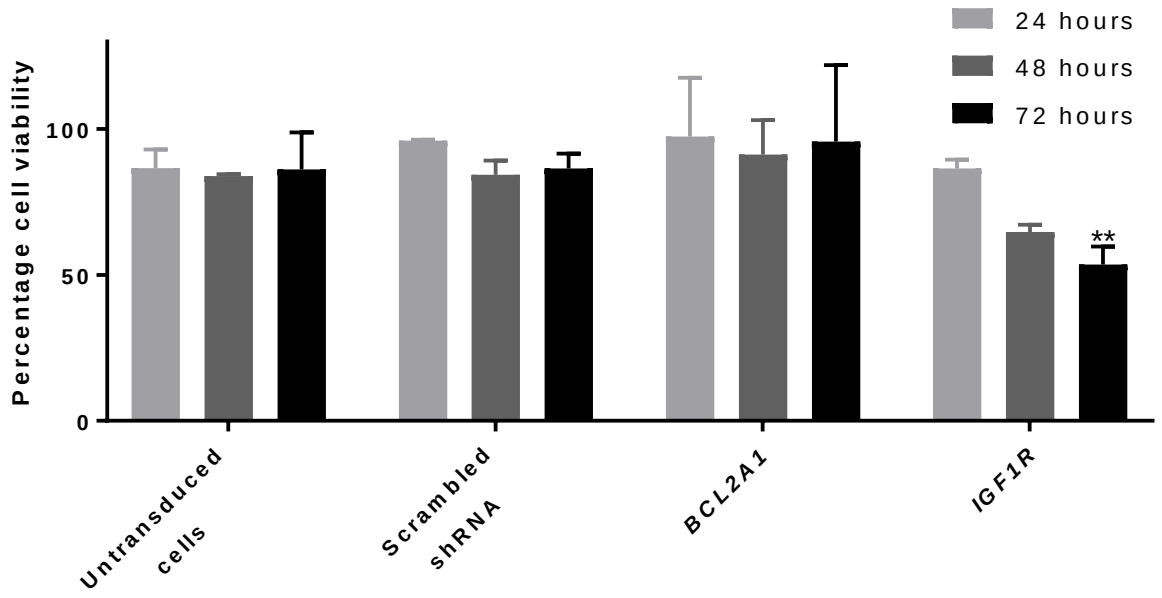

Fig. 5.9.6: **Contribution of mediators in AML cell killing using shRNA-mediated knockdown.** Viability of HL-60 cells after shRNA-mediated gene knockdown of essential mediators BCL2A1 and IGF1R for 24, 48, and 72 hours. Percentage cell viability compared to untransduced cells, taken as 100%, was calculated. Mann-Whitney test was performed to identify significant change in the viability. (** represents q value < 0.01). Data are represented as mean values ± SD and derived from 3 biological replicates.

5.10 Emulators are cytotoxic and synergize with etoposide

Using the CMap resource, I identified gene modulations and drugs that cause GEC either similar or contrary to those evoked by etoposide. There were 32 gene knockdowns and 76 drugs whose application led to etoposide-like GEC. They were referred to as putative etoposide-*like* emulators. The majority of the drugs belonged to the classes mTOR inhibition, topoisomerase inhibition, and

HDAC inhibition. I also identified 12 drugs evoking opposite GEC, which are referred to as putative etoposide-*contrary* emulators (**Table 5.10.1** and **Table 5.10.2**).

Table 5.10.1: **Emulators (gene knockdowns) evoking gene expression changes (GEC) either similar (etoposide-like) or opposite (etoposide-contrary) to those evoked by etoposide.** Emulators were identified by uploading top 300 etoposide-evoked GEC overlapping in 10 AML cell lines to Connectivity Map (CMap) resource. The connectivity score ranging from -100 to 100 depicts the fraction of reference genes exhibiting similarity with the query. Emulators with connectivity score greater than |90| were considered as significant.

Etoposide-like emulators (gene knockdowns)		
ID	Target	Connectivity score
CGS001-6240	*RRM1*	99.66
CGS001-4609	***MYC***	99.14
CGS001-1027	*CDKN1B*	98.15
CGS001-4998	*ORC1*	97.18
CGS001-4067	*LYN*	97.04
CGS001-1666	*DECR1*	96.86
CGS001-3815	*KIT*	96.73
CGS001-4199	*ME1*	96.33
CGS001-11331	*PHB2*	95.7
CGS001-29890	*RBM15B*	95.25
CGS001-9020	*MAP3K14*	94.59
CGS001-5373	*PMM2*	94.51
CGS001-3226	*HOXC10*	94.22
CGS001-5591	*PRKDC*	93.49
CGS001-998	*CDC42*	93.31
CGS001-291	*SLC25A4*	93.26
CGS001-2852	*GPER*	92.76
CGS001-4191	*MDH2*	92.52
CGS001-2872	*MKNK2*	92.35
CGS001-5245	*PHB*	91.58
CGS001-5690	*PSMB2*	91.49
CGS001-5770	*PTPN1*	91.43
CGS001-2355	*FOSL2*	91.26
CGS001-10247	*HRSP12*	91.08
CGS001-2581	*GALC*	90.52
CGS001-11245	*GPR176*	90.44
CGS001-4792	*NFKBIA*	90.44
CGS001-5184	*PEPD*	90.41
CGS001-79724	*ZNF768*	90.4
CGS001-64116	*SLC39A8*	90.21
CGS001-63933	*CCDC90A*	90.15
CGS001-4143	*MAT1A*	90.04

Etoposide-contrary emulators (gene knockdowns)		
CGS001-64805	*P2RY12*	-97.83
CGS001-2153	*F5*	-95.66
CGS001-1622	*DBI*	-95.5
CGS001-25805	*BAMBI*	-94.21
CGS001-4312	*MMP1*	-92.97
CGS001-136	*ADORA2B*	-92.66
CGS001-57819	*LSM2*	-92.39
CGS001-79796	*ALG9*	-92.37
CGS001-991	*CDC20*	-92.27
CGS001-7535	*ZAP70*	-91.91
CGS001-25925	*ZNF521*	-91.68
CGS001-6046	*BRD2*	-91.6
CGS001-6478	*SIAH2*	-90.91
CGS001-9128	*PRPF4*	-90.81
CGS001-7132	*TNFRSF1A*	-90.63
CGS001-9575	*CLOCK*	-90.34
CGS001-83593	*RASSF5*	-90.31

Table 5.10.2: Emulators (drug treatments) evoking gene expression changes (GEC) either similar (etoposide-like) or opposite (etoposide-contrary) to those evoked by etoposide. Emulators were identified by uploading top 300 etoposide-evoked GEC overlapping in 10 AML cell lines to Connectivity Map (CMap) resource. The connectivity score ranging from -100 to 100 depicts the fraction of reference genes exhibiting similarity with the query. Emulators with connectivity score greater than |90| were considered as significant.

Etoposide-like emulators (drug treatment)

ID	Drug	Drug target	Drug class	Connectivity score
BRD-A62025033	temsirolimus	MTOR, PTEN	**MTOR inhibitor**	96.06
BRD-K68174511	torin-2	MTOR		94.2
BRD-K69932463	AZD-8055	MTOR		91.51
BRD-A45498368	WYE-125132	MTOR, PIK3CA		91.3
BRD-K77008974	WYE-354	MTOR		90.52
BRD-A79768653	sirolimus	MTOR, FKBP1A, CCR5, FGF2		93.94
BRD-K84937637	sirolimus	MTOR, FKBP1A, CCR5, FGF2		93.47
BRD-A75409952	wortmannin	PIK3CA, PIK3CG, PLK1, ATM, ATR, MTOR, PI4KA, PI4KB, PIK3CD, PIK3R1, PLK3, PRKDC		95.03
BRD-K06750613	GSK-1059615	PIK3CA, PIK3CG		97.99
BRD-K12184916	NVP-BEZ235	MTOR, PIK3CA, PIK3CG, PIK3CD, ATR, PIK3CB		90.56
BRD-A36630025	SN-38	TOP1	Topoisomerase inhibitor	97.88
BRD-K98490050	amsacrine	TOP2A, KCNH2		97.84
BRD-K56334280	amonafide	TOP2A, TOP2B		96.72
BRD-A35588707	teniposide	TOP2A, CYP3A5		96.42

BRD-K37798499	etoposide	TOP2A, CYP2E1, CYP3A5, TOP2B		93.68
BRD-K08547377	irinotecan	TOP1, CYP3A5, TOP1MT		91.08
BRD-K85985071	ellipticine	TOP2A, TOP2B		90.54
BRD-A71390734	idarubicin	TOP2A		98.49
BRD-A52530684	doxorubicin	TOP2A		97.24
BRD-A18419789	etoposide	TOP2A, CYP2E1, CYP3A5, TOP2B		94.59
BRD-K52522949	NCH-51	HDAC1, HDAC10, HDAC11, HDAC2, HDAC3, HDAC4, HDAC5, HDAC6, HDAC7, HDAC8, HDAC9	**HDAC inhibitor**	96.18
BRD-K81418486	vorinostat	HDAC1, HDAC2, HDAC3, HDAC6, HDAC8, HDAC10, HDAC11, HDAC5, HDAC9		93.6
BRD-K77908580	entinostat	HDAC1, HDAC2, HDAC3, HDAC9		92.85
BRD-K74733595	APHA-compound-8	HDAC8		91.88
BRD-K13169950	NSC-3852	HDAC1		91.72
BRD-K16485616	mocetinostat	HDAC1, HDAC2, HDAC3, HDAC11		91.51
BRD-K64606589	apicidin	HDAC1, HDAC10, HDAC11, HDAC2, HDAC3, HDAC4, HDAC5, HDAC6, HDAC7, HDAC8, HDAC9		90.53
BRD-K68336408	tyrphostin-AG-1478	EGFR, MAPK14	EGFR inhibitor	93.44
BRD-K85606544	neratinib	EGFR, ERBB2, ERBB4, KDR		92.27
BRD-U25771771	WZ-4-145	CSF1R, DDR1, EGFR, PDGFRA, TIE1		91.63
BRD-K50168500	canertinib	EGFR, ERBB2, ERBB4, AKT1		91.2
BRD-A25687296	emetine	RPS2	Protein synthesis inhibitor	96.9

BRD-A28970875	puromycin	NHP2L1, RPL10L, RPL11, RPL13A, RPL15, RPL19, RPL23, RPL23A, RPL26L1, RPL3, RPL37, RPL8, RSL24D1		95.88
BRD-K76674262	homoharringtonine	RPL3		95.2
BRD-K80348542	cephaeline	RPS2		94.76
BRD-K15108141	gemcitabine	RRM1, CMPK1, RRM2, TYMS	Ribonucleotide reductase inhibitor	97.28
BRD-K33106058	cytarabine	POLB, POLA1		96.48
BRD-A82371568	clofarabine	RRM1, POLA1, RRM2, SLC22A8		96.35
BRD-K50836978	purvalanol-a	CDK1, CDK2, CDK4, CDK5, CCND1, CCNE1, CSNK1G3, RPS6KA1, SRC	CDK inhibitor	97.58
BRD-K07762753	aminopurvalanol-a	CDK1, CDK2, CDK5, CDK6		96.96
BRD-K31542390	mycophenolic-acid	IMPDH1, IMPDH2	IMPDH inhibitor	97.57
BRD-K92428153	mycophenolate-mofetil	IMPDH1, IMPDH2, HCAR2		90.42
BRD-A49680073	cucurbitacin-i	JAK2, STAT3	JAK-STAT inhibitor	97.96
BRD-A28105619	cucurbitacin-i	JAK2, STAT3		95.86
BRD-A15079084	phorbol-12-myristate-13-acetate	CD4, KCNT2, PRKCA, TRPV4	PKC activator	97.25
BRD-A52650764	ingenol	PRKCD, PRKCE		95.15
BRD-A89434049	sarmentogenin	ATP1A1	ATPase inhibitor	91.79
BRD-K51018020	VAMA-37	PRKDC	DNA dependent protein kinase inhibitor	92.46
BRD-A48237631	mitomycin-c		DNA synthesis inhibitor	94.44

BRD-K13646352	midostaurin	FLT3, KIT, CCNB1, FLT1, KDR, PDGFRB, PRKCA, PRKCG, VEGFA	FLT3 inhibitor, PDGFR/KIT inhibitor, PKC inhibitor, VEGFR inhibitor	96.9
BRD-A81772229	simvastatin	HMGCR, CYP2C8, CYP3A4, CYP3A5, ITGB2	HMGCR inhibitor	93.91
BRD-K13049116	BMS-754807	IGF1R, AKT1	IGF-1 inhibitor	94.69
BRD-K47983010	BX-795	PDPK1, CDK2, CHEK1, GSK3B, IKBKE, KDR, PDK1, TBK1	IKK inhibitor	98.8
BRD-A11678676	wortmannin	PIK3CA, PIK3CG, PLK1, ATM, ATR, MTOR, PI4KA, PI4KB, PIK3CD, PIK3R1, PLK3, PRKDC	PI3K inhibitor	97.02
BRD-K82823804	SA-792987	WEE1	PKC inhibitor	98.3
BRD-K87343924	wortmannin	PIK3CA, PIK3CG, PLK1, ATM, ATR, MTOR, PI4KA, PI4KB, PIK3CD, PIK3R1, PLK3, PRKDC	-	98.5
BRD-M86331534	pyrvinium-pamoate	AR	-	96.6
BRD-K30677119	PP-30	RAF1	-	96.14
BRD-K03067624	emetine	RPS2	-	95.87
BRD-A24643465	homoharringtonine	RPL3	-	95.63
BRD-A55484088	BNTX	OPRD1, OPRK1, OPRM1	-	95.38
BRD-K91370081	anisomycin	NHP2L1, RPL10L, RPL11, RPL13A, RPL15, RPL19, RPL23, RPL23A, RPL26L1, RPL3, RPL37, RPL8, RSL24D1	-	94.36
BRD-K61829047	7b-cis	XPO1	-	94.35
BRD-A19248578	latrunculin-b	ACTA1, MKL1, SPIRE2	-	94.34
BRD-K74402642	NSC-632839	USP2, USP7, SENP2, USP1	-	94.33
BRD-K37392901	NSC-632839	USP2, USP7, SENP2, USP1	-	94.2

BRD-K36007650	puromycin	NHP2L1, RPL10L, RPL11, RPL13A, RPL15, RPL19, RPL23, RPL23A, RPL26L1, RPL3, RPL37, RPL8, RSL24D1	-	94.01
BRD-U86922168	QL-XII-47	BMX, BTK	-	93.74
BRD-K67439147	SIB-1893	GRM5, GRM4	-	93.65
BRD-K17140735	SCH-79797	F2R	-	93.26
BRD-A50737080	CGK-733	ATM, ATR	-	92.59
BRD-K14821540	FCCP		-	91.53
BRD-K28907958	CD-437	RARG	-	91.36
BRD-K89930444	AG-592		-	91.02
BRD-K73610817	BRD-K73610817		-	90.76
BRD-K30351863	BRD-K30351863	APEX1	-	90
Etoposide-contrary emulators (drug treatment)				
BRD-K23875128	**RHO-kinase-inhibitor-III[rockout]**	**IMPDH2, ROCK1**	-	-98.78
BRD-A35108200	dexamethasone	ANXA1, CYP3A4, CYP3A5, NOS2, NR0B1, NR3C1, NR3C2	Glucocorticoid receptor agonist	-97.76
BRD-A69951442	dexamethasone	ANXA1, CYP3A4, CYP3A5, NOS2, NR0B1, NR3C1, NR3C2		-97.65
BRD-K89687904	PKCbeta-inhibitor	PRKCB	-	-96.99
BRD-K32107296	temozolomide	TOP2A	Topoisomerase inhibitor	-94.48
BRD-A68631409	evodiamine	TRPV1	-	-94.22

BRD-K32536677	AGK-2	SIRT2	-	-93.98
BRD-A14985772	ascorbyl-palmitate		-	-93.73
BRD-K59184148	SB-216763	GSK3B, CCNA2, CDK2, GSK3A	Glycogen synthase kinase inhibitor	-93.31
BRD-K59222562	BRD-K59222562	CLK1, CLK4, DYRK1A, DYRK1B	-	-91.84
BRD-K01638814	rilmenidine	NISCH	Imidazoline ligand	-91.2
BRD-K98372770	L-2167	PPARD	-	-90.8

I then measured cell viability in AML cell lines treated with inhibitors targeting the protein products of selected putative etoposide-like emulators individually, as well as in combination with etoposide (IC_{25} concentrations) for 24 hours. Targeting of the etoposide-like emulator *MYC* with TWS-119 led to cytotoxicity in all AML cell lines except MONO-MAC-6 (**Fig. 5.10.1A** and **Table 5.8.3**). Similarly, inhibition of etoposide-like emulators mTOR with rapamycin and of HDAC with vorinostat evoked cell death in in 9 and 6 AML cell lines, respectively (**Fig. 5.10.1B** and **C**, and **Table 5.8.3**). Interestingly, vorinostat and rapamycin also exhibited synergy or additivity with etoposide in 9 and 6 AML cell lines, respectively (**Table 5.8.3**, **Appendix table 4**, and **Appendix table 5**).

The etoposide-contrary emulator *ROCK1* also synergized or exhibited additivity with etoposide in 7 out of 11 AML cell lines, when inhibited with rockout. Inhibition of ROCK1 was cytotoxic in only 3 AML cell lines (**Table 5.8.3** and **Appendix table 4**). The target specificity of rockout was confirmed by demonstrating cytotoxicity in HL-60 cells upon shRNA-mediated knockdown of *ROCK1* (**Fig. 5.10.3**).

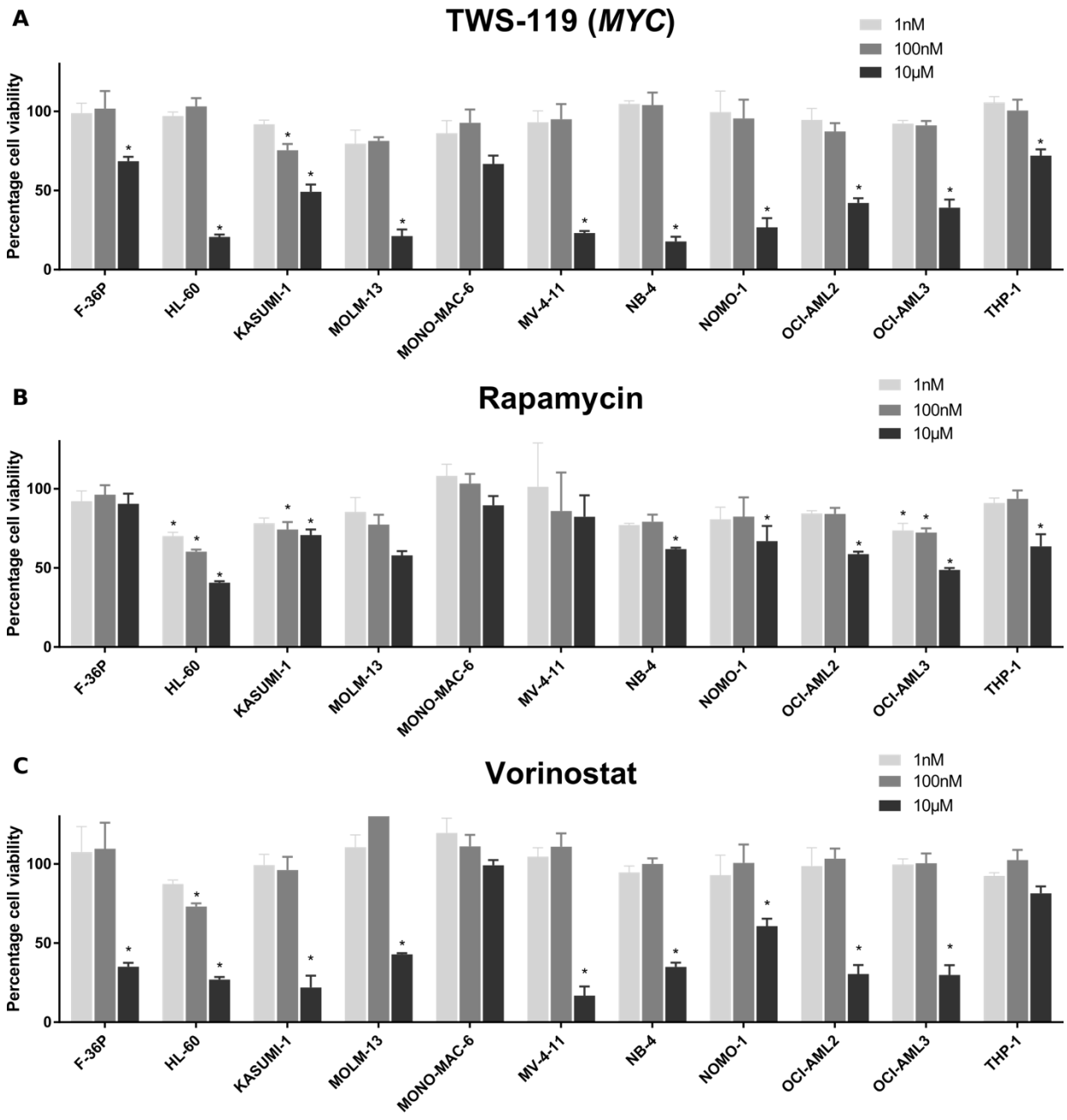

Fig. 5.10.1: **AML cell viability in response to emulators.** Percentage of cell viability in response to an inhibitor of the etoposide-like transcriptional driver (A) MYC, (B) rapamycin (mTOR inhibitor), and (C) vorinostat (HDAC inhibitor) respectively after 24 hours treatment. Percentage cell viability compared to vehicle-treated control, taken as 100%, was calculated. Two-way ANOVA with Benjamini and Hochberg FDR test was performed to quantify significant difference. Data are represented as mean values ± SD and derived from 3 biological replicates. (* p-value < 0.05).

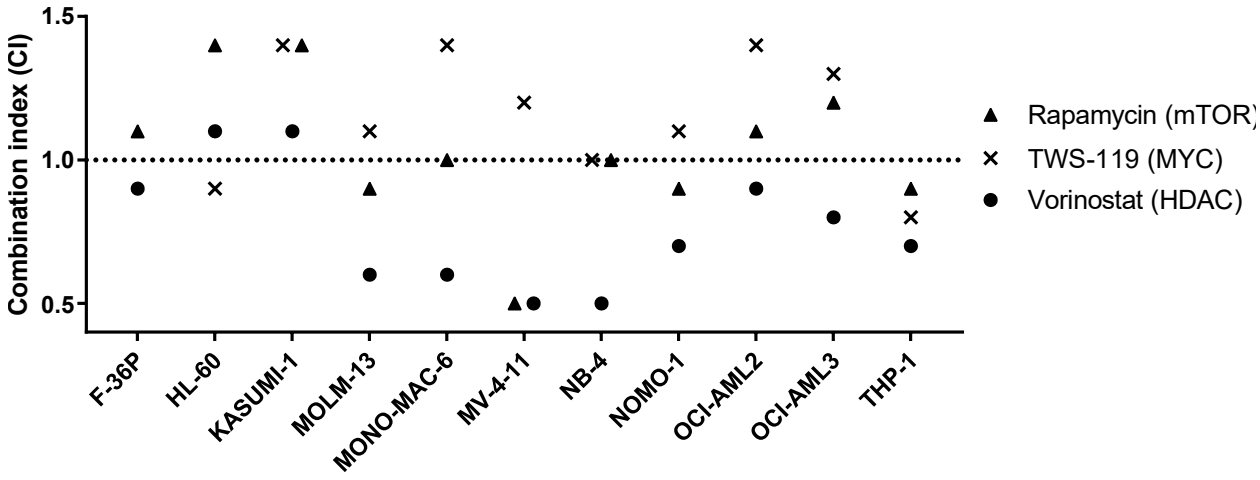

Fig. 5.10.2: **Synergy of emulators with etoposide in AML cells.** Combination index of etoposide treatment with protein inhibitor targeting the etoposide-like transcriptional drivers MYC, vorinostat, and rapamycin. CI < 1: synergism, CI = 1 (dotted line): additivity, CI > 1: antagonism.

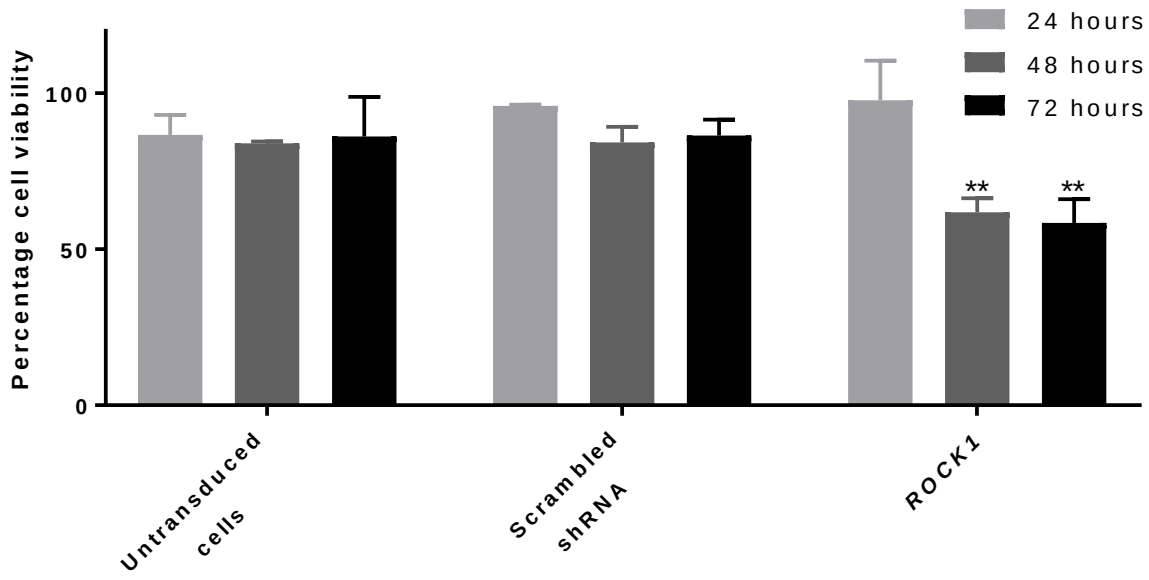

Fig. 5.10.3: **Viability of HL-60 cells after shRNA-mediated gene knockdown of the etoposide-contrary emulator *ROCK1*.** Percentage cell viability compared to untransduced cells, taken as 100%, was calculated. Mann-Whitney test was performed to identify significant change in the viability. (** represents q value < 0.01). Data are represented as mean values ± SD and derived from 3 biological replicates.

5.11 Etoposide-driver combinations exert cytotoxicity without increasing DNA damage

To investigate the safety of the identified combinations of etoposide with other drugs, their effect on DNA damage in HL-60 cell line was investigated. I measured the FITC-conjugated Anti-

phospho H2A.X-labelled HL-60 cells by flow cytometry before and after the treatment with etoposide, alone or in combination with other inhibitors for 24 hours. Etoposide caused, as an effect of TOP2-poisoning, DNA damage in 45% of cells when treated at IC_{25} concentration. None of the investigated etoposide-combinations elevated the amount of DNA damage in comparison to etoposide alone **(Fig. 5.11.1**). Furthermore, the BIR inhibitor GDC-0152 increased the cytotoxicity in combination with etoposide, while reducing the amount of DNA damage in comparison to etoposide alone.

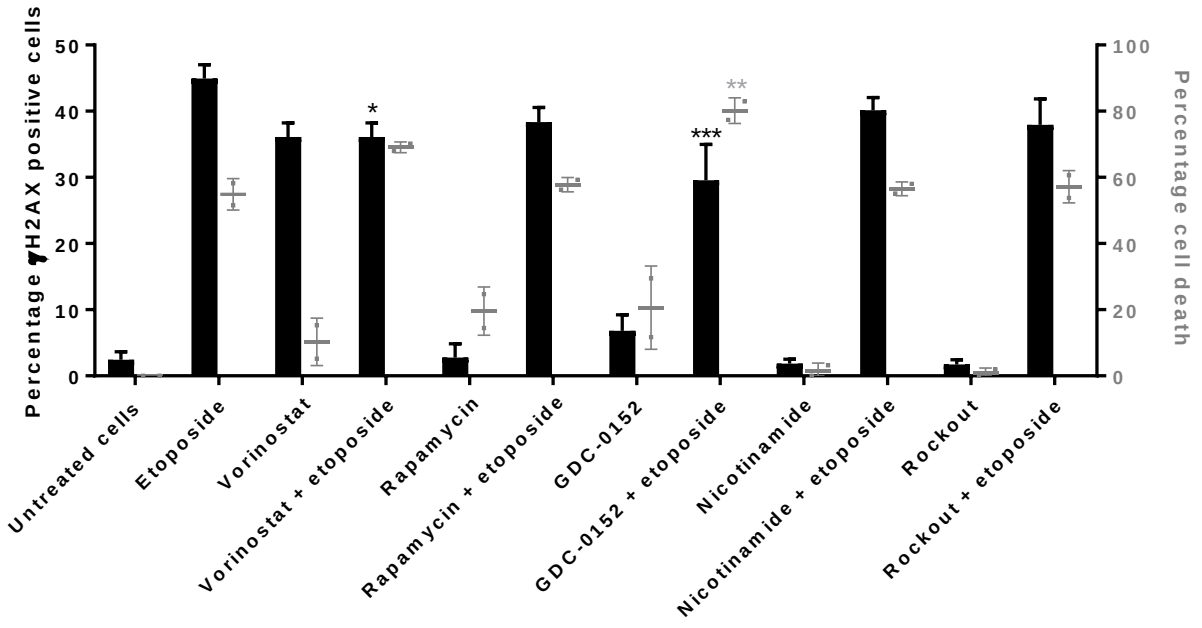

Fig. 5.11.1: **DNA damage after etoposide treatment in combination with its cytotoxicity drivers.** Bar plot representing percentage of phospho-H2A.X positive cells counted using flow cytometry and percentage cell death after treatment with different inhibitors alone as well as in combination with IC_{25} concentration of etoposide in HL-60 cell line. Mann-Whitney test was performed using GraphPad Prism software to identify significant effect compared to etoposide alone.

5.12 Drivers of etoposide cytotoxicity form unfavorable prognostic markers in AML patients

To assess the clinical relevance of identified drivers, I inspected the gene expression and clinical data for 173 patients from TCGA and compared with gene expression in 30 normal blood samples

from GTEx. The analysis revealed an association between high expression of *BCL2A1* and *PARP9* with poor survival in AML patients (**Fig. 5.12.1A** and **B**). Furthermore, these genes were highly expressed in AML patients compared to healthy individuals (**Fig. 5.12.1C** and **D**).

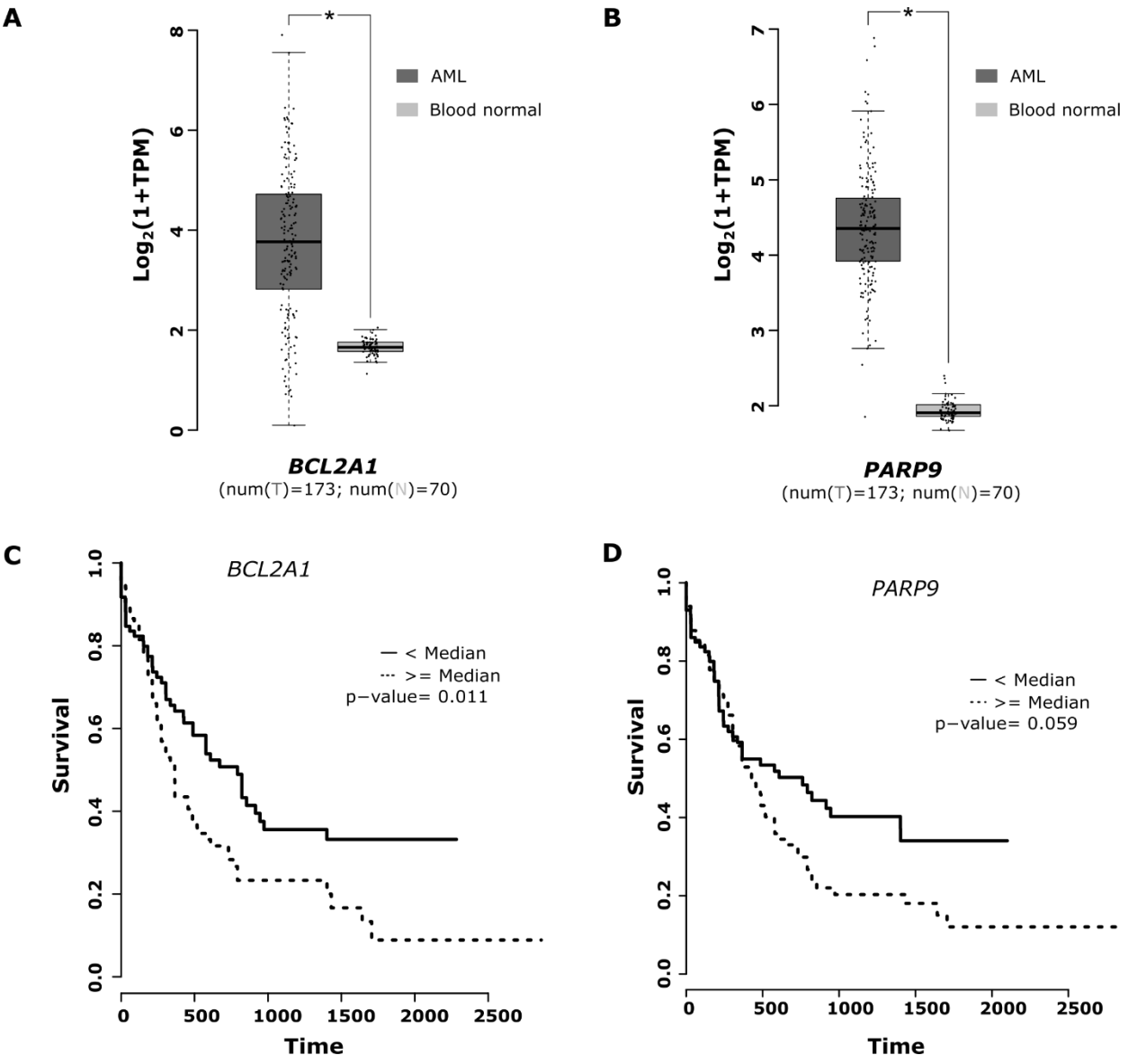

Fig. 5.12.1: **Relevance of etoposide cytotoxicity drivers in AML patients.** Basal expression of (A) *BCL2A1* and (B) *PARP9* respectively in AML and normal blood cells using the RNA-Seq data from TCGA and GTEx. Kaplan–Meier plot representing survival analysis of the AML patients with high and low expression of (A) *BCL2A1* and (B) *PARP9* respectively, obtained from TCGA.

Additionally, the Human Protein Atlas resource revealed high expression of *BIRC5* or *PLK1* to be association poor survival in renal, liver, and lung cancer patients (**Fig. 5.12.2**) and high expression of *ROCK1* to be a marker of unfavorable prognosis in pancreatic cancer (**Fig. 5.12.3**).

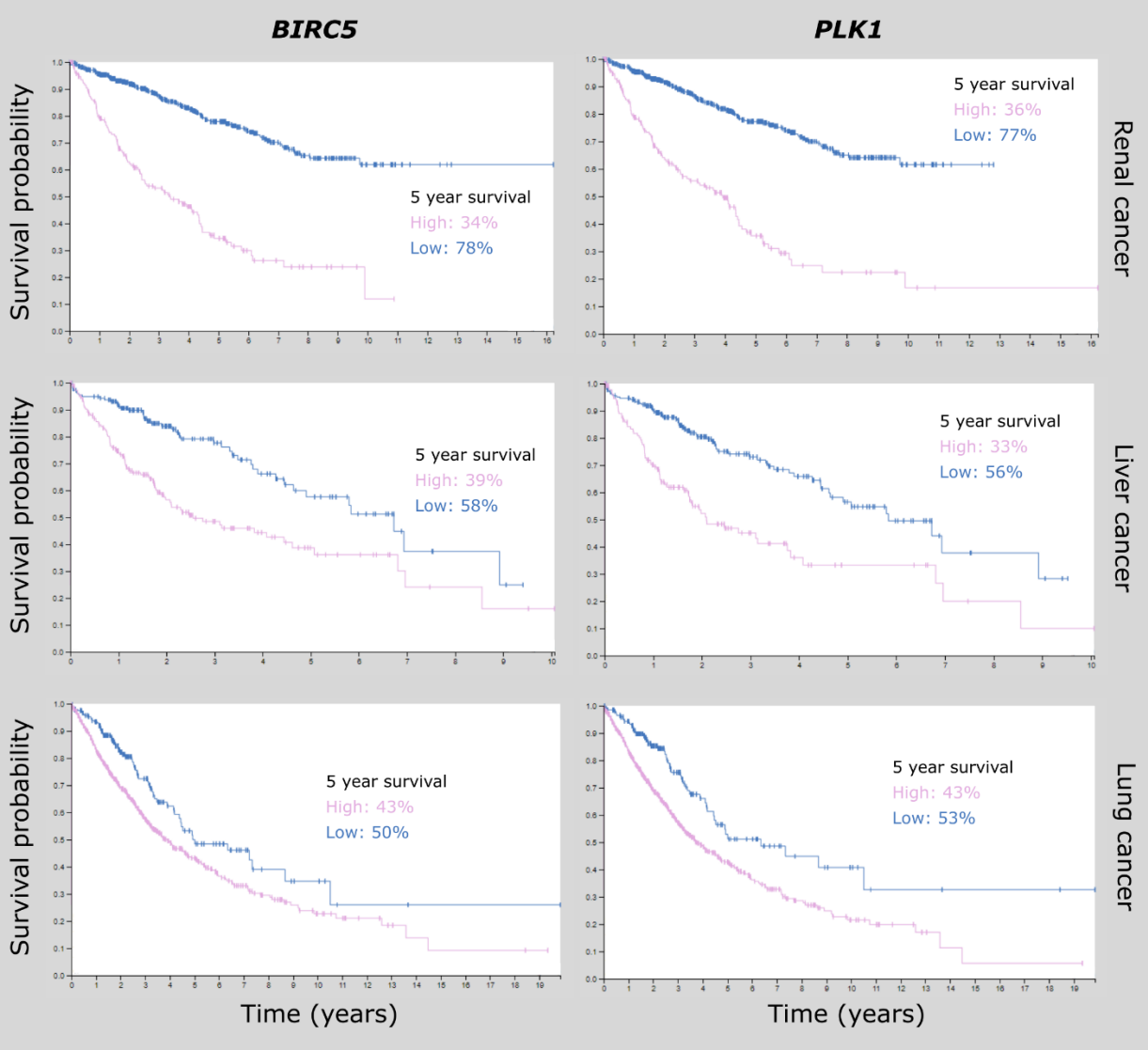

Fig. 5.12.2: **Kaplan–Meier plot representing survival analysis for cancer patients with low or high expression of *BIRC5* and *PLK1*, obtained from The Human Protein Atlas resource.**

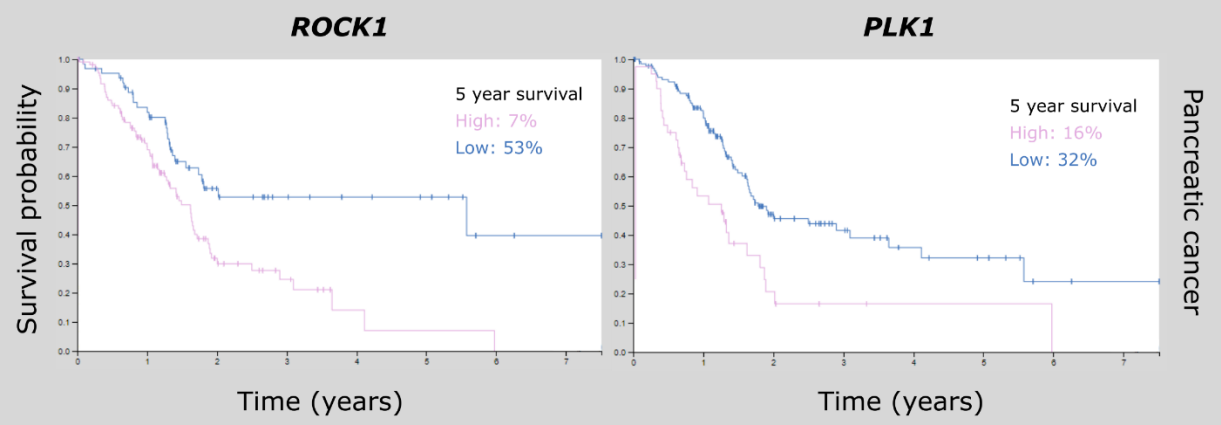

Fig. 5.12.3: **Kaplan–Meier plot representing survival analysis for cancer patients with low or high expression of *ROCK1* and *PLK1*, obtained from The Human Protein Atlas resource.**

6 Discussion

In this work, I demonstrate that etoposide kills cancer cells depending on expression levels of driver genes, some of which it modulates. This effect is distinct from the etoposide concentration-driven increase in DNA double stranded breaks (Smart, Halicka et al. 2008). Targeting these drivers genetically or pharmacologically mimics or augments the response to etoposide, indicating a potential for clinical exploration. The pipeline used to discover drivers of etoposide cytotoxicity is applicable to other TOP2 inhibitors and to cytotoxic drugs in general.

Furthermore, using HTETOP cell line model, I found the TOP2A dependency of etoposide for cytotoxic response. Both TOP2 poisons, doxorubicin and etoposide, inhibit re-ligation of transient DSB, which triggers cell death. However, the dependency of etoposide for TOP2A was striking. Doxorubicin poisons TOP2 as well as intercalates into DNA. Doxorubicin is oxidized to semiquinone and then converted back to original state generating reactive oxygen species (ROS) in the process. ROS generates oxidative stress and contributes to DNA damage and apoptosis. This pathway is most likely upregulated after doxorubicin treatment in the absence of TOP2A,

overruling the need of TOP2A for cytotoxic response (Thorn, Oshiro et al. 2011). On the other hand, etoposide seems to exert its action predominantly via TOP2A poisoning.

Altogether, this work demonstrates that:

- Modulators synergized with etoposide
- Mediators exhibited standalone cytotoxicity
- Emulators exhibited standalone cytotoxicity and synergized with etoposide

These drivers of etoposide cytotoxicity have been exploited to enhance the efficacy of etoposide.

6.1 Gene expression changes-mediated cytotoxicity of etoposide

Since the response of cancer cells to TOP2 poisons is variable, attempts have been made to explain it via pre-treatment gene expression levels (Zoppoli, Regairaz et al. 2012, Reinhold, Varma et al. 2015, Yadav, Gopalacharyulu et al. 2015, Liu, Yang et al. 2016, Sun, Zhang et al. 2016). *SLFN11* (Zoppoli, Regairaz et al. 2012, Rees, Seashore-Ludlow et al. 2016) and *SMARCA4* (Lee, Celik et al. 2018), re-discovered in this study, have been identified as modulators of TOP2 poisons, including etoposide, but failed to make clinical impact. Treatment-driven GEC have been likewise reported (Woo, Shimoni et al. 2015, Huang, Hsieh et al. 2018), but not explored for optimizing response to TOP2 poisons. I considered both pre-treatment gene expression levels *and* drug-evoked changes, as a surrogate of pre- and post-treatment protein expression levels. Post-treatment transcriptomes turned out to be particularly important, since they were essential for the discovery of most of the functionally confirmed drivers (i.e. of all mediators and emulators).

Most of the etoposide-evoked GEC were likely secondary, judging from the predominance of gene inductions over reductions. Indeed, only expression reductions can be expected to arise directly from DNA damage within regulatory or coding gene sequences. This is well reflected in a

HTETOP cell model, where predominance of gene repression was observed. However, I could not confirm the etoposide-evoked predominance of gene repression in other cancer cell lines, including a panel of AML cell lines, as well as in other cells lines obtained from GEO, except in OCI-Ly3 (B-cell lymphoma). The explanation for this observation could be variable etoposide concentrations and treatment times in GEO set of cell lines. The HTETOP cell line was treated with 20 µM of etoposide (IC_{50} being 7.7 µM) for 24 hours. None of the cell line from GEO set was treated with comparable concentration and time-points. Furthermore, HTETOP is an engineered cell line derived from fibrosarcoma HT-1080 cell line, with artificially high TOP2A expression (Carpenter and Porter 2004). Hence, the predominance of repressing GEC after etoposide treatment seems to be a specific attribute of HTETOP cell line. Etoposide treatment generates limited numbers of DSB foci (Roos and Kaina 2013), which could have been reflected in lower number of gene repressions in other cancer cell lines. The predominance of gene inductions in other cancer cell lines is most likely resulted from secondary effectors of etoposide.

Nevertheless, these GEC could themselves contribute to cytotoxicity, especially repressions in the oncogenic targets and inductions in the tumor repressor targets. Considering off-target effects of classical anti-cancer drugs, such essential GEC could provide effective alternative for targeted cancer therapies. Analysis of etoposide-treated HTETOP cell line revealed majority of etoposide-evoked gene repressions to be involved in cancer and cell proliferation processes, indicating their repression could be exploited as a potential therapeutic strategy.

6.2 Mediators as standalone targets for etoposide replacement

The mediators *PFKP* and *PLAU* reduced the viability of HTETOP cells when suppressed using siRNA. PFKP (phosphofructokinase) catalyzes the initial step of glycolysis by phosphorylating D-fructose 6-phosphate to fructose 1,6-bisphosphate. Many cancer cell types depend on glycolysis

rather than more efficient oxidative phosphorylation for energy metabolism because of hypoxic environment and mutations in the mitochondrial DNA (Ganapathy-Kanniappan & Geschwind, 2013). Hence, targeting the enzymes involved in glycolytic processes provides an effective strategy for managing tumor growth (Zheng, 2012). In consistent with this, *PFKP* is highly expressed in HTETOP and its high expression is associated with poor survival of liver cancer and head and neck cancer patients (Uhlén et al., 2015).

PLAU (plasminogen activator, urokinase) is a serine protease responsible for tumor migration because of its function in degrading the extracellular matrix. I found PLAU overexpressed in HTETOP cell line and its overexpression reduced the survival in pancreatic, head and neck, renal, and lung cancer patients, most likely contributing to secondary tumors at different sites. Reduction in the cell viability of HTETOP cell line after PLAU knockdown suggests its utility as an alternate target for therapy.

Other investigated mediators of etoposide cytotoxicity in AML cell lines also represent critical processes in cancer survival and were confirmed to be essential. B-cell lymphoma 2-related protein A1 (BCL2A1) is a member of BCL2 family proteins having anti-apoptotic function (Vogler 2012). BCL2A1 expression is frequently deregulated in many types of cancers, including overexpression in AML patients. Insulin-like growth factor receptor 1 (IGF1R), a tyrosine kinase receptor, augment the cell proliferation and it's use as anti-cancer target in combination with other chemotherapeutic drugs is under investigation (Chen and Sharon 2013). Polo-like kinase 1 (PLK1) plays critical role during mitosis (Brandwein 2015). I predicted *PLK1* to be essential for 4 AML survival. Interestingly, PLK1 inhibition was cytotoxic in all 11 AML cell lines. This suggests that targets derived from small sample size can even be applicable for large cohort. Protein kinase c eta (PRKCH) in involved many cellular processes including cell proliferation and differentiation.

It is required for maintaining hematopoietic stem cell function. PRKCH is highly expressed in leukemia and its high expression is associated with poor prognosis in AML patients (Porter and Magee 2017).

These mediators exhibited synergy with etoposide only in 2 out of 11 AML cell lines each. Similar results were obtained using HTETOP cell line. None of the knockdowns sensitized the HTETOP cell line to etoposide treatment in combination experiment. This may be due to different pathways governing the cytotoxicity getting triggered after treatment with inhibitors compared to etoposide. AML cells are likely to be committed to the dominant response pathway triggered either by essential mediator or by etoposide. Altogether, results confirmed the contribution of etoposide-evoked GEC to its anti-cancer activity. Such essential mediators could even replace the classical anti-cancer drugs because of their specificity. These specific targets could replicate the cytotoxicity of non-specific anti-cancer drugs with less side-effects.

6.3 Modulators for overcoming drug resistance

The comparison of co-expression networks before and after etoposide-treatment identified the etoposide-relevant biological processes such as response to DNA damage, DNA repair, and apoptosis regulation to be affected by the treatment. The potential negative modulators investigated in detail, BIRC5 and PARP9, sensitized AML cell lines to etoposide treatment. BIRC5, also known as survivin, is a member of inhibitor of apoptosis family. It is involved in cell proliferation and apoptosis inhibition, and frequently overexpressed in cancer cells (Tanaka, Iwamoto et al. 2000). The results demonstrated the involvement of BIRC5 in etoposide resistance by AML cell lines as confirmed by increased etoposide sensitivity in combination with survivin inhibitor. Several clinical trials are undergoing to evaluate effectiveness of survivin inhibitors in combination with idarubicin and cytarabine (NCT00620321 and NCT01398462). The other

investigated negative modulator, *PARP9* (also abbreviated as *ARTD9* or *BAL1*), plays a role in cell migration (Aguiar, Yakushijin et al. 2000). The high expression of catalytically inactive PARP9 is associated with upregulated cell motility. The experiments using nicotinamide, NAD and NADP pre-cursor and PARP inhibitor, revealed either etoposide-synergy or additive effects in 10 out of 11 investigated AML cell lines. As nicotinamide is not a selective inhibitor of PARP9, further investigation using shRNA-mediated *PARP9* knockdown in HL-60 cell line revealed essentiality for cell survival. Furthermore, high expression of *PARP9* is associated with poor survival of AML patients. PARP inhibitors are currently being investigate in AML patients in combination with TOP1 poison topotecan (NCT03289910 and NCT00588991). Altogether, the results indicated the essential role of *PARP9* for AML cell survival and a role in DNA damage response inferred by etoposide-synergy in AML cell lines. I also investigated *NOTCH1* as a positive modulator of etoposide cytotoxicity with high expression in the etoposide-responsive AML cell lines. As expected, treatment with Notch inhibitor did not exert cytotoxicity or etoposide synergy. Interestingly, Notch inhibition in F-36P cell line further reduced the etoposide cytotoxicity of this cell line.

Using this approach, I re-discovered the etoposide cytotoxicity modulators *SLFN11* (Zoppoli, Regairaz et al. 2012, Rees, Seashore-Ludlow et al. 2016) and *SMARCA4* (Lee, Celik et al. 2018), reported previously, correlating with etoposide sensitivity. However, the predicted effector targets *MYC*, *BRD4*, and *SIRT1* were enriched only after integrating the etoposide-evoked GEC, confirming their additional value for predicting the sensitivity-relevant modulators. MALT1 (Mucosa Associated Lymphoid Tissue Lymphoma Translocation Gene 1) enhances BCL10-mediated NF-$_K$B activation, triggering the proliferating and anti-apoptotic program (Hadian and Krappmann 2011). I observed *MALT1* induction after etoposide treatment in the AML cell lines

less responsive to etoposide treatment, especially in the most resistant F-36P cell line. SIRT1 (Sirtuin 1) enhances the DNA damage repair by deacetylating the repair proteins TP53 and Ku70 (Jeong, Juhn et al. 2007). I observed *SIRT1* induction in the AML cell lines less responsive to etoposide treatment. Altogether, these results suggest the efficient repair and apoptosis regulation to be key processes for differential etoposide response in the investigated AML cell lines. Furthermore, results also suggest involvement of epigenetic regulation enhancing the DNA repair processes and could be the possible mechanism for the observed synergy with etoposide and a HDAC inhibitor vorinostat. Inhibiting such targets, those affect the downstream pathways of etoposide, can provide effective strategy to overcome resistance to this drug.

6.4 Rational combination partners using etoposide-like emulators

After confirming the respective etoposide-synergy and cytotoxicity of modulators and mediators of etoposide cytotoxicity, I hypothesized that the next-generation etoposide-combinations can be designed using etoposide-evoked GEC. The CMap resource (Subramanian, Narayan et al. 2017) provided other specific targets as well as drugs which evoke GEC either similar (etoposide-like emulators) or opposite (etoposide-contrary emulators) to those evoked by etoposide. I expected that etoposide-like emulators could exert etoposide-like cytotoxic response and etoposide-contrary emulators could synergize with etoposide, hypothesizing that such targets would induce the genes which are direct or indirect targets of etoposide. Interestingly, along with other TOP2 poisons, I identified mTOR and HDAC inhibitors as etoposide-like emulators. This analysis surprisingly identified, along with other topoisomerase inhibitors, class of HDAC inhibitor and mTOR inhibitors evoking GEC similar to those evoked by etoposide. The etoposide-synergy with HDAC (Thurn, Thomas et al. 2011) and mTOR inhibitors (Xu, Thompson et al. 2005) is well documented and undergoing clinical trials, which I confirmed in AML using vorinostat and rapamycin. Due to

the interaction of TOP2 with HDAC1 and 2 (Montecucco, Zanetta et al. 2015), etoposide-evoked DNA double-strand breaks could affect the chromatin architecture. This could be plausible explanation for similar GEC after treatment with etoposide and HDAC inhibitor, as well as the basis for synergy.

6.5 Potential application to AML and other cancers

Etoposide effects can be clearly optimized by targeting drivers of its toxicity, but how relevant is this strategy to AML management? AML accounts for 80% of leukemia cases in adult patients and have poor prognosis in patients (De Kouchkovsky and Abdul-Hay 2016, Pearsall, Lincz et al. 2018). Chemotherapy is the major form of treatment for AML management (Dombret and Gardin 2016). However, treatment strategies for relapsed AML are not yet clearly defined. MEC regimen (mitoxantrone in combination with etoposide and cytarabine) is one of the common regimens used for relapsed AML. However, it is associated with increased side-effects in AML patients (Ramos, Mo et al. 2015, Thol, Schlenk et al. 2015). Hence, there is a need to improve efficacy and reduce the toxicity of these treatment regimens. Similar needs exist for other etoposide applications, such as testicular, prostate and small cell lung cancer.

Interestingly, some of the drivers investigated in this work have been or are currently undergoing testing. This provides an additional validation of our approach. Supplementing etoposide with the inhibitor of its emulator mTOR with rapamycin has already been shown to reduce the survival of cancer cells in a mouse model of AML (Xu, Thompson et al. 2005). A phase II trial for managing high-risk AML patients with rapamycin in combination with MEC regimen is ongoing (NCT02583893). The etoposide-synergy with HDAC is currently undergoing testing for AML (NCT02553460). Due to the interaction of TOP2 with HDAC1 and 2, etoposide-evoked DNA double strand breaks could affect the chromatin architecture (Montecucco, Zanetta et al. 2015).

Interestingly, we observed etoposide-evoked induction in *SIRT1*. It is evident that SIRT1 induction synergizes with HDAC inhibition (Scuto, Kirschbaum et al. 2013). This is in agreement with the observed etoposide-evoked induction of *SIRT1* and its observed synergy with vorinostat.

Improved clinical outcomes in AML patients have been already reported for the PLK1 inhibitor volasertib (Kobayashi, Yamauchi et al. 2015) and a Phase III trial is ongoing (NCT01721876). Strikingly, PLK1 inhibition with volasertib was cytotoxic in all 11 AML cell lines. This suggests that cytotoxicity drivers can be efficient beyond the cohort subset in which they were detected. Inhibition of IGF1R has been found to be efficacious together with etoposide and cisplatin in small-cell lung cancer (Ellis, Shepherd et al. 2014) and further clinical trials are undergoing with other drugs and cancer types.

This work also tries to address the most common drawback of chemotherapy – side effects. The use of DNA damaging drugs, including etoposide, is associated with increased risk of secondary leukemia because of chromosomal aberrations (Ezoe, 2012; Kollmannsberger et al., 1998). Hence, it is crucial to formulate the combination partners which don't raise the risk further. My primary investigation using DSB marker gH2A.X revealed that none of the combination partners elevated the DNA damage compared to etoposide alone. Moreover, the inhibitor GDC-0152 targeting BIR protein reduced the amount of DNA damage caused by etoposide alone. GDC-0152 targets the anti-apoptotic BIR family proteins and hence most likely triggers the apoptotic pathways effectively in combination with etoposide.

6.6 Limitations and perspective

Utilizing etoposide-evoked GEC, I have demonstrated a unique pipeline to identify its specific targets and combination partners. However, this has certain limitations and caveats, beginning with the assumption of gene expression reflecting protein expression. While this assumption is

generally true, the expression and activity levels of some proteins are regulated without changes in the RNA expression level. Nevertheless, all potential drivers selected for validation displayed standalone toxicity or modified that of etoposide. Altogether, using transcriptome data is sufficiently sensitive and specific to detect and confirm cytotoxicity drivers worth further exploration in animal models and in the clinic.

Furthermore, it seems that some drivers serve as markers of, additional, undetected drivers. For example, inhibiting the etoposide modulator BCL2A1 with sabutoclax caused cytotoxicity in all AML cells. In contrast, a shRNA-mediated knockdown of BCL2A1 in HL-60 cells had no effect. Additional members of the Bcl2 family may have contributed to the effect of sabutoclax, a pan-Bcl2 inhibitor. shRNA-mediated knockdowns did confirm the specific involvements of *IGF1R* and *ROCK1*. On the other hand, results using chemical inhibitors are clinically more relevant. Especially drivers like BCL2A1 and PARP9, which showed relevance for AML patients, exhibit high potential and are currently under clinical investigation. Nevertheless, if possible, putative drivers should undergo verification both by genetic *and* pharmacological means.

Even though drug evoked GEC are found to be ideal for retrospective identification of cytotoxicity drivers, they are impossible to obtain in advance from cancer patients. However, it would be possible to model these GEC by applying machine learning to high throughput genomics data. The next generation CMap is an example of such efforts, which extrapolate the genome-wide GEC based-on expression change in 1000 genes using machine learning. Considering numerous ongoing big data initiatives including Cancer Cell Line Encyclopedia (CCLE), Genomics of Drug Sensitivity in Cancer (GDSC), Connectivity Map (CMap), project DREAM, and Cancer Target Discovery and Development (CTD^2), the drug-evoked changes could be predicted in patient beforehand to optimize the treatment for maximum efficacy with least side-effects.

7 References

Aguiar, R. C., Y. Yakushijin, S. Kharbanda, R. Salgia, J. A. Fletcher and M. A. Shipp (2000). "BAL is a novel risk-related gene in diffuse large B-cell lymphomas that enhances cellular migration." Blood **96**(13): 4328-4334.

Alexander, S. P., D. Fabbro, E. Kelly, N. V. Marrion, J. A. Peters, E. Faccenda, S. D. Harding, A. J. Pawson, J. L. Sharman, C. Southan, J. A. Davies and C. Collaborators (2017). "THE CONCISE GUIDE TO PHARMACOLOGY 2017/18: Enzymes." Br J Pharmacol **174 Suppl 1**: S272-S359.

An, X., A. K. Tiwari, Y. Sun, P. R. Ding, C. R. Ashby, Jr. and Z. S. Chen (2010). "BCR-ABL tyrosine kinase inhibitors in the treatment of Philadelphia chromosome positive chronic myeloid leukemia: a review." Leuk Res **34**(10): 1255-1268.

Arbiser, J. L. (2007). "Why targeted therapy hasn't worked in advanced cancer." J Clin Invest **117**(10): 2762-2765.

Ben-Ari Fuchs, S., I. Lieder, G. Stelzer, Y. Mazor, E. Buzhor, S. Kaplan, Y. Bogoch, I. Plaschkes, A. Shitrit, N. Rappaport, A. Kohn, R. Edgar, L. Shenhav, M. Safran, D. Lancet, Y. Guan-Golan, D. Warshawsky and R. Shtrichman (2016). "GeneAnalytics: An Integrative Gene Set Analysis Tool for Next Generation Sequencing, RNAseq and Microarray Data." OMICS **20**(3): 139-151.

Benjamini, Y. and Y. Hochberg (1995). "Controlling the False Discovery Rate - a Practical and Powerful Approach to Multiple Testing." Journal of the Royal Statistical Society Series B-Statistical Methodology **57**(1): 289-300.

Benyahia, B., S. Huguet, X. Decleves, K. Mokhtari, E. Criniere, J. F. Bernaudin, J. M. Scherrmann and J. Y. Delattre (2004). "Multidrug resistance-associated protein MRP1 expression in human gliomas: chemosensitization to vincristine and etoposide by indomethacin in human glioma cell lines overexpressing MRP1." J Neurooncol **66**(1-2): 65-70.

Brandwein, J. M. (2015). "Targeting polo-like kinase 1 in acute myeloid leukemia." Ther Adv Hematol **6**(2): 80-87.

Bray, F., F. Jacques, S. Isabelle, Siegel, R. L., Torre, L. A. and A. Jemal (2018). "Global Cancer Statistics 2018: GLOBOCAN Estimates of Incidence and Mortality Worldwide for 36 Cancers in 185 Countries." CA: A Cancer Journal for Clinicians.

Carpenter, A. J. and A. C. Porter (2004). "Construction, characterization, and complementation of a conditional-lethal DNA topoisomerase IIalpha mutant human cell line." Mol Biol Cell **15**(12): 5700-5711.

Chemocare. (2019). "Chemocare." Retrieved 15.02.2019, from http://chemocare.com/default.aspx.

Chen, H. X. and E. Sharon (2013). "IGF-1R as an anti-cancer target--trials and tribulations." Chin J Cancer **32**(5): 242-252.

Cowell, I. G. and C. A. Austin (2012). "Mechanism of generation of therapy related leukemia in response to anti-topoisomerase II agents." Int J Environ Res Public Health **9**(6): 2075-2091.

De Kouchkovsky, I. and M. Abdul-Hay (2016). "'Acute myeloid leukemia: a comprehensive review and 2016 update'." Blood Cancer J **6**(7): e441.

Dobin, A., C. A. Davis, F. Schlesinger, J. Drenkow, C. Zaleski, S. Jha, P. Batut, M. Chaisson and T. R. Gingeras (2013). "STAR: ultrafast universal RNA-seq aligner." Bioinformatics **29**(1): 15-21.

Dombret, H. and C. Gardin (2016). "An update of current treatments for adult acute myeloid leukemia." Blood **127**(1): 53-61.

Ellis, P. M., F. A. Shepherd, S. A. Laurie, G. D. Goss, M. Olivo, J. Powers, L. Seymour and P. A. Bradbury (2014). "NCIC CTG IND.190 phase I trial of dalotuzumab (MK-0646) in combination with cisplatin and etoposide in extensive-stage small-cell lung cancer." J Thorac Oncol **9**(3): 410-413.

Foucquier, J. and M. Guedj (2015). "Analysis of drug combinations: current methodological landscape." Pharmacol Res Perspect **3**(3): e00149.

Hadian, K. and D. Krappmann (2011). "Signals from the nucleus: activation of NF-kappaB by cytosolic ATM in the DNA damage response." Sci Signal **4**(156): pe2.

Hanahan, D. and R. A. Weinberg (2011). "Hallmarks of cancer: the next generation." Cell **144**(5): 646-674.

Huang, C. T., C. H. Hsieh, Y. J. Oyang, H. C. Huang and H. F. Juan (2018). "A Large-Scale Gene Expression Intensity-Based Similarity Metric for Drug Repositioning." iScience **7**: 40-52.

Iorio, F., R. Tagliaferri and D. di Bernardo (2009). "Identifying network of drug mode of action by gene expression profiling." J Comput Biol **16**(2): 241-251.

Jeong, J., K. Juhn, H. Lee, S. H. Kim, B. H. Min, K. M. Lee, M. H. Cho, G. H. Park and K. H. Lee (2007). "SIRT1 promotes DNA repair activity and deacetylation of Ku70." Exp Mol Med **39**(1): 8-13.

Kanavos, P. (2006). "The rising burden of cancer in the developing world." Ann Oncol **17 Suppl 8**: viii15-viii23.

Kobayashi, Y., T. Yamauchi, H. Kiyoi, T. Sakura, T. Hata, K. Ando, A. Watabe, A. Harada, T. Taube, Y. Miyazaki and T. Naoe (2015). "Phase I trial of volasertib, a Polo-like kinase inhibitor, in Japanese patients with acute myeloid leukemia." Cancer Sci **106**(11): 1590-1595.

Langfelder, P. and S. Horvath (2008). "WGCNA: an R package for weighted correlation network analysis." BMC Bioinformatics **9**: 559.

Lee, S. I., S. Celik, B. A. Logsdon, S. M. Lundberg, T. J. Martins, V. G. Oehler, E. H. Estey, C. P. Miller, S. Chien, J. Dai, A. Saxena, C. A. Blau and P. S. Becker (2018). "A machine learning approach to integrate big data for precision medicine in acute myeloid leukemia." Nat Commun **9**(1): 42.

Legrand, O., R. Zittoun and J. P. Marie (1999). "Role of MRP1 in multidrug resistance in acute myeloid leukemia." Leukemia **13**(4): 578-584.

Li, J., D. Zhou, W. Qiu, Y. Shi, J. J. Yang, S. Chen, Q. Wang and H. Pan (2018). "Application of Weighted Gene Co-expression Network Analysis for Data from Paired Design." Sci Rep **8**(1): 622.

Liu, X., J. Yang, Y. Zhang, Y. Fang, F. Wang, J. Wang, X. Zheng and J. Yang (2016). "A systematic study on drug-response associated genes using baseline gene expressions of the Cancer Cell Line Encyclopedia." Sci Rep **6**: 22811.

Marinello, J., M. Delcuratolo and G. Capranico (2018). "Anthracyclines as Topoisomerase II Poisons: From Early Studies to New Perspectives." Int J Mol Sci **19**(11).

McGowan, J. V., R. Chung, A. Maulik, I. Piotrowska, J. M. Walker and D. M. Yellon (2017). "Anthracycline Chemotherapy and Cardiotoxicity." Cardiovasc Drugs Ther **31**(1): 63-75.

Montecucco, A., F. Zanetta and G. Biamonti (2015). "Molecular mechanisms of etoposide." EXCLI J **14**: 95-108.

Nitiss, J. L. (2009). "Targeting DNA topoisomerase II in cancer chemotherapy." Nat Rev Cancer **9**(5): 338-350.

Ossenkoppele, G. and B. Lowenberg (2015). "How I treat the older patient with acute myeloid leukemia." Blood **125**(5): 767-774.

Pearsall, E. A., L. F. Lincz and K. A. Skelding (2018). "The Role of DNA Repair Pathways in AML Chemosensitivity." Curr Drug Targets **19**(10): 1205-1219.

Pendleton, M., R. H. Lindsey, Jr., C. A. Felix, D. Grimwade and N. Osheroff (2014). "Topoisomerase II and leukemia." Ann N Y Acad Sci **1310**: 98-110.

Pommier, Y. (2013). "Drugging topoisomerases: lessons and challenges." ACS Chem Biol **8**(1): 82-95.

Pommier, Y., E. Leo, H. Zhang and C. Marchand (2010). "DNA topoisomerases and their poisoning by anticancer and antibacterial drugs." Chem Biol **17**(5): 421-433.

Pommier, Y., Y. Sun, S. N. Huang and J. L. Nitiss (2016). "Roles of eukaryotic topoisomerases in transcription, replication and genomic stability." Nat Rev Mol Cell Biol **17**(11): 703-721.

Porter, S. N. and J. A. Magee (2017). "PRKCH regulates hematopoietic stem cell function and predicts poor prognosis in acute myeloid leukemia." Exp Hematol **53**: 43-47.

R Core Team (2014). "R: A language and environment for statistical computing." R Foundation for Statistical Computing, Vienna, Austria.

Ramos, N. R., C. C. Mo, J. E. Karp and C. S. Hourigan (2015). "Current Approaches in the Treatment of Relapsed and Refractory Acute Myeloid Leukemia." J Clin Med **4**(4): 665-695.

Rees, M. G., B. Seashore-Ludlow, J. H. Cheah, D. J. Adams, E. V. Price, S. Gill, S. Javaid, M. E. Coletti, V. L. Jones, N. E. Bodycombe, C. K. Soule, B. Alexander, A. Li, P. Montgomery, J. D. Kotz, C. S. Hon, B. Munoz, T. Liefeld, V. Dancik, D. A. Haber, C. B. Clish, J. A. Bittker, M. Palmer, B. K. Wagner, P. A. Clemons, A. F. Shamji and S. L. Schreiber (2016). "Correlating chemical sensitivity and basal gene expression reveals mechanism of action." Nat Chem Biol **12**(2): 109-116.

Reinhold, W. C., S. Varma, V. N. Rajapakse, A. Luna, F. G. Sousa, K. W. Kohn and Y. G. Pommier (2015). "Using drug response data to identify molecular effectors, and molecular "omic" data to identify candidate drugs in cancer." Hum Genet **134**(1): 3-11.

Robert, J., A. Vekris, P. Pourquier and J. Bonnet (2004). "Predicting drug response based on gene expression." Crit Rev Oncol Hematol **51**(3): 205-227.

Robinson, M. D., D. J. McCarthy and G. K. Smyth (2010). "edgeR: a Bioconductor package for differential expression analysis of digital gene expression data." Bioinformatics **26**(1): 139-140.

Roos, W. P. and B. Kaina (2013). DNA damage-induced cell death: From specific DNA lesions to the DNA damage response and apoptosis. Cancer Letters, Elsevier. **332:** 237-248.

Samur, M. K. (2014). "RTCGAToolbox: a new tool for exporting TCGA Firehose data." PLoS One **9**(9): e106397.

Schilsky, R. L. and L. E. Schnipper (2018). "Hans Christian Andersen and the Value of New Cancer Treatments." J Natl Cancer Inst **110**(5): 441-442.

Scuto, A., M. Kirschbaum, R. Buettner, M. Kujawski, J. M. Cermak, P. Atadja and R. Jove (2013). "SIRT1 activation enhances HDAC inhibition-mediated upregulation of GADD45G by repressing the binding of NF-kappaB/STAT3 complex to its promoter in malignant lymphoid cells." Cell Death Dis **4**: e635.

Siegel, R. L., K. D. Miller and A. Jemal (2018). "Cancer statistics, 2018." CA: A Cancer Journal for Clinicians **68**(1): 7-30.

Smart, D. J., H. D. Halicka, G. Schmuck, F. Traganos, Z. Darzynkiewicz and G. M. Williams (2008). "Assessment of DNA double-strand breaks and gammaH2AX induced by the topoisomerase II poisons etoposide and mitoxantrone." Mutat Res **641**(1-2): 43-47.

Stein, E. M., C. D. DiNardo, D. A. Pollyea, A. T. Fathi, G. J. Roboz, J. K. Altman, R. M. Stone, D. J. DeAngelo, R. L. Levine, I. W. Flinn, H. M. Kantarjian, R. Collins, M. R. Patel, A. E. Frankel, A. Stein, M. A. Sekeres, R. T. Swords, B. C. Medeiros, C. Willekens, P. Vyas, A. Tosolini, Q. Xu, R. D. Knight, K. E. Yen, S. Agresta, S. de Botton and M.

S. Tallman (2017). "Enasidenib in mutant IDH2 relapsed or refractory acute myeloid leukemia." Blood **130**(6): 722-731.

Stone, R. M., S. J. Mandrekar, B. L. Sanford, K. Laumann, S. Geyer, C. D. Bloomfield, C. Thiede, T. W. Prior, K. Dohner, G. Marcucci, F. Lo-Coco, R. B. Klisovic, A. Wei, J. Sierra, M. A. Sanz, J. M. Brandwein, T. de Witte, D. Niederwieser, F. R. Appelbaum, B. C. Medeiros, M. S. Tallman, J. Krauter, R. F. Schlenk, A. Ganser, H. Serve, G. Ehninger, S. Amadori, R. A. Larson and H. Dohner (2017). "Midostaurin plus Chemotherapy for Acute Myeloid Leukemia with a FLT3 Mutation." N Engl J Med **377**(5): 454-464.

Subramanian, A., R. Narayan, S. M. Corsello, D. D. Peck, T. E. Natoli, X. Lu, J. Gould, J. F. Davis, A. A. Tubelli, J. K. Asiedu, D. L. Lahr, J. E. Hirschman, Z. Liu, M. Donahue, B. Julian, M. Khan, D. Wadden, I. C. Smith, D. Lam, A. Liberzon, C. Toder, M. Bagul, M. Orzechowski, O. M. Enache, F. Piccioni, S. A. Johnson, N. J. Lyons, A. H. Berger, A. F. Shamji, A. N. Brooks, A. Vrcic, C. Flynn, J. Rosains, D. Y. Takeda, R. Hu, D. Davison, J. Lamb, K. Ardlie, L. Hogstrom, P. Greenside, N. S. Gray, P. A. Clemons, S. Silver, X. Wu, W. N. Zhao, W. Read-Button, X. Wu, S. J. Haggarty, L. V. Ronco, J. S. Boehm, S. L. Schreiber, J. G. Doench, J. A. Bittker, D. E. Root, B. Wong and T. R. Golub (2017). "A Next Generation Connectivity Map: L1000 Platform and the First 1,000,000 Profiles." Cell **171**(6): 1437-1452 e1417.

Sun, J., Q. Wei, Y. Zhou, J. Wang, Q. Liu and H. Xu (2017). "A systematic analysis of FDA-approved anticancer drugs." BMC Syst Biol **11**(Suppl 5): 87.

Sun, Y., W. Zhang, Y. Chen, Q. Ma, J. Wei and Q. Liu (2016). "Identifying anti-cancer drug response related genes using an integrative analysis of transcriptomic and genomic variations with cell line-based drug perturbations." Oncotarget **7**(8): 9404-9419.

Tanaka, K., S. Iwamoto, G. Gon, T. Nohara, M. Iwamoto and N. Tanigawa (2000). "Expression of survivin and its relationship to loss of apoptosis in breast carcinomas." Clin Cancer Res **6**(1): 127-134.

Tang, Z., C. Li, B. Kang, G. Gao, C. Li and Z. Zhang (2017). "GEPIA: a web server for cancer and normal gene expression profiling and interactive analyses." Nucleic Acids Res **45**(W1): W98-W102.

Tarazona, S., P. Furio-Tari, D. Turra, A. D. Pietro, M. J. Nueda, A. Ferrer and A. Conesa (2015). "Data quality aware analysis of differential expression in RNA-seq with NOISeq R/Bioc package." Nucleic Acids Res **43**(21): e140.

Thol, F., R. F. Schlenk, M. Heuser and A. Ganser (2015). "How I treat refractory and early relapsed acute myeloid leukemia." Blood **126**(3): 319-327.

Thorn, C. F., C. Oshiro, S. Marsh, T. Hernandez-Boussard, H. McLeod, T. E. Klein and R. B. Altman (2011). "Doxorubicin pathways: Pharmacodynamics and adverse effects." Pharmacogenetics and Genomics **21**(7): 440-446.

Thorn, C. F., C. Oshiro, S. Marsh, T. Hernandez-Boussard, H. McLeod, T. E. Klein and R. B. Altman (2011). "Doxorubicin pathways: pharmacodynamics and adverse effects." Pharmacogenet Genomics **21**(7): 440-446.

Thurn, K. T., S. Thomas, A. Moore and P. N. Munster (2011). "Rational therapeutic combinations with histone deacetylase inhibitors for the treatment of cancer." Future Oncol **7**(2): 263-283.

Tsherniak, A., F. Vazquez, P. G. Montgomery, B. A. Weir, G. Kryukov, G. S. Cowley, S. Gill, W. F. Harrington, S. Pantel, J. M. Krill-Burger, R. M. Meyers, L. Ali, A. Goodale, Y. Lee, G. Jiang, J. Hsiao, W. F. J. Gerath, S. Howell, E. Merkel, M. Ghandi, L. A. Garraway, D. E. Root, T. R. Golub, J. S. Boehm and W. C. Hahn (2017). "Defining a Cancer Dependency Map." Cell **170**(3): 564-576 e516.

Urruticoechea, A., R. Alemany, J. Balart, A. Villanueva, F. Vinals and G. Capella (2010). "Recent advances in cancer therapy: an overview." Curr Pharm Des **16**(1): 3-10.

Vogler, M. (2012). "BCL2A1: the underdog in the BCL2 family." Cell Death Differ **19**(1): 67-74.

Vural, S., R. Simon and J. Krushkal (2018). "Correlation of gene expression and associated mutation profiles of APOBEC3A, APOBEC3B, REV1, UNG, and FHIT with chemosensitivity of cancer cell lines to drug treatment." Hum Genomics **12**(1): 20.

Whyte, D. B. and S. L. Holbeck (2006). "Correlation of PIK3Ca mutations with gene expression and drug sensitivity in NCI-60 cell lines." Biochem Biophys Res Commun **340**(2): 469-475.

Widakowich, C., G. de Castro, Jr., E. de Azambuja, P. Dinh and A. Awada (2007). "Review: side effects of approved molecular targeted therapies in solid cancers." Oncologist **12**(12): 1443-1455.

Woo, J. H., Y. Shimoni, W. S. Yang, P. Subramaniam, A. Iyer, P. Nicoletti, M. Rodriguez Martinez, G. Lopez, M. Mattioli, R. Realubit, C. Karan, B. R. Stockwell, M. Bansal and A. Califano (2015). "Elucidating Compound Mechanism of Action by Network Perturbation Analysis." Cell **162**(2): 441-451.

Woo, J. H., Y. Shimoni, W. S. Yang, P. Subramaniam, A. Iyer, P. Nicoletti, M. Rodríguez Martínez, G. López, M. Mattioli, R. Realubit, C. Karan, B. R. Stockwell, M. Bansal and A. Califano (2015). "Elucidating Compound Mechanism of Action by Network Perturbation Analysis." Cell **162**(2): 441-451.

Xu, Q., J. E. Thompson and M. Carroll (2005). "mTOR regulates cell survival after etoposide treatment in primary AML cells." Blood **106**(13): 4261-4268.

Yadav, B., P. Gopalacharyulu, T. Pemovska, S. A. Khan, A. Szwajda, J. Tang, K. Wennerberg and T. Aittokallio (2015). "From drug response profiling to target addiction scoring in cancer cell models." Dis Model Mech **8**(10): 1255-1264.

Yan, T., S. Deng, A. Metzger, U. Godtel-Armbrust, A. C. Porter and L. Wojnowski (2009). "Topoisomerase II{alpha}-dependent and -independent apoptotic effects of dexrazoxane and doxorubicin." Mol Cancer Ther **8**(5): 1075-1085.

Zhang, H. and J. Chen (2018). "Current status and future directions of cancer immunotherapy." J Cancer **9**(10): 1773-1781.

Zhang, N., H. Wang, Y. Fang, J. Wang, X. Zheng and X. S. Liu (2015). "Predicting Anticancer Drug Responses Using a Dual-Layer Integrated Cell Line-Drug Network Model." PLoS Comput Biol **11**(9): e1004498.

Zoppoli, G., M. Regairaz, E. Leo, W. C. Reinhold, S. Varma, A. Ballestrero, J. H. Doroshow and Y. Pommier (2012). "Putative DNA/RNA helicase Schlafen-11 (SLFN11) sensitizes cancer cells to DNA-damaging agents." Proc Natl Acad Sci U S A **109**(37): 15030-15035.

8 Appendix

Appendix table 1: All siRNAs sequences used in this work. The Project Achilles (PAch) database was used to identify siRNA targeting selected mediator genes.

Target	siRNA sequence
ANLN	UGCUGGAGCGAACCCGUGCC
CDC20	ACAGAGGAUAUAUAUUCCCC
CDK6	AGUUCAGAUGUUGAUCAACU
DLGAP5	GAUGUUCGAGCAAUCCGACC
FOXM1	AUAGCCUAUCCAACAUCCAG
IGF2B	CACCACUGCCGUCUCACUCU
KIF20A	CCCCUGCCGUCAUGUCGCAA
MCM6	GAGUUUACCCUUACCUGUGU
MED1	UAAGCUUGUGCGUCAAGUCA
NCAPD2	CACGUUCUGCUAGUUCUGUC
PFKP	CGUCCCCGCCGAUCACACAC
RPA2	GCCGCCGGCUCCCCCGUAUG
SLC7A5	UACAGCGGCCUCUUUGCCUA
TOPBP1	UGUCUUUGAUCACCUCAAAA
TPX2	AUUGUCACACCUUUGAAACC
YWHAH	AAGCGACCUCUGCUAAGUAG

Appendix table 2: List of primers used for gene expression quantification using SYBR green qPCR.

Gene	5' - 3'	3' - 5'
ANLN	TCTGACATTCACTACTACATTTACTCTGC	GCCATGACTGAAGAATGAATGTTG
BCL2A1	CAGGAGAATGGATAAGGCAAA	CCAGCCAGATTTAGGTTCAAA
BIRC5	CCACCGCATCTCTACATTCA	TATGTTCCTCTATGGGGTCG
CDC20	GGCACCAGTGATCGACACATTCGCAT	GCCATAGCCTCAGGGTCTCATCTGCT
CDK6	TGGAGACCTTCGAGCACC	CACTCCAGGCTCTGGAACTT
CENPF	TACTGAGTTTGAGCCAGAGGGACT	CATGGTTGTTCTTCGCAGGATAT
DLGAP5	GGAAGACCTGCCAAAAATGTAG	TGTGCCAAAATTTCTTTTGTTG
FOSL1	GGGCATGTTCCGACACTT	CCACTCATGGTGTTGATGCT
FOXM1	GGAGGCAGCGACAGGTTAAGG	GTTGATGGCGAATTGTATCATGG
HDAC6	TGGCTATTGCATGTTCAACC	TCGAAGGTGAACTGTGTTCCT
HMGA2	AAGTTGTTCAGAAGAAGCCTGCTCA	TGGAAAGACCATGGCAATACAGAAT
IGF1R	GCCACTACTACTATGCCGGTG	GTGCATCCTTGGAGCATCT
IGF2BP1	GCGGCCAGTTCTTGGTCAA	TTGGGCACCGAATGTTCAATC
KIF20A	CTACAAGCACCCAAGGACTCTT	AGATGGAGAAGCGAATGTTTG
MCM6	TGGTGGCATCAATGGTCATG	TTAAGGAGGCTTTGGGAGCA
MED1	TGCGTCAAGTCATGGAGAAG	CCACTGGCACTGAGATGAGA
NCAPD2	TGGAGGGGTGAATCAGTATGT	GCGGGATACCACTTTTATCAGG
PARP9	GCAAAGAGGTCCAAGATGCT	CCTCACACATCTCTTCCACGT
PFKP	GCATGGGTATCTACGTGGGG	CTCTGCGATGTTTGAGCCTC
PLAU	CACGCAAGGGGAGATGAA	ACAGCATTTTGGTGGTGACTT
ROCK1	AAAGAAAGGATGGAGGATGAAGT	TGTAACAACAGCCGCTTATTTG
RPA2	GCACCTTCTCAAGCCGAAAA	CAGCTGACATATAGTACAGGGCACAA
SLC7A5	GCTGGTGTACGTGCTGACC	GCCCAGGTGATAGTTCCCG
TOPBP1	TGTGACCCTTTTAGTGGCGTT	CTTGGGACACATGGCTGG
TPX2	CCAGACCTTGCCCTACTAAGATT	AATGTGGCACAGGTTGAGC
YWHAH	CGCTATGAAGGCGGTGAC	TGCTAATGACCCTCCAGGAA

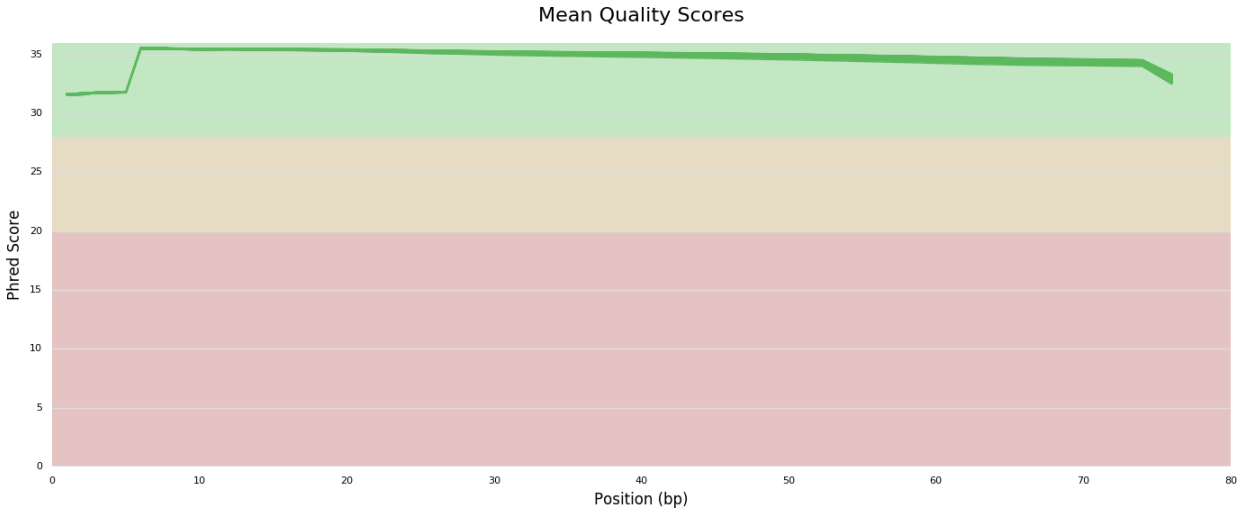

Appendix figure 1: Mean quality scores for all RNA-Seq raw reads from AML cell lines.

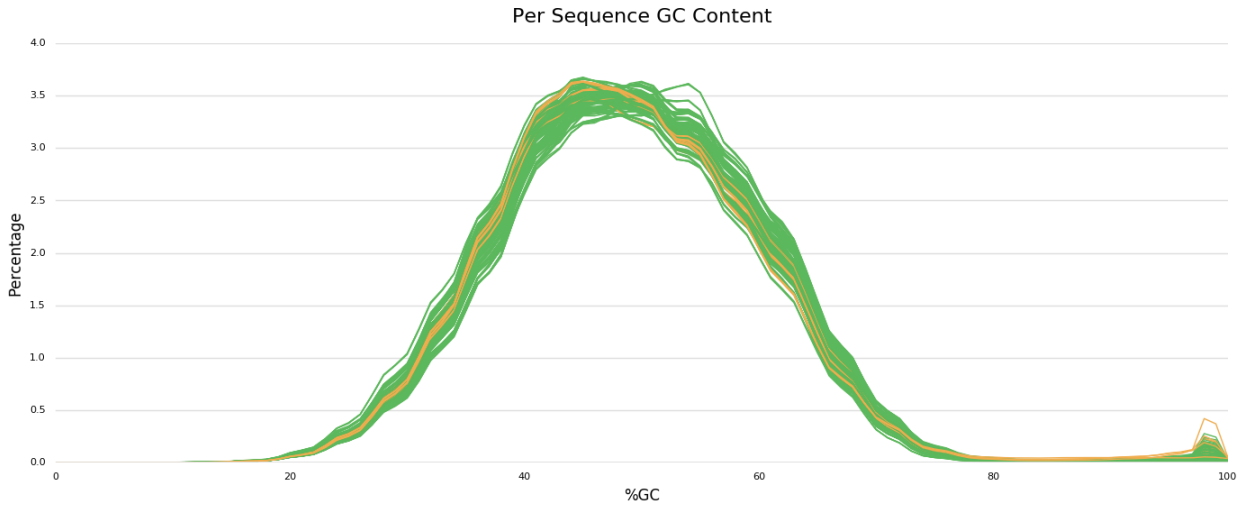

Appendix figure 2: GC content in the raw RNA-Seq reads from AML cell lines.

Appendix table 3: Percentage of reads mapped to the human reference genome hg38.

Sample Name	% Aligned	Million Aligned
F36P_CTR_1	87.70%	21
F36P_CTR_2	87.30%	21.4
F36P_CTR_3	88.50%	22.6
F36P_ETP_2	87.70%	21
F36P_ETP_3	88.50%	21.9
HL60_CTR_1	87.30%	22.9
HL60_CTR_2	87.00%	22.8
HL60_CTR_3	87.00%	20.8
HL60_ETP_1	87.30%	21
HL60_ETP_2	86.90%	21.2
HL60_ETP_3	86.70%	23
KASUMI1_CTR_1	87.20%	23.8
KASUMI1_CTR_2	87.00%	23.1
KASUMI1_CTR_3	86.60%	21.9
KASUMI1_ETP_1	86.80%	24.7
KASUMI1_ETP_2	85.50%	23
KASUMI1_ETP_3	86.40%	23.5
MOLM13_CTR_1	87.20%	22.9
MOLM13_CTR_2	86.90%	22.6
MOLM13_CTR_3	87.10%	22.7
MOLM13_ETP_1	85.20%	20.5
MOLM13_ETP_2	85.60%	22.5
MOLM13_ETP_3	85.40%	22.5
MONOMAC6_CTR_1	89.10%	23
MONOMAC6_CTR_2	88.90%	23.6
MONOMAC6_CTR_3	89.00%	24
MONOMAC6_ETP_1	88.50%	24.4
MONOMAC6_ETP_2	88.20%	23.3
MONOMAC6_ETP_3	88.50%	24.9
MV411_CTR_1	88.00%	22.7
MV411_CTR_2	87.90%	20.9
MV411_CTR_3	88.00%	22.9
MV411_ETP_3	87.90%	26.2
NB4_CTR_1	88.70%	23.9
NB4_CTR_2	88.30%	22.1
NB4_CTR_3	87.80%	21.1
NB4_ETP_1	87.60%	24.2
NB4_ETP_2	87.10%	22.5
NB4_ETP_3	86.90%	22.8
NOMO1_CTR_1	88.20%	22.7
NOMO1_CTR_2	88.00%	23.5

NOMO1_CTR_3	88.10%	21.5
NOMO1_ETP_1	88.10%	21.8
NOMO1_ETP_2	88.00%	22.1
NOMO1_ETP_3	88.40%	22.2
OCIAML2_CTR_1	87.70%	23.8
OCIAML2_CTR_2	87.70%	22
OCIAML2_CTR_3	87.40%	22.2
OCIAML2_ETP_3	87.50%	21.2
OCIAML3_CTR_1	89.00%	23.1
OCIAML3_CTR_2	88.80%	22.8
OCIAML3_CTR_3	88.60%	23.8
OCIAML3_ETP_1	89.00%	24.1
OCIAML3_ETP_2	89.00%	25.2
OCIAML3_ETP_3	88.80%	24.8
THP1_CTR_1	88.00%	22
THP1_CTR_2	87.10%	22.7
THP1_CTR_3	87.60%	21.8
THP1_ETP_1	88.00%	23.8
THP1_ETP_2	87.40%	22.3
THP1_ETP_3	87.30%	24.3

Appendix table 4: Standalone cytotoxicity of the drugs inhibiting selected drivers in AML cell line. Cells were treated with 3 concentrations of each drug for 24 hours. Two-way ANOVA with Benjamini and Hochberg FDR correction test was performed to determine significant standalone cytotoxicity

Drug (driver)	Treatment concentration (μM)	Mean difference	q value										
			F-36P	HL-60	KASUMI-1	MOLM-13	MONO-MAC-6	MV-4-11	NB-4	NOMO-1	OCI-AML2	OCI-AML3	THP-1
GDC-0152 (BIRC5)	10	10.68	0.9717	0.4994	0.5955	0.8723	0.8661	0.3159	0.2301	0.6627	0.2204	**0.0408**	0.1738
	0.1	1.532	0.9717	0.5612	0.5955	0.7171	0.8943	0.8857	0.2777	0.9505	0.3106	**0.0408**	0.9151
	0.001	-1.963	0.9717	0.83	0.8623	0.7191	0.8943	0.7337	0.8791	0.8579	0.12	**0.0291**	0.7585
GSK-1838705A (IGF1R)	10	85.3	**<0.0001**	**<0.0001**	**<0.0001**	0.1719	0.3331	**<0.0001**	**<0.0001**	**<0.0001**	**<0.0001**	**<0.0001**	**<0.0001**
	0.1	4.08	0.9717	**0.0041**	0.5574	0.9473	0.8661	0.7337	0.7725	0.3015	0.2204	**0.0169**	0.9515
	0.001	3.502	0.9717	0.5541	0.6986	0.8	0.8661	0.7515	0.9004	0.4933	0.537	0.0549	0.719
LY-3039478 (NOTCH1)	10	-2.693	0.9717	0.4994	0.7399	0.7171	0.8661	0.9605	0.0652	0.5825	0.796	**0.0108**	0.719
	0.1	1.129	0.9717	0.2832	0.6941	0.7171	0.8661	0.9124	**0.0306**	0.5421	0.8944	**0.0096**	0.719
	0.001	-4.146	0.9717	0.1466	0.7682	0.7519	0.8661	0.906	0.602	0.4933	0.8298	**0.0035**	0.719
Nicotinamide (PARP9)	10	-4.48	0.9717	0.5399	0.5955	0.7171	0.8661	0.7337	0.7725	0.9576	0.9715	0.2969	0.7856
	0.1	-6.55	0.9717	0.4416	0.5955	0.7191	0.8943	0.9605	0.8871	0.8015	0.5624	0.742	0.719
	0.001	-8.173	0.9717	0.9966	0.5574	0.6617	0.8661	0.7337	0.1449	0.7631	0.3182	0.7829	0.9151
Rapamycin (mTOR)	10	9.511	0.9717	**<0.0001**	**0.0065**	0.2481	0.8661	0.6897	**0.0198**	**0.0375**	**<0.0001**	**<0.0001**	**0.0006**
	0.1	3.771	0.9717	**0.0003**	**0.0205**	0.7036	0.8943	0.7337	0.2301	0.3861	0.1208	**<0.0001**	0.719
	0.001	7.931	0.9717	**0.0091**	0.0602	0.7225	0.8661	0.9605	0.2056	0.3695	0.1273	**<0.0001**	0.719
Rockout (ROCK1)	10	1.961	0.9717	0.0663	0.59	0.7876	0.8661	0.9558	0.1748	0.3015	**0.0264**	**0.0062**	**0.0255**
	0.1	-6.848	0.9717	0.8752	0.5955	0.7171	0.8943	0.9693	0.3002	0.9576	**0.0104**	0.3993	0.719
	0.001	1.646	0.9717	0.6357	0.5574	0.5752	0.8661	0.9605	0.8791	0.9576	**0.0264**	**0.0266**	0.719
Sabutoclax (BCL2A1)	10	42.76	**0.0007**	**<0.0001**	**<0.0001**	**0.0192**	**0.0003**	**<0.0001**	**<0.0001**	**<0.0001**	**<0.0001**	**<0.0001**	**<0.0001**
	0.1	-1.232	0.9717	0.6357	0.8634	0.8073	0.8943	0.8636	0.1748	0.5421	0.9976	0.1612	0.719
	0.001	-5.607	0.9717	0.5052	0.5955	0.7171	0.8661	0.7941	0.2301	0.6471	0.9887	0.0744	0.1215
Sotrastaurin (PRKCH)	10	29.98	**0.0292**	**<0.0001**	**<0.0001**	**0.0109**	0.7467	**0.0008**	0.1748	0.3861	**<0.0001**	**<0.0001**	0.9594
	0.1	6.969	0.9717	0.6734	0.5955	0.9699	0.8661	0.5377	0.7543	0.86	**0.001**	0.0549	0.719
	0.001	6.241	0.9717	0.7203	0.5574	0.7171	0.8661	0.5377	0.7725	0.8579	**0.0375**	0.0549	0.9151
TWS-119 (MYC)	10	31.54	**0.0233**	**<0.0001**	**<0.0001**	**0.0087**	0.2445	**<0.0001**	**<0.0001**	**<0.0001**	**<0.0001**	**<0.0001**	**0.0152**
	0.1	-1.689	0.9717	0.83	**0.0277**	0.8723	0.8661	0.906	0.8791	0.8579	0.2239	0.0928	0.9594
	0.001	1.202	0.9717	0.83	0.5955	0.8723	0.8661	0.8857	0.8791	0.9649	0.6895	0.1425	0.719

Volasertib (PLK1)	10	83.03	**<0.0001**	**<0.0001**	**<0.0001**	**0.0008**	**<0.0001**	**<0.0001**	**<0.0001**	**<0.0001**	**<0.0001**	**<0.0001**	**<0.0001**
	0.1	21.08	0.255	**<0.0001**	**<0.0001**	**0.0192**	0.8661	**0.0001**	**<0.0001**	**<0.0001**	**<0.0001**	**<0.0001**	0.1596
	0.001	14.07	0.8191	**0.0149**	0.9294	0.2001	0.8661	0.7337	0.8791	**0.0015**	0.4652	**<0.0001**	0.719
Vorinostat (HDAC)	10	64.95	**<0.0001**	**<0.0001**	**<0.0001**	**0.0225**	0.9508	**<0.0001**	**<0.0001**	**0.0089**	**<0.0001**	**<0.0001**	0.1596
	0.1	-9.609	0.9717	**0.0177**	0.7682	0.5752	0.8661	0.7674	0.997	0.9649	0.8731	0.9865	0.906
	0.001	-7.394	0.9717	0.3912	0.9294	0.4114	0.8661	0.906	0.8791	0.7631	0.9388	0.9865	0.719

Appendix table 5: Synergy with etoposide of the drugs inhibiting selected drivers in AML cell line. Cells were treated with 3 concentrations of each drug in combination with IC_{25} concentration of etoposide for 24 hours. Combination index (CI) was calculated to determine either synergistic (CI<1), additive (CI=1), or antagonist (CI>1) effects.

Drug (driver)	Treatment concentration (µM)	Combination index (CI)										
		F-36P	HL-60	KASUMI-1	MOLM-13	MONO-MAC-6	MV-4-11	NB-4	NOMO-1	OCI-AML2	OCI-AML3	THP-1
GDC-0152 (BIRC5)	10	**0.7**	**0.9**	1.1	**0.9**	**1.0**	1.4	**0.9**	1.4	1.3	1.3	1.2
	0.1	**0.7**	**0.9**	1.1	**0.8**	**0.8**	1.2	**1.0**	**1.0**	1.1	1.3	**0.8**
	0.001	**0.8**	**0.7**	**1.0**	**0.7**	**0.8**	1.2	**1.0**	**0.8**	**1.0**	1.2	**0.8**
GSK-1838705A (IGF1R)	10	1.4	**1.0**	1.2	1.4	1.3	1.6	**0.5**	1.3	1.3	1.5	**0.8**
	0.1	1.2	1.4	1.1	1.2	1.4	1.3	**0.9**	1.2	1.4	1.4	**0.7**
	0.001	1.3	1.5	1.5	1.1	1.3	1.4	1.2	1.3	1.4	1.6	1.2
LY-3039478 (NOTCH1)	10	3.2	1.2	1.3	**0.7**	1.3	1.3	**1.0**	1.3	1.1	1.6	1.3
	0.1	1.3	1.2	1.2	**0.8**	1.1	1.2	1.8	1.3	1.1	1.5	1.3
	0.001	10.3	1.3	1.3	**0.8**	1.1	1.5	1.2	1.3	1.1	1.7	**0.8**
Nicotinamide (PARP9)	10	**1.0**	**1.0**	1.2	**0.9**	1.5	1.9	1.2	2.3	1.3	1.2	**1.0**
	0.1	**0.8**	1.1	1.2	**0.8**	1.1	**0.6**	**0.7**	1.4	**0.9**	**1.0**	**0.9**
	0.001	**0.6**	1.1	**1.0**	**0.8**	1.3	**0.6**	**0.7**	**0.9**	**0.9**	**1.0**	**0.8**
Rapamycin (mTOR)	10	1.8	1.3	1.6	**0.9**	1.4	**0.5**	1.2	1.4	1.5	1.3	1.1
	0.1	1.1	1.6	1.6	**0.9**	1.1	**1.0**	2.3	1.1	1.5	1.2	**0.9**
	0.001	1.9	1.4	1.4	1.1	**1.0**	**0.8**	**1.0**	**0.9**	1.1	1.3	1.1
Rockout (ROCK1)	10	**1.0**	**0.9**	1.2	**0.7**	**0.8**	**0.7**	1.2	**0.8**	1.4	1.4	1.1
	0.1	1.2	**0.7**	1.3	1.1	**0.9**	**0.5**	1.3	**0.7**	1.4	1.6	**1.0**
	0.001	1.1	**1.0**	1.3	**0.6**	**1.0**	**0.7**	1.5	1.1	1.3	1.5	1.3
Sabutoclax (BCL2A1)	10	-	1.1	1.8	**0.8**	1.2	1.4	1.5	1.4	1.1	1.6	1.7
	0.1	-	1.3	1.5	**0.9**	1.1	1.3	1.5	1.7	1.3	1.4	1.6
	0.001	1.2	1.5	1.6	1.3	1.5	1.4	1.3	1.4	1.6	1.6	1.3
Sotrastaurin (PRKCH)	10	1.4	1.1	1.2	**0.9**	1.3	1.4	1.5	1.4	1.4	1.3	**0.8**
	0.1	1.1	**1.0**	1.2	**0.7**	**1.0**	1.5	1.1	1.1	1.5	1.3	**0.8**
	0.001	1.3	1.5	1.5	1.2	1.2	1.3	1.2	**0.8**	1.2	1.6	**0.6**
TWS-119 (MYC)	10	1.6	**0.9**	1.4	1.1	1.4	1.2	**1.0**	1.1	1.4	1.4	**0.8**
	0.1	4.3	1.3	1.5	1.2	1.4	1.2	1.7	1.4	1.6	1.3	1.1
	0.001	4.4	2.8	1.6	1.3	1.4	1.5	1.9	3.6	1.6	2.1	1.4
Volasertib (PLK1)	10	20.1	1.3	1.1	1.2	1.4	2.6	**0.5**	3.0	1.7	1.5	1.2
	0.1	2.8	2.3	2.0	2.0	2.0	15.2	2.0	5.2	1.8	3.0	1.4
	0.001	1.3	1.4	1.6	1.2	1.4	1.2	1.2	1.3	1.3	1.4	1.4
Vorinostat (HDAC)	10	1.3	1.1	1.1	**0.7**	1.7	**0.6**	**0.7**	1.1	**0.9**	**0.9**	**0.9**
	0.1	**0.9**	1.1	1.1	**0.6**	1.1	**0.5**	**0.5**	**0.7**	1.1	**0.8**	**0.7**
	0.001	1.1	1.4	1.5	1.1	**0.6**	1.2	1.1	**0.7**	1.2	1.2	**0.8**

R script developed in this work for comprehensive analysis of RNA-Seq data

```
#' ---
#' title: "AML_VP16_RNA-Seq-2017_edgeR"
#' author: "Piyush More"
#' date: "September 1st, 2017"
#' output: html_document
#' ---

library(edgeR)
library(Homo.sapiens)

setwd("/media/piyush/372429ff-0d6e-45d6-b529-527e3fb69028/RNA-
seq/AML_IMB_2017/Analysis/STAR/Gene_counts/edgeR")

# Read individual count files (.tab) into edgeR
files <- dir(pattern="*\\.tab$")

# Remove OCIAML2 samples
files <- files[ !grepl("OCIAML2", files) ]

# While loading counts define the groups
RG <- readDGE(files, columns = c(1,2), sep = " ", group = rep(1:20, times = 1, length.out = 60, each = 3))

rownames(RG$samples) <-
c("F36P_CTR_1","F36P_CTR_2","F36P_CTR_3","F36P_VP16_1","F36P_VP16_2","F36P_VP16_3","HL60_CTR
_1","HL60_CTR_2","HL60_CTR_3","HL60_VP16_1","HL60_VP16_2","HL60_VP16_3","Kasumi1_CTR_1","Ka
sumi1_CTR_2","Kasumi1_CTR_3","Kasumi1_VP16_1","Kasumi1_VP16_2","Kasumi1_VP16_3","MOLM13_CT
R_1","MOLM13_CTR_2","MOLM13_CTR_3","MOLM13_VP16_1","MOLM13_VP16_2","MOLM13_VP16_3",
"MONOMAC6_CTR_1","MONOMAC6_CTR_2","MONOMAC6_CTR_3","MONOMAC6_VP16_1","MONOMA
C6_VP16_2","MONOMAC6_VP16_3","MV411_CTR_1","MV411_CTR_2","MV411_CTR_3","MV411_VP16_1
","MV411_VP16_2","MV411_VP16_3","NB4_CTR_1","NB4_CTR_2","NB4_CTR_3","NB4_VP16_1","NB4_VP
16_2","NB4_VP16_3","NOMO1_CTR_1","NOMO1_CTR_2","NOMO1_CTR_3","NOMO1_VP16_1","NOMO1_
VP16_2","NOMO1_VP16_3","OCIAML3_CTR_1","OCIAML3_CTR_2","OCIAML3_CTR_3","OCIAML3_VP1
6_1","OCIAML3_VP16_2","OCIAML3_VP16_3","THP1_CTR_1","THP1_CTR_2","THP1_CTR_3","THP1_VP1
6_1","THP1_VP16_2","THP1_VP16_3")

colnames(RG$counts) <-
c("F36P_CTR_1","F36P_CTR_2","F36P_CTR_3","F36P_VP16_1","F36P_VP16_2","F36P_VP16_3","HL60_CTR
_1","HL60_CTR_2","HL60_CTR_3","HL60_VP16_1","HL60_VP16_2","HL60_VP16_3","Kasumi1_CTR_1","Ka
sumi1_CTR_2","Kasumi1_CTR_3","Kasumi1_VP16_1","Kasumi1_VP16_2","Kasumi1_VP16_3","MOLM13_CT
R_1","MOLM13_CTR_2","MOLM13_CTR_3","MOLM13_VP16_1","MOLM13_VP16_2","MOLM13_VP16_3",
"MONOMAC6_CTR_1","MONOMAC6_CTR_2","MONOMAC6_CTR_3","MONOMAC6_VP16_1","MONOMA
C6_VP16_2","MONOMAC6_VP16_3","MV411_CTR_1","MV411_CTR_2","MV411_CTR_3","MV411_VP16_1
","MV411_VP16_2","MV411_VP16_3","NB4_CTR_1","NB4_CTR_2","NB4_CTR_3","NB4_VP16_1","NB4_VP
16_2","NB4_VP16_3","NOMO1_CTR_1","NOMO1_CTR_2","NOMO1_CTR_3","NOMO1_VP16_1","NOMO1_
VP16_2","NOMO1_VP16_3","OCIAML3_CTR_1","OCIAML3_CTR_2","OCIAML3_CTR_3","OCIAML3_VP1
6_1","OCIAML3_VP16_2","OCIAML3_VP16_3","THP1_CTR_1","THP1_CTR_2","THP1_CTR_3","THP1_VP1
6_1","THP1_VP16_2","THP1_VP16_3")

RG$samples
View(RG$counts)

# Add gene annotation to the DGEList object
geneid <- row.names(RG)
```

```
geneid <- substr(geneid, 1, 15)
head(geneid)
genes <- select(Homo.sapiens, keys=geneid, columns=c("ENTREZID", "SYMBOL", "TXCHROM",
"DEFINITION", "OMIM"), keytype="ENSEMBL")
head(genes)
genes <- genes[!duplicated(genes$ENSEMBL),]
head(genes)
RG$genes <- genes
y <- RG

library("DESeq2")
library("edgeR")
library("hexbin")
library("latticeExtra")
library("vsn")
library("gplots")
library("RColorBrewer")
library("topGO")
library("gplots")
library("genefilter")
library("rtracklayer")
library("xtable")
library("GO.db")
library("goseq")
library("GenomicFeatures")
library("pathview")
library("NMF")
library("pheatmap")
library("GOplot")
library(knitr)
library("pcaExplorer")
library(DT)
library(ideal)
library("dplyr")

# Filter low counts: 3 are the minimum numbers of samples in each group and CPM 1 corresponds to counts of 6-7
keep <- rowSums(cpm(y)>1) >= 3

# Recalculate the library size
y <- y[keep, , keep.lib.sizes=FALSE]

# Create design for glm edgeR
group <- factor(y$samples$group)
group
levels(y$samples$group)

design <- model.matrix(~0+group, data=y$samples)
design

# DESeq object

samplesDesign <- read.csv("/media/piyush/372429ff-0d6e-45d6-b529-527e3fb69028/RNA-
seq/AML_IMB_2017/Analysis/STAR/Gene_counts/DESeq2/sampleDesign_New2.csv", sep = ",", header = T,
stringsAsFactors = F)
dds <- DESeqDataSetFromMatrix(y$counts ,samplesDesign, design = ~ celltype + condition)
colnames(dds) <- samplesDesign$sampleID
```

```
dds <- DESeq(dds)

# Variance stabilizing transformation
dds <- estimateSizeFactors(dds)
baseMean <- rowMeans(counts(dds, normalized=TRUE))
sum(baseMean > 1)
idx <- sample(which(baseMean > 5), 1000)
dds.sub <- dds[idx, ]
dds.sub <- estimateDispersions(dds.sub)
dispersionFunction(dds) <- dispersionFunction(dds.sub)
vsd <- varianceStabilizingTransformation(dds, blind=FALSE)

colnames(vsd) <-
c("F36P_CTR_1","F36P_CTR_2","F36P_CTR_3","F36P_VP16_1","F36P_VP16_2","F36P_VP16_3","HL60_CTR
_1","HL60_CTR_2","HL60_CTR_3","HL60_VP16_1","HL60_VP16_2","HL60_VP16_3","Kasumi1_CTR_1","Ka
sumi1_CTR_2","Kasumi1_CTR_3","Kasumi1_VP16_1","Kasumi1_VP16_2","Kasumi1_VP16_3","MOLM13_CT
R_1","MOLM13_CTR_2","MOLM13_CTR_3","MOLM13_VP16_1","MOLM13_VP16_2","MOLM13_VP16_3",
"MONOMAC6_CTR_1","MONOMAC6_CTR_2","MONOMAC6_CTR_3","MONOMAC6_VP16_1","MONOMA
C6_VP16_2","MONOMAC6_VP16_3","MV411_CTR_1","MV411_CTR_2","MV411_CTR_3","MV411_VP16_1
","MV411_VP16_2","MV411_VP16_3","NB4_CTR_1","NB4_CTR_2","NB4_CTR_3","NB4_VP16_1","NB4_VP
16_2","NB4_VP16_3","NOMO1_CTR_1","NOMO1_CTR_2","NOMO1_CTR_3","NOMO1_VP16_1","NOMO1_
VP16_2","NOMO1_VP16_3","OCIAML3_CTR_1","OCIAML3_CTR_2","OCIAML3_CTR_3","OCIAML3_VP1
6_1","OCIAML3_VP16_2","OCIAML3_VP16_3","THP1_CTR_1","THP1_CTR_2","THP1_CTR_3","THP1_VP1
6_1","THP1_VP16_2","THP1_VP16_3")

library(pheatmap)
pheatmap(as.matrix(dist(t(assay(vsd)))))
dev.print(pdf, './edgeR_Results/AML-global_pheatmap.pdf', width = 12, height = 12)

library(pcaExplorer)
pcaplot(vsd, title = "pcaplot - global", ellipse = F)
dev.print(pdf, './edgeR_Results/AML_pca_global.pdf', width = 12, height = 12)
pcaplot(vsd, intgroup = "celltype", title = "pcaplot celltype - global", ellipse = F)
dev.print(pdf, './edgeR_Results/AML_pca_global_celltype.pdf', width = 12, height = 12)

# Sample distances
sampleDists <- dist( t( assay(vsd) ) )
library("gplots")
library("RColorBrewer")
sampleDistMatrix <- as.matrix( sampleDists )
rownames(sampleDistMatrix) <- colnames(y$counts)
colors <- colorRampPalette( rev(brewer.pal(9, "Blues")) )(255)
hc <- hclust(sampleDists)
heatmap.2( sampleDistMatrix, Rowv=as.dendrogram(hc),
        symm=TRUE, trace="none", col=colors,
        margins=c(2,10), labCol=FALSE )
dev.print(pdf, './edgeR_Results/AML-global_heatmap.pdf', width = 12, height = 12)

# PCA plot
z <- plotPCA(vsd, intgroup = "condition")
nudge <- position_nudge(y = 2)
z + geom_label(aes(label = name), position = nudge)
dev.print(pdf, './edgeR_Results/AML_pca.pdf', width = 12, height = 12)
(data <- plotPCA(vsd, intgroup = "condition", returnData=TRUE))
percentVar <- round(100 * attr(data, "percentVar"))
library("ggplot2")
```

```
qplot(PC1, PC2, color=condition, shape=name, data=data) +
  xlab(paste0("PC1: ",percentVar[1],"% variance")) +
  ylab(paste0("PC2: ",percentVar[2],"% variance"))

# Calculate library normalization factor
y <- calcNormFactors(y)

# MDS plot to identify outliers
plotMDS(y, col = rainbow(22))
dev.print(pdf, './edgeR_Results/AML-global_MDS_plot.pdf', width = 12, height = 12)
y <- estimateDisp(y, design)
plotMeanVar(y, show.tagwise.vars = TRUE, NBline = TRUE)
dev.print(pdf, './edgeR_Results/AML-global_mean_var.pdf')
plotBCV(y)
dev.print(pdf, './edgeR_Results/AML-global_BCV.pdf', width = 12, height = 12)
fit <- glmFit(y, design)

# Make all contrasts together
my.contrasts <- makeContrasts(f36p=group2-group1, hl60=group4-group3, kasumi1=group6-group5,
molm13=group8-group7, monomac6=group10-group9, mv411=group12-group11, nb4=group14-group13,
nomo1=group16-group15, luciaml3=group18-group17, thp1=group20-group19, levels = design)
my.contrasts
my.contrasts2 <- makeContrasts(resistant=group2-group8, resistant.ctr=group1-group7, levels = design)
my.contrasts2

# Differential expression
f36p.vp16.VS.ctr <- glmLRT(fit, contrast = my.contrasts[,"f36p"])
hl60.vp16.VS.ctr <- glmLRT(fit, contrast = my.contrasts[,"hl60"])
kasumi1.vp16.VS.ctr <- glmLRT(fit, contrast = my.contrasts[,"kasumi1"])
molm13.vp16.VS.ctr <- glmLRT(fit, contrast = my.contrasts[,"molm13"])
monomac6.vp16.VS.ctr <- glmLRT(fit, contrast = my.contrasts[,"monomac6"])
mv411.vp16.VS.ctr <- glmLRT(fit, contrast = my.contrasts[,"mv411"])
nb4.vp16.VS.ctr <- glmLRT(fit, contrast = my.contrasts[,"nb4"])
nomo1.vp16.VS.ctr <- glmLRT(fit, contrast = my.contrasts[,"nomo1"])
luciaml3.vp16.VS.ctr <- glmLRT(fit, contrast = my.contrasts[,"luciaml3"])
thp1.vp16.VS.ctr <- glmLRT(fit, contrast = my.contrasts[,"thp1"])
f36p.vp16.VS.molm13.vp16 <- glmLRT(fit, contrast = my.contrasts2[,"resistant"])
f36p.VS.molm13.ctr <- glmLRT(fit, contrast = my.contrasts2[,"resistant.ctr"])

# Filter top DEG according to FDR
res_f36p.vp16.VS.ctr <- topTags(f36p.vp16.VS.ctr, n = nrow(f36p.vp16.VS.ctr), sort.by = "PValue", p.value = 0.05)
res_hl60.vp16.VS.ctr <- topTags(hl60.vp16.VS.ctr, n = nrow(hl60.vp16.VS.ctr), sort.by = "PValue", p.value = 0.05)
res_kasumi1.vp16.VS.ctr <- topTags(kasumi1.vp16.VS.ctr, n = nrow(kasumi1.vp16.VS.ctr), sort.by = "PValue",
p.value = 0.05)
res_molm13.vp16.VS.ctr <- topTags(molm13.vp16.VS.ctr, n = nrow(molm13.vp16.VS.ctr), sort.by = "PValue",
p.value = 0.05)
res_monomac6.vp16.VS.ctr <- topTags(monomac6.vp16.VS.ctr, n = nrow(monomac6.vp16.VS.ctr), sort.by =
"PValue", p.value = 0.05)
res_mv411.vp16.VS.ctr <- topTags(mv411.vp16.VS.ctr, n = nrow(mv411.vp16.VS.ctr), sort.by = "PValue", p.value
= 0.05)
res_nb4.vp16.VS.ctr <- topTags(nb4.vp16.VS.ctr, n = nrow(nb4.vp16.VS.ctr), sort.by = "PValue", p.value = 0.05)
res_nomo1.vp16.VS.ctr <- topTags(nomo1.vp16.VS.ctr, n = nrow(nomo1.vp16.VS.ctr), sort.by = "PValue", p.value
= 0.05)
res_luciaml3.vp16.VS.ctr <- topTags(luciaml3.vp16.VS.ctr, n = nrow(luciaml3.vp16.VS.ctr), sort.by = "PValue",
p.value = 0.05)
res_thp1.vp16.VS.ctr <- topTags(thp1.vp16.VS.ctr, n = nrow(thp1.vp16.VS.ctr), sort.by = "PValue", p.value = 0.05)
```

```
res_f36p.vp16.VS.molm13.vp16 <- topTags(f36p.vp16.VS.molm13.vp16, n = nrow(f36p.vp16.VS.molm13.vp16), sort.by = "PValue", p.value = 0.05)
res_f36p.VS.molm13.ctr <- topTags(f36p.VS.molm13.ctr, n = nrow(f36p.VS.molm13.ctr), sort.by = "PValue", p.value = 0.05)

# Filter DEG with logFC >= |1|
keep_f36p <- abs(res_f36p.vp16.VS.ctr$table$logFC) >= 1
res_f36p.vp16.VS.ctr <- res_f36p.vp16.VS.ctr[keep_f36p, ]
keep_hl60 <- abs(res_hl60.vp16.VS.ctr$table$logFC) >= 1
res_hl60.vp16.VS.ctr <- res_hl60.vp16.VS.ctr[keep_hl60, ]
keep_kasumi1 <- abs(res_kasumi1.vp16.VS.ctr$table$logFC) >= 1
res_kasumi1.vp16.VS.ctr <- res_kasumi1.vp16.VS.ctr[keep_kasumi1, ]
keep_molm13 <- abs(res_molm13.vp16.VS.ctr$table$logFC) >= 1
res_molm13.vp16.VS.ctr <- res_molm13.vp16.VS.ctr[keep_molm13, ]
keep_monomac6 <- abs(res_monomac6.vp16.VS.ctr$table$logFC) >= 1
res_monomac6.vp16.VS.ctr <- res_monomac6.vp16.VS.ctr[keep_monomac6, ]
keep_mv411 <- abs(res_mv411.vp16.VS.ctr$table$logFC) >= 1
res_mv411.vp16.VS.ctr <- res_mv411.vp16.VS.ctr[keep_mv411, ]
keep_nb4 <- abs(res_nb4.vp16.VS.ctr$table$logFC) >= 1
res_nb4.vp16.VS.ctr <- res_nb4.vp16.VS.ctr[keep_nb4, ]
keep_nomo1 <- abs(res_nomo1.vp16.VS.ctr$table$logFC) >= 1
res_nomo1.vp16.VS.ctr <- res_nomo1.vp16.VS.ctr[keep_nomo1, ]
keep_ociaml3 <- abs(res_ociaml3.vp16.VS.ctr$table$logFC) >= 1
res_ociaml3.vp16.VS.ctr <- res_ociaml3.vp16.VS.ctr[keep_ociaml3, ]
keep_thp1 <- abs(res_thp1.vp16.VS.ctr$table$logFC) >= 1
res_thp1.vp16.VS.ctr <- res_thp1.vp16.VS.ctr[keep_thp1, ]
keep_resistant <- abs(res_f36p.vp16.VS.molm13.vp16$table$logFC) >= 1
res_f36p.vp16.VS.molm13.vp16 <- res_f36p.vp16.VS.molm13.vp16[keep_resistant, ]
keep_resistant.ctr <- abs(res_f36p.VS.molm13.ctr$table$logFC) >= 1
res_f36p.VS.molm13.ctr <- res_f36p.VS.molm13.ctr[keep_resistant.ctr, ]

plotMD(f36p.vp16.VS.ctr)
abline(h=c(-1, 1), col="blue")
dev.print(pdf, 'f36p_MD_plot.pdf')
plotMD(hl60.vp16.VS.ctr)
abline(h=c(-1, 1), col="blue")
dev.print(pdf, 'hl60_MD_plot.pdf')
plotMD(kasumi1.vp16.VS.ctr)
abline(h=c(-1, 1), col="blue")
dev.print(pdf, 'kasumi1_MD_plot.pdf')
plotMD(molm13.vp16.VS.ctr)
abline(h=c(-1, 1), col="blue")
dev.print(pdf, 'molm13_MD_plot.pdf')
plotMD(monomac6.vp16.VS.ctr)
abline(h=c(-1, 1), col="blue")
dev.print(pdf, 'monomac6_MD_plot.pdf')
plotMD(mv411.vp16.VS.ctr)
abline(h=c(-1, 1), col="blue")
dev.print(pdf, 'mv411_MD_plot.pdf')
plotMD(nb4.vp16.VS.ctr)
abline(h=c(-1, 1), col="blue")
dev.print(pdf, 'nb4_MD_plot.pdf')
plotMD(nomo1.vp16.VS.ctr)
abline(h=c(-1, 1), col="blue")
dev.print(pdf, 'nomo1_MD_plot.pdf')
plotMD(ociaml3.vp16.VS.ctr)
```

```
abline(h=c(-1, 1), col="blue")
dev.print(pdf, 'ociaml3_MD_plot.pdf')
plotMD(thp1.vp16.VS.ctr)
abline(h=c(-1, 1), col="blue")
dev.print(pdf, 'thp1_MD_plot.pdf')
plotMD(f36p.vp16.VS.molm13.vp16)
abline(h=c(-1, 1), col="blue")
dev.print(pdf, 'f36p_vs_molm13_vp16_MD_plot.pdf')
plotMD(f36p.VS.molm13.ctr)
abline(h=c(-1, 1), col="blue")
dev.print(pdf, 'f36p_vs_molm13_ctr_MD_plot.pdf')

# Inspect depth-adjusted reads per million for some top DEGs
nc <- cpm(y, normalized.lib.sizes = TRUE)
rn_f36p <- rownames(topTags(f36p.vp16.VS.ctr)$table)
rn_hl60 <- rownames(topTags(hl60.vp16.VS.ctr)$table)
rn_kasumi1 <- rownames(topTags(kasumi1.vp16.VS.ctr)$table)
rn_molm13 <- rownames(topTags(molm13.vp16.VS.ctr)$table)
rn_monomac6 <- rownames(topTags(monomac6.vp16.VS.ctr)$table)
rn_mv411 <- rownames(topTags(mv411.vp16.VS.ctr)$table)
rn_nb4 <- rownames(topTags(nb4.vp16.VS.ctr)$table)
rn_nomo1 <- rownames(topTags(nomo1.vp16.VS.ctr)$table)
rn_ociaml3 <- rownames(topTags(ociaml3.vp16.VS.ctr)$table)
rn_thp1 <- rownames(topTags(thp1.vp16.VS.ctr)$table)
rn_resistant <- rownames(topTags(f36p.vp16.VS.molm13.vp16)$table)
rn_resistant.ctr <- rownames(topTags(f36p.VS.molm13.ctr)$table)

# MA plot
# F36P
deg_f36p <- rn_f36p[topTags(f36p.vp16.VS.ctr)$table$FDR < .05]
plotSmear(y, de.tags = deg_f36p, main = "F36P - VP16 VS Control")
dev.print(pdf, './edgeR_Results/f36p_smear_plot.pdf')
tt_f36p <- topTags(f36p.vp16.VS.ctr, n=nrow(y))
plot(-log10(PValue) ~ logFC, tt_f36p, pch=20)
title(main = "F36P - VP16 VS Control")
with(subset(tt_f36p$table, FDR < .05), points(logFC, -log10(PValue), col = "red"))
with(subset(tt_f36p$table, abs(logFC) > 1), points(logFC, -log10(PValue),col = "orange"))
with(subset(tt_f36p$table, FDR < 0.05 & abs(logFC) > 1), points(logFC, -log10(PValue), col = "green"))
legend("topright", legend = c("FDR < 0.05", "logFC > 1", "Both"), pch = 16, col = c("red", "orange", "green"))
dev.print(pdf, './edgeR_Results/f36p_volcano_plot.pdf')

# HL60
deg_hl60 <- rn_hl60[topTags(hl60.vp16.VS.ctr)$table$FDR < .05]
plotSmear(y, de.tags = deg_hl60, main = "HL60 - VP16 VS Control")
dev.print(pdf, './edgeR_Results/hl60_smear_plot.pdf')
tt_hl60 <- topTags(hl60.vp16.VS.ctr, n=nrow(y))
plot(-log10(PValue) ~ logFC, tt_hl60, pch=20)
title(main = "HL60 - VP16 VS Control")
with(subset(tt_hl60$table, FDR < .05), points(logFC, -log10(PValue), col = "red"))
with(subset(tt_hl60$table, abs(logFC) > 1), points(logFC, -log10(PValue),col = "orange"))
with(subset(tt_hl60$table, FDR < 0.05 & abs(logFC) > 1), points(logFC, -log10(PValue), col = "green"))
legend("topright", legend = c("FDR < 0.05", "logFC > 1", "Both"), pch = 16, col = c("red", "orange", "green"))
dev.print(pdf, './edgeR_Results/hl60_volcano_plot.pdf')

# KASUMI1
deg_kasumi1 <- rn_kasumi1[topTags(kasumi1.vp16.VS.ctr)$table$FDR < .05]
```

```
plotSmear(y, de.tags = deg_kasumi1, main = "KASUMI1 - VP16 VS Control")
dev.print(pdf, './edgeR_Results/kasumi1_smear_plot.pdf')
tt_kasumi1 <- topTags(kasumi1.vp16.VS.ctr, n=nrow(y))
plot(-log10(PValue) ~ logFC, tt_kasumi1, pch=20)
title(main = "KASUMI1 - VP16 VS Control")
with(subset(tt_kasumi1$table, FDR < .05), points(logFC, -log10(PValue), col = "red"))
with(subset(tt_kasumi1$table, abs(logFC) > 1), points(logFC, -log10(PValue),col = "orange"))
with(subset(tt_kasumi1$table, FDR < 0.05 & abs(logFC) > 1), points(logFC, -log10(PValue), col = "green"))
legend("topright", legend = c("FDR < 0.05", "logFC > 1", "Both"), pch = 16, col = c("red", "orange", "green"))
dev.print(pdf, './edgeR_Results/kasumi1_volcano_plot.pdf')

# MOLM13
deg_molm13 <- rn_molm13[topTags(molm13.vp16.VS.ctr)$table$FDR < .05]
plotSmear(y, de.tags = deg_molm13, main = "MOLM13 - VP16 VS Control")
dev.print(pdf, './edgeR_Results/molm13_smear_plot.pdf')
tt_molm13 <- topTags(molm13.vp16.VS.ctr, n=nrow(y))
plot(-log10(PValue) ~ logFC, tt_molm13, pch=20)
title(main = "MOLM13 - VP16 VS Control")
with(subset(tt_molm13$table, FDR < .05), points(logFC, -log10(PValue), col = "red"))
with(subset(tt_molm13$table, abs(logFC) > 1), points(logFC, -log10(PValue),col = "orange"))
with(subset(tt_molm13$table, FDR < 0.05 & abs(logFC) > 1), points(logFC, -log10(PValue), col = "green"))
legend("topright", legend = c("FDR < 0.05", "logFC > 1", "Both"), pch = 16, col = c("red", "orange", "green"))
dev.print(pdf, './edgeR_Results/molm13_volcano_plot.pdf')

# MONOMAC6
deg_monomac6 <- rn_monomac6[topTags(monomac6.vp16.VS.ctr)$table$FDR < .05]
plotSmear(y, de.tags = deg_monomac6, main = "MONOMAC6 - VP16 VS Control")
dev.print(pdf, './edgeR_Results/monomac6_smear_plot.pdf')
tt_monomac6 <- topTags(monomac6.vp16.VS.ctr, n=nrow(y))
plot(-log10(PValue) ~ logFC, tt_monomac6, pch=20)
title(main = "MONOMAC6 - VP16 VS Control")
with(subset(tt_monomac6$table, FDR < .05), points(logFC, -log10(PValue), col = "red"))
with(subset(tt_monomac6$table, abs(logFC) > 1), points(logFC, -log10(PValue),col = "orange"))
with(subset(tt_monomac6$table, FDR < 0.05 & abs(logFC) > 1), points(logFC, -log10(PValue), col = "green"))
legend("topright", legend = c("FDR < 0.05", "logFC > 1", "Both"), pch = 16, col = c("red", "orange", "green"))
dev.print(pdf, './edgeR_Results/monomac6_volcano_plot.pdf')

# MV411
deg_mv411 <- rn_mv411[topTags(mv411.vp16.VS.ctr)$table$FDR < .05]
plotSmear(y, de.tags = deg_mv411, main = "MV411 - VP16 VS Control")
dev.print(pdf, './edgeR_Results/mv411_smear_plot.pdf')
tt_mv411 <- topTags(mv411.vp16.VS.ctr, n=nrow(y))
plot(-log10(PValue) ~ logFC, tt_mv411, pch=20)
title(main = "MV411 - VP16 VS Control")
with(subset(tt_mv411$table, FDR < .05), points(logFC, -log10(PValue), col = "red"))
with(subset(tt_mv411$table, abs(logFC) > 1), points(logFC, -log10(PValue),col = "orange"))
with(subset(tt_mv411$table, FDR < 0.05 & abs(logFC) > 1), points(logFC, -log10(PValue), col = "green"))
legend("topright", legend = c("FDR < 0.05", "logFC > 1", "Both"), pch = 16, col = c("red", "orange", "green"))
dev.print(pdf, './edgeR_Results/mv411_volcano_plot.pdf')

# NB4
deg_nb4 <- rn_nb4[topTags(nb4.vp16.VS.ctr)$table$FDR < .05]
plotSmear(y, de.tags = deg_nb4, main = "NB4 - VP16 VS Control")
dev.print(pdf, './edgeR_Results/nb4_smear_plot.pdf')
tt_nb4 <- topTags(nb4.vp16.VS.ctr, n=nrow(y))
plot(-log10(PValue) ~ logFC, tt_nb4, pch=20)
```

```
title(main = "NB4 - VP16 VS Control")
with(subset(tt_nb4$table, FDR < .05), points(logFC, -log10(PValue), col = "red"))
with(subset(tt_nb4$table, abs(logFC) > 1), points(logFC, -log10(PValue),col = "orange"))
with(subset(tt_nb4$table, FDR < 0.05 & abs(logFC) > 1), points(logFC, -log10(PValue), col = "green"))
legend("topright", legend = c("FDR < 0.05", "logFC > 1", "Both"), pch = 16, col = c("red", "orange", "green"))
dev.print(pdf, './edgeR_Results/nb4_volcano_plot.pdf')

# NOMO1
deg_nomo1 <- rn_nomo1[topTags(nomo1.vp16.VS.ctr)$table$FDR < .05]
plotSmear(y, de.tags = deg_nomo1, main = "NOMO1 - VP16 VS Control")
dev.print(pdf, './edgeR_Results/nomo1_smear_plot.pdf')
tt_nomo1 <- topTags(nomo1.vp16.VS.ctr, n=nrow(y))
plot(-log10(PValue) ~ logFC, tt_nomo1, pch=20)
title(main = "NOMO1 - VP16 VS Control")
with(subset(tt_nomo1$table, FDR < .05), points(logFC, -log10(PValue), col = "red"))
with(subset(tt_nomo1$table, abs(logFC) > 1), points(logFC, -log10(PValue),col = "orange"))
with(subset(tt_nomo1$table, FDR < 0.05 & abs(logFC) > 1), points(logFC, -log10(PValue), col = "green"))
legend("topright", legend = c("FDR < 0.05", "logFC > 1", "Both"), pch = 16, col = c("red", "orange", "green"))
dev.print(pdf, './edgeR_Results/nomo1_volcano_plot.pdf')

# OCIAML3
deg_ociaml3 <- rn_ociaml3[topTags(ociaml3.vp16.VS.ctr)$table$FDR < .05]
plotSmear(y, de.tags = deg_ociaml3, main = "OCIAML3 - VP16 VS Control")
dev.print(pdf, './edgeR_Results/ociaml3_smear_plot.pdf')
tt_ociaml3 <- topTags(ociaml3.vp16.VS.ctr, n=nrow(y))
plot(-log10(PValue) ~ logFC, tt_ociaml3, pch=20)
title(main = "OCIAML3 - VP16 VS Control")
with(subset(tt_ociaml3$table, FDR < .05), points(logFC, -log10(PValue), col = "red"))
with(subset(tt_ociaml3$table, abs(logFC) > 1), points(logFC, -log10(PValue),col = "orange"))
with(subset(tt_ociaml3$table, FDR < 0.05 & abs(logFC) > 1), points(logFC, -log10(PValue), col = "green"))
legend("topright", legend = c("FDR < 0.05", "logFC > 1", "Both"), pch = 16, col = c("red", "orange", "green"))
dev.print(pdf, './edgeR_Results/ociaml3_volcano_plot.pdf')

# THP1
deg_thp1 <- rn_thp1[topTags(thp1.vp16.VS.ctr)$table$FDR < .05]
plotSmear(y, de.tags = deg_thp1, main = "THP1 - VP16 VS Control")
dev.print(pdf, './edgeR_Results/thp1_smear_plot.pdf')
tt_thp1 <- topTags(thp1.vp16.VS.ctr, n=nrow(y))
plot(-log10(PValue) ~ logFC, tt_thp1, pch=20)
title(main = "THP1 - VP16 VS Control")
with(subset(tt_thp1$table, FDR < .05), points(logFC, -log10(PValue), col = "red"))
with(subset(tt_thp1$table, abs(logFC) > 1), points(logFC, -log10(PValue),col = "orange"))
with(subset(tt_thp1$table, FDR < 0.05 & abs(logFC) > 1), points(logFC, -log10(PValue), col = "green"))
legend("topright", legend = c("FDR < 0.05", "logFC > 1", "Both"), pch = 16, col = c("red", "orange", "green"))
dev.print(pdf, './edgeR_Results/thp1_volcano_plot.pdf')

# F36P VS MOLM13 VP16
deg_resistant <- rn_resistant[topTags(f36p.vp16.VS.molm13.vp16)$table$FDR < .05]
plotSmear(y, de.tags = deg_resistant, main = "F36P VP16 VS MOLM13 VP16")
dev.print(pdf, './edgeR_Results/f36p-vp16_VS_mol13-vp16_smear_plot.pdf')
tt_resistant <- topTags(f36p.vp16.VS.molm13.vp16, n=nrow(y))
plot(-log10(PValue) ~ logFC, tt_resistant, pch=20)
title(main = "F36P VP16 VS MOLM13 VP16")
with(subset(tt_resistant$table, FDR < .05), points(logFC, -log10(PValue), col = "red"))
with(subset(tt_resistant$table, abs(logFC) > 1), points(logFC, -log10(PValue),col = "orange"))
with(subset(tt_resistant$table, FDR < 0.05 & abs(logFC) > 1), points(logFC, -log10(PValue), col = "green"))
```

```
legend("topright", legend = c("FDR < 0.05", "logFC > 1", "Both"), pch = 16, col = c("red", "orange", "green"))
dev.print(pdf, './edgeR_Results/f36p-vp16_VS_molm13-vp16_volcano_plot.pdf')

# F36P VS MOLM13 CTR
deg_resistant.ctr <- rn_resistant[topTags(f36p.VS.molm13.ctr)$table$FDR < .05]
plotSmear(y, de.tags = deg_resistant.ctr, main = "F36P VP16 VS MOLM13 CTR")
dev.print(pdf, './edgeR_Results/f36p-vp16_VS_mol13-ctr_smear_plot.pdf')
tt_resistant.ctr <- topTags(f36p.VS.molm13.ctr, n=nrow(y))
plot(-log10(PValue) ~ logFC, tt_resistant.ctr, pch=20)
title(main = "F36P VP16 VS MOLM13 CTR")
with(subset(tt_resistant.ctr$table, FDR < .05), points(logFC, -log10(PValue), col = "red"))
with(subset(tt_resistant.ctr$table, abs(logFC) > 1), points(logFC, -log10(PValue),col = "orange"))
with(subset(tt_resistant.ctr$table, FDR < 0.05 & abs(logFC) > 1), points(logFC, -log10(PValue), col = "green"))
legend("topright", legend = c("FDR < 0.05", "logFC > 1", "Both"), pch = 16, col = c("red", "orange", "green"))
dev.print(pdf, './edgeR_Results/f36p_VS_molm13-ctr_volcano_plot.pdf')

# Create result table
# Define functions to create links

createLinkGO <- function(val) {
  sprintf('<a href="http://amigo.geneontology.org/amigo/term/%s" target="_blank" class="btn btn-
primary">%s</a>',val,val)
}

createLinkENS  <- function(val, species="Homo_sapiens") {
  paste0('<a href="http://www.ensembl.org/',species,'/Gene/Summary?g=',val,'" target="_blank" class="btn btn-
primary">',val,'</a>')
}

createLinkGeneSymbol <- function(val) {
  paste0('<a href="http://www.genecards.org/cgi-bin/carddisp.pl?gene=',val,'" target="_blank" class="btn btn-
primary">',val,'</a>')
}

# Create tables
# F36P
tbl_res_f36p.vp16.VS.ctr <- res_f36p.vp16.VS.ctr$table
etbl_res_f36p.vp16.VS.ctr <- tbl_res_f36p.vp16.VS.ctr
etbl_res_f36p.vp16.VS.ctr$ENSEMBL <- createLinkENS(etbl_res_f36p.vp16.VS.ctr$ENSEMBL, species =
"Homo_sapiens")
etbl_res_f36p.vp16.VS.ctr$SYMBOL <- createLinkGeneSymbol(etbl_res_f36p.vp16.VS.ctr$SYMBOL)
datatable(etbl_res_f36p.vp16.VS.ctr, caption = "F36P - VP16 vs Control, DE genes", escape=F)
write.table(tbl_res_f36p.vp16.VS.ctr, "./edgeR_Results/DEG_Table_f36p.txt", sep = "\t", row.names = F)

# HL60
tbl_res_hl60.vp16.VS.ctr <- res_hl60.vp16.VS.ctr$table
etbl_res_hl60.vp16.VS.ctr <- tbl_res_hl60.vp16.VS.ctr
etbl_res_hl60.vp16.VS.ctr$ENSEMBL <- createLinkENS(etbl_res_hl60.vp16.VS.ctr$ENSEMBL, species =
"Homo_sapiens")
etbl_res_hl60.vp16.VS.ctr$SYMBOL <- createLinkGeneSymbol(etbl_res_hl60.vp16.VS.ctr$SYMBOL)
datatable(etbl_res_hl60.vp16.VS.ctr, caption = "HL60 - VP16 vs Control, DE genes", escape=F)
write.table(tbl_res_hl60.vp16.VS.ctr, "./edgeR_Results/DEG_Table_hl60.txt", sep = "\t", row.names = F)

# KASUMI1
tbl_res_kasumi1.vp16.VS.ctr <- res_kasumi1.vp16.VS.ctr$table
etbl_res_kasumi1.vp16.VS.ctr <- tbl_res_kasumi1.vp16.VS.ctr
```

```
etbl_res_kasumi1.vp16.VS.ctr$ENSEMBL <- createLinkENS(etbl_res_kasumi1.vp16.VS.ctr$ENSEMBL, species =
"Homo_sapiens")
etbl_res_kasumi1.vp16.VS.ctr$SYMBOL <- createLinkGeneSymbol(etbl_res_kasumi1.vp16.VS.ctr$SYMBOL)
datatable(etbl_res_kasumi1.vp16.VS.ctr, caption = "KASUMI1 - VP16 vs Control, DE genes", escape=F)
write.table(tbl_res_kasumi1.vp16.VS.ctr, "./edgeR_Results/DEG_Table_kasumi1.txt", sep = "\t", row.names = F)

# MOLM13
tbl_res_molm13.vp16.VS.ctr <- res_molm13.vp16.VS.ctr$table
etbl_res_molm13.vp16.VS.ctr <- tbl_res_molm13.vp16.VS.ctr
etbl_res_molm13.vp16.VS.ctr$ENSEMBL <- createLinkENS(etbl_res_molm13.vp16.VS.ctr$ENSEMBL, species =
"Homo_sapiens")
etbl_res_molm13.vp16.VS.ctr$SYMBOL <- createLinkGeneSymbol(etbl_res_molm13.vp16.VS.ctr$SYMBOL)
datatable(etbl_res_molm13.vp16.VS.ctr, caption = "MOLM13 - VP16 vs Control, DE genes", escape=F)
write.table(tbl_res_molm13.vp16.VS.ctr, "./edgeR_Results/DEG_Table_molm13.txt", sep = "\t", row.names = F)

# MONOMAC6
tbl_res_monomac6.vp16.VS.ctr <- res_monomac6.vp16.VS.ctr$table
etbl_res_monomac6.vp16.VS.ctr <- tbl_res_monomac6.vp16.VS.ctr
etbl_res_monomac6.vp16.VS.ctr$ENSEMBL <- createLinkENS(etbl_res_monomac6.vp16.VS.ctr$ENSEMBL,
species = "Homo_sapiens")
etbl_res_monomac6.vp16.VS.ctr$SYMBOL <-
createLinkGeneSymbol(etbl_res_monomac6.vp16.VS.ctr$SYMBOL)
datatable(etbl_res_monomac6.vp16.VS.ctr, caption = "MONOMAC6 - VP16 vs Control, DE genes", escape=F)
write.table(tbl_res_monomac6.vp16.VS.ctr, "./edgeR_Results/DEG_Table_monomac6.txt", sep = "\t", row.names =
F)

# MV411
tbl_res_mv411.vp16.VS.ctr <- res_mv411.vp16.VS.ctr$table
etbl_res_mv411.vp16.VS.ctr <- tbl_res_mv411.vp16.VS.ctr
etbl_res_mv411.vp16.VS.ctr$ENSEMBL <- createLinkENS(etbl_res_mv411.vp16.VS.ctr$ENSEMBL, species =
"Homo_sapiens")
etbl_res_mv411.vp16.VS.ctr$SYMBOL <- createLinkGeneSymbol(etbl_res_mv411.vp16.VS.ctr$SYMBOL)
datatable(etbl_res_mv411.vp16.VS.ctr, caption = "MV411 - VP16 vs Control, DE genes", escape=F)
write.table(tbl_res_mv411.vp16.VS.ctr, "./edgeR_Results/DEG_Table_mv411.txt", sep = "\t", row.names = F)

# NB4
tbl_res_nb4.vp16.VS.ctr <- res_nb4.vp16.VS.ctr$table
etbl_res_nb4.vp16.VS.ctr <- tbl_res_nb4.vp16.VS.ctr
etbl_res_nb4.vp16.VS.ctr$ENSEMBL <- createLinkENS(etbl_res_nb4.vp16.VS.ctr$ENSEMBL, species =
"Homo_sapiens")
etbl_res_nb4.vp16.VS.ctr$SYMBOL <- createLinkGeneSymbol(etbl_res_nb4.vp16.VS.ctr$SYMBOL)
datatable(etbl_res_nb4.vp16.VS.ctr, caption = "NB4 - VP16 vs Control, DE genes", escape=F)
write.table(tbl_res_nb4.vp16.VS.ctr, "./edgeR_Results/DEG_Table_nb4.txt", sep = "\t", row.names = F)

# NOMO1
tbl_res_nomo1.vp16.VS.ctr <- res_nomo1.vp16.VS.ctr$table
etbl_res_nomo1.vp16.VS.ctr <- tbl_res_nomo1.vp16.VS.ctr
etbl_res_nomo1.vp16.VS.ctr$ENSEMBL <- createLinkENS(etbl_res_nomo1.vp16.VS.ctr$ENSEMBL, species =
"Homo_sapiens")
etbl_res_nomo1.vp16.VS.ctr$SYMBOL <- createLinkGeneSymbol(etbl_res_nomo1.vp16.VS.ctr$SYMBOL)
datatable(etbl_res_nomo1.vp16.VS.ctr, caption = "NOMO1 - VP16 vs Control, DE genes", escape=F)
write.table(tbl_res_nomo1.vp16.VS.ctr, "./edgeR_Results/DEG_Table_nomo1.txt", sep = "\t", row.names = F)

# OCIAML3
tbl_res_ociaml3.vp16.VS.ctr <- res_ociaml3.vp16.VS.ctr$table
etbl_res_ociaml3.vp16.VS.ctr <- tbl_res_ociaml3.vp16.VS.ctr
```

```
etbl_res_ociaml3.vp16.VS.ctr$ENSEMBL <- createLinkENS(etbl_res_ociaml3.vp16.VS.ctr$ENSEMBL, species =
"Homo_sapiens")
etbl_res_ociaml3.vp16.VS.ctr$SYMBOL <- createLinkGeneSymbol(etbl_res_ociaml3.vp16.VS.ctr$SYMBOL)
datatable(etbl_res_ociaml3.vp16.VS.ctr, caption = "OCIAML3 - VP16 vs Control, DE genes", escape=F)
write.table(tbl_res_ociaml3.vp16.VS.ctr, "./edgeR_Results/DEG_Table_ociaml3.txt", sep = "\t", row.names = F)

# THP1
tbl_res_thp1.vp16.VS.ctr <- res_thp1.vp16.VS.ctr$table
etbl_res_thp1.vp16.VS.ctr <- tbl_res_thp1.vp16.VS.ctr
etbl_res_thp1.vp16.VS.ctr$ENSEMBL <- createLinkENS(etbl_res_thp1.vp16.VS.ctr$ENSEMBL, species =
"Homo_sapiens")
etbl_res_thp1.vp16.VS.ctr$SYMBOL <- createLinkGeneSymbol(etbl_res_thp1.vp16.VS.ctr$SYMBOL)
datatable(etbl_res_thp1.vp16.VS.ctr, caption = "THP1 - VP16 vs Control, DE genes", escape=F)
write.table(tbl_res_thp1.vp16.VS.ctr, "./edgeR_Results/DEG_Table_thp1.txt", sep = "\t", row.names = F)

# F36P VS MOLM13 VP16
tbl_res_f36p.vp16.VS.molm13.vp16 <- res_f36p.vp16.VS.molm13.vp16$table
etbl_res_f36p.vp16.VS.molm13.vp16 <- tbl_res_f36p.vp16.VS.molm13.vp16
etbl_res_f36p.vp16.VS.molm13.vp16$ENSEMBL <-
createLinkENS(etbl_res_f36p.vp16.VS.molm13.vp16$ENSEMBL, species = "Homo_sapiens")
etbl_res_f36p.vp16.VS.molm13.vp16$SYMBOL <-
createLinkGeneSymbol(etbl_res_f36p.vp16.VS.molm13.vp16$SYMBOL)
datatable(etbl_res_f36p.vp16.VS.molm13.vp16, caption = "F36P VS MOLM13 VP16, DE genes", escape=F)
write.table(tbl_res_f36p.vp16.VS.molm13.vp16, "./edgeR_Results/DEG_Table_f36p-vp16_VS-molm13-vp16.txt",
sep = "\t", row.names = F)

# F36P VS MOLM13 CTR
tbl_res_f36p.VS.molm13.ctr <- res_f36p.VS.molm13.ctr$table
etbl_res_f36p.VS.molm13.ctr <- tbl_res_f36p.VS.molm13.ctr
etbl_res_f36p.VS.molm13.ctr$ENSEMBL <- createLinkENS(etbl_res_f36p.VS.molm13.ctr$ENSEMBL, species =
"Homo_sapiens")
etbl_res_f36p.VS.molm13.ctr$SYMBOL <- createLinkGeneSymbol(etbl_res_f36p.VS.molm13.ctr$SYMBOL)
datatable(etbl_res_f36p.VS.molm13.ctr, caption = "F36P VS MOLM13 Control, DE genes", escape=F)
write.table(tbl_res_f36p.VS.molm13.ctr, "./edgeR_Results/DEG_Table_f36p_VS-molm13-ctr.txt", sep = "\t",
row.names = F)

# Functional interpretation
# Create annotation file

annoHuman <- import("/media/piyush/372429ff-0d6e-45d6-b529-527e3fb69028/RNA-
seq/AML_IMB_2017/Analysis/STAR/NOISeq/Gencode_v25_GRCh38.p7/gencode.v25.annotation.gtf")
cm2=data.frame(ensid=mcols(annoHuman)$gene_id,fromgtf=mcols(annoHuman)$gene_name,stringsAsFactors =
FALSE)
cm2 <- cm2[!duplicated(cm2),]
rownames(cm2) <- cm2$ensid
anno_df <- data.frame(gene_id = rownames(dds), stringsAsFactors = F)
anno_df$gene_name <- cm2$fromgtf[match(anno_df$gene_id,rownames(cm2))]
rownames(anno_df) <- anno_df$gene_id
head(anno_df)

# Create list of universally expressed genes
expressedInAssay <- (rowSums(assay(dds))>0)
geneUniverseExprENS <- rownames(dds)[expressedInAssay]
geneUniverseExpr <- anno_df$gene_name[match(geneUniverseExprENS,anno_df$gene_id)]
```

```
# Use topGOtable to annotate DEGs for biological processesGObps_f36p.vp16.VS.ctr <- topGOtable(DEgenes = res_f36p.vp16.VS.ctr$table$SYMBOL, BGgenes = geneUniverseExpr, ontology = "BP", geneID = "symbol", addGeneToTerms = TRUE, mapping = "org.Hs.eg.db")
# F36P
GObps_f36p.vp16.VS.ctr <- topGOtable(DEgenes = res_f36p.vp16.VS.ctr$table$SYMBOL, BGgenes = geneUniverseExpr, ontology = "BP", geneID = "symbol", addGeneToTerms = TRUE, mapping = "org.Hs.eg.db")
eGObps_f36p.vp16.VS.ctr <- GObps_f36p.vp16.VS.ctr
eGObps_f36p.vp16.VS.ctr$GO.ID <- createLinkGO(eGObps_f36p.vp16.VS.ctr$GO.ID)
eGObps_f36p.vp16.VS.ctr %>% datatable(caption = "topGO - Biological processes enriched in DE genes - F36P- VP16 vs Control", options = list(pageLength = 20),escape = FALSE)
write.table(GObps_f36p.vp16.VS.ctr, "./edgeR_Results/topGO_BP_f36p_vp16_VS_ctr.txt", sep = "\t", row.names = F)

# HL60
GObps_hl60.vp16.VS.ctr <- topGOtable(DEgenes = res_hl60.vp16.VS.ctr$table$SYMBOL, BGgenes = geneUniverseExpr, ontology = "BP", geneID = "symbol", addGeneToTerms = TRUE, mapping = "org.Hs.eg.db")
eGObps_hl60.vp16.VS.ctr <- GObps_hl60.vp16.VS.ctr
eGObps_hl60.vp16.VS.ctr$GO.ID <- createLinkGO(eGObps_hl60.vp16.VS.ctr$GO.ID)
eGObps_hl60.vp16.VS.ctr %>% datatable(caption = "topGO - Biological processes enriched in DE genes - HL60- VP16 vs Control", options = list(pageLength = 20),escape = FALSE)
write.table(GObps_hl60.vp16.VS.ctr, "./edgeR_Results/topGO_BP_hl60_vp16_VS_ctr.txt", sep = "\t", row.names = F)

# KASUMI1
GObps_kasumi1.vp16.VS.ctr <- topGOtable(DEgenes = res_kasumi1.vp16.VS.ctr$table$SYMBOL, BGgenes = geneUniverseExpr, ontology = "BP", geneID = "symbol", addGeneToTerms = TRUE, mapping = "org.Hs.eg.db")
eGObps_kasumi1.vp16.VS.ctr <- GObps_kasumi1.vp16.VS.ctr
eGObps_kasumi1.vp16.VS.ctr$GO.ID <- createLinkGO(eGObps_kasumi1.vp16.VS.ctr$GO.ID)
eGObps_kasumi1.vp16.VS.ctr %>% datatable(caption = "topGO - Biological processes enriched in DE genes - KASUMI1- VP16 vs Control", options = list(pageLength = 20),escape = FALSE)
write.table(GObps_kasumi1.vp16.VS.ctr, "./edgeR_Results/topGO_BP_kasumi1_vp16_VS_ctr.txt", sep = "\t", row.names = F)

# MOLM13
GObps_molm13.vp16.VS.ctr <- topGOtable(DEgenes = res_molm13.vp16.VS.ctr$table$SYMBOL, BGgenes = geneUniverseExpr, ontology = "BP", geneID = "symbol", addGeneToTerms = TRUE, mapping = "org.Hs.eg.db")
eGObps_molm13.vp16.VS.ctr <- GObps_molm13.vp16.VS.ctr
eGObps_molm13.vp16.VS.ctr$GO.ID <- createLinkGO(eGObps_molm13.vp16.VS.ctr$GO.ID)
eGObps_molm13.vp16.VS.ctr %>% datatable(caption = "topGO - Biological processes enriched in DE genes - MOLM13- VP16 vs Control", options = list(pageLength = 20),escape = FALSE)
write.table(GObps_molm13.vp16.VS.ctr, "./edgeR_Results/topGO_BP_molm13_vp16_VS_ctr.txt", sep = "\t", row.names = F)

# MONOMAC6
GObps_monomac6.vp16.VS.ctr <- topGOtable(DEgenes = res_monomac6.vp16.VS.ctr$table$SYMBOL, BGgenes = geneUniverseExpr, ontology = "BP", geneID = "symbol", addGeneToTerms = TRUE, mapping = "org.Hs.eg.db")
eGObps_monomac6.vp16.VS.ctr <- GObps_monomac6.vp16.VS.ctr
eGObps_monomac6.vp16.VS.ctr$GO.ID <- createLinkGO(eGObps_monomac6.vp16.VS.ctr$GO.ID)
eGObps_monomac6.vp16.VS.ctr %>% datatable(caption = "topGO - Biological processes enriched in DE genes - MONOMAC6- VP16 vs Control", options = list(pageLength = 20),escape = FALSE)
write.table(GObps_monomac6.vp16.VS.ctr, "./edgeR_Results/topGO_BP_monomac6_vp16_VS_ctr.txt", sep = "\t", row.names = F)

# MV411
GObps_mv411.vp16.VS.ctr <- topGOtable(DEgenes = res_mv411.vp16.VS.ctr$table$SYMBOL, BGgenes = geneUniverseExpr, ontology = "BP", geneID = "symbol", addGeneToTerms = TRUE, mapping = "org.Hs.eg.db")
```

```
eGObps_mv411.vp16.VS.ctr <- GObps_mv411.vp16.VS.ctr
eGObps_mv411.vp16.VS.ctr$GO.ID <- createLinkGO(eGObps_mv411.vp16.VS.ctr$GO.ID)
eGObps_mv411.vp16.VS.ctr %>% datatable(caption = "topGO - Biological processes enriched in DE genes - MV411- VP16 vs Control", options = list(pageLength = 20),escape = FALSE)
write.table(GObps_mv411.vp16.VS.ctr, "./edgeR_Results/topGO_BP_mv411_vp16_VS_ctr.txt", sep = "\t", row.names = F)

# NB4
GObps_nb4.vp16.VS.ctr <- topGOtable(DEgenes = res_nb4.vp16.VS.ctr$table$SYMBOL, BGgenes = geneUniverseExpr, ontology = "BP", geneID = "symbol", addGeneToTerms = TRUE, mapping = "org.Hs.eg.db")
eGObps_nb4.vp16.VS.ctr <- GObps_nb4.vp16.VS.ctr
eGObps_nb4.vp16.VS.ctr$GO.ID <- createLinkGO(eGObps_nb4.vp16.VS.ctr$GO.ID)
eGObps_nb4.vp16.VS.ctr %>% datatable(caption = "topGO - Biological processes enriched in DE genes - NB4- VP16 vs Control", options = list(pageLength = 20),escape = FALSE)
write.table(GObps_nb4.vp16.VS.ctr, "./edgeR_Results/topGO_BP_nb4_vp16_VS_ctr.txt", sep = "\t", row.names = F)

# NOMO1
GObps_nomo1.vp16.VS.ctr <- topGOtable(DEgenes = res_nomo1.vp16.VS.ctr$table$SYMBOL, BGgenes = geneUniverseExpr, ontology = "BP", geneID = "symbol", addGeneToTerms = TRUE, mapping = "org.Hs.eg.db")
eGObps_nomo1.vp16.VS.ctr <- GObps_nomo1.vp16.VS.ctr
eGObps_nomo1.vp16.VS.ctr$GO.ID <- createLinkGO(eGObps_nomo1.vp16.VS.ctr$GO.ID)
eGObps_nomo1.vp16.VS.ctr %>% datatable(caption = "topGO - Biological processes enriched in DE genes - NOMO1- VP16 vs Control", options = list(pageLength = 20),escape = FALSE)
write.table(GObps_nomo1.vp16.VS.ctr, "./edgeR_Results/topGO_BP_nomo1_vp16_VS_ctr.txt", sep = "\t", row.names = F)

# OCIAML3
GObps_ociaml3.vp16.VS.ctr <- topGOtable(DEgenes = res_ociaml3.vp16.VS.ctr$table$SYMBOL, BGgenes = geneUniverseExpr, ontology = "BP", geneID = "symbol", addGeneToTerms = TRUE, mapping = "org.Hs.eg.db")
eGObps_ociaml3.vp16.VS.ctr <- GObps_ociaml3.vp16.VS.ctr
eGObps_ociaml3.vp16.VS.ctr$GO.ID <- createLinkGO(eGObps_ociaml3.vp16.VS.ctr$GO.ID)
eGObps_ociaml3.vp16.VS.ctr %>% datatable(caption = "topGO - Biological processes enriched in DE genes - OCIAML3- VP16 vs Control", options = list(pageLength = 20),escape = FALSE)
write.table(GObps_ociaml3.vp16.VS.ctr, "./edgeR_Results/topGO_BP_ociaml3_vp16_VS_ctr.txt", sep = "\t", row.names = F)

# THP1
GObps_thp1.vp16.VS.ctr <- topGOtable(DEgenes = res_thp1.vp16.VS.ctr$table$SYMBOL, BGgenes = geneUniverseExpr, ontology = "BP", geneID = "symbol", addGeneToTerms = TRUE, mapping = "org.Hs.eg.db")
eGObps_thp1.vp16.VS.ctr <- GObps_thp1.vp16.VS.ctr
eGObps_thp1.vp16.VS.ctr$GO.ID <- createLinkGO(eGObps_thp1.vp16.VS.ctr$GO.ID)
eGObps_thp1.vp16.VS.ctr %>% datatable(caption = "topGO - Biological processes enriched in DE genes - THP1- VP16 vs Control", options = list(pageLength = 20),escape = FALSE)
write.table(GObps_thp1.vp16.VS.ctr, "./edgeR_Results/topGO_BP_thp1_vp16_VS_ctr.txt", sep = "\t", row.names = F)

# F36P VS MOLM13 VP16
GObps_f36p.vp16.VS.molm13.vp16 <- topGOtable(DEgenes = res_f36p.vp16.VS.molm13.vp16$table$SYMBOL, BGgenes = geneUniverseExpr, ontology = "BP", geneID = "symbol", addGeneToTerms = TRUE, mapping = "org.Hs.eg.db")
eGObps_f36p.vp16.VS.molm13.vp16 <- GObps_f36p.vp16.VS.molm13.vp16
eGObps_f36p.vp16.VS.molm13.vp16$GO.ID <- createLinkGO(eGObps_f36p.vp16.VS.molm13.vp16$GO.ID)
eGObps_f36p.vp16.VS.molm13.vp16 %>% datatable(caption = "topGO - Biological processes enriched in DE genes - F36P-VP16 VS MOLM13-VP16", options = list(pageLength = 20),escape = FALSE)
```

```
write.table(GObps_f36p.vp16.VS.molm13.vp16, "./edgeR_Results/topGO_BP_f36p-vp16_VS_molm13-vp16.txt",
sep = "\t", row.names = F)

# F36P VS MOLM13 CTR
GObps_f36p.VS.molm13.ctr <- topGOtable(DEgenes = res_f36p.VS.molm13.ctr$table$SYMBOL, BGgenes =
geneUniverseExpr, ontology = "BP", geneID = "symbol", addGeneToTerms = TRUE, mapping = "org.Hs.eg.db")
eGObps_f36p.VS.molm13.ctr <- GObps_f36p.VS.molm13.ctr
eGObps_f36p.VS.molm13.ctr$GO.ID <- createLinkGO(eGObps_f36p.VS.molm13.ctr$GO.ID)
eGObps_f36p.VS.molm13.ctr %>% datatable(caption = "topGO - Biological processes enriched in DE genes - F36P
VS MOLM13 Control", options = list(pageLength = 20),escape = FALSE)
write.table(GObps_f36p.VS.molm13.ctr, "./edgeR_Results/topGO_BP_f36p_VS_molm13-control.txt", sep = "\t",
row.names = F)

# remove NA values in ENTREZ and SYMBOL field
deg_table_f36p <- data.frame(tbl_res_f36p.vp16.VS.ctr[complete.cases(tbl_res_f36p.vp16.VS.ctr[,2:3]),])
deg_table_hl60 <- data.frame(tbl_res_hl60.vp16.VS.ctr[complete.cases(tbl_res_hl60.vp16.VS.ctr[,2:3]),])
deg_table_kasumi1 <-
data.frame(tbl_res_kasumi1.vp16.VS.ctr[complete.cases(tbl_res_kasumi1.vp16.VS.ctr[,2:3]),])
deg_table_molm13 <-
data.frame(tbl_res_molm13.vp16.VS.ctr[complete.cases(tbl_res_molm13.vp16.VS.ctr[,2:3]),])
deg_table_monomac6 <-
data.frame(tbl_res_monomac6.vp16.VS.ctr[complete.cases(tbl_res_monomac6.vp16.VS.ctr[,2:3]),])
deg_table_mv411 <- data.frame(tbl_res_mv411.vp16.VS.ctr[complete.cases(tbl_res_mv411.vp16.VS.ctr[,2:3]),])
deg_table_nb4 <- data.frame(tbl_res_nb4.vp16.VS.ctr[complete.cases(tbl_res_nb4.vp16.VS.ctr[,2:3]),])
deg_table_nomo1 <- data.frame(tbl_res_nomo1.vp16.VS.ctr[complete.cases(tbl_res_nomo1.vp16.VS.ctr[,2:3]),])
deg_table_ociaml3 <- data.frame(tbl_res_ociaml3.vp16.VS.ctr[complete.cases(tbl_res_ociaml3.vp16.VS.ctr[,2:3]),])
deg_table_thp1 <- data.frame(tbl_res_thp1.vp16.VS.ctr[complete.cases(tbl_res_thp1.vp16.VS.ctr[,2:3]),])

# DEG statistics
deg_stat <- data.frame("Total_DEG" = c(length(deg_table_f36p$SYMBOL), length(deg_table_hl60$SYMBOL),
length(deg_table_kasumi1$SYMBOL), length(deg_table_molm13$SYMBOL),
length(deg_table_monomac6$SYMBOL), length(deg_table_mv411$SYMBOL), length(deg_table_nb4$SYMBOL),
length(deg_table_nomo1$SYMBOL), length(deg_table_ociaml3$SYMBOL), length(deg_table_thp1$SYMBOL)),
"UP" = c(length(which(deg_table_f36p$logFC >= 1)), length(which(deg_table_hl60$logFC >= 1)),
length(which(deg_table_kasumi1$logFC >= 1)), length(which(deg_table_molm13$logFC >= 1)),
length(which(deg_table_monomac6$logFC >= 1)), length(which(deg_table_mv411$logFC >= 1)),
length(which(deg_table_nb4$logFC >= 1)), length(which(deg_table_nomo1$logFC >= 1)),
length(which(deg_table_ociaml3$logFC >= 1)), length(which(deg_table_thp1$logFC >= 1))), "DOWN" =
c(length(which(deg_table_f36p$logFC <= 1)), length(which(deg_table_hl60$logFC <= 1)),
length(which(deg_table_kasumi1$logFC <= 1)), length(which(deg_table_molm13$logFC <= 1)),
length(which(deg_table_monomac6$logFC <= 1)), length(which(deg_table_mv411$logFC <= 1)),
length(which(deg_table_nb4$logFC <= 1)), length(which(deg_table_nomo1$logFC <= 1)),
length(which(deg_table_ociaml3$logFC <= 1)), length(which(deg_table_thp1$logFC <= 1))))
deg_stat$"%_Up" <- round(((deg_stat$UP / deg_stat$Total_DEG) * 100), digits = 2)
deg_stat$"%_Down" <- round(((deg_stat$DOWN / deg_stat$Total_DEG) * 100), digits = 2)
rownames(deg_stat) <- c("F36-P", "HL-60", "KASUMI-1", "MOLM-13", "MONO-MAC-6", "MV-4-11", "NB-4",
"NOMO-1", "OCI-AML3", "THP-1")
deg_stat$"VP16-IC50 (µM)" <- c(98.81, 0.74, 6.80, 0.39, 4.39, 1.33, 0.50, 1.65, 1.00, 1.01)
deg_stat %>% datatable(caption = "DEG statistics (VP16 VS Control)", escape = F)


deg_table_UP_f36p <- data.frame(deg_table_f36p[which(deg_table_f36p$logFC >= 1),])
deg_table_DOWN_f36p <- data.frame(deg_table_f36p[which(deg_table_f36p$logFC <= 1),])
deg_table_UP_hl60 <- data.frame(deg_table_hl60[which(deg_table_hl60$logFC >= 1),])
deg_table_DOWN_hl60 <- data.frame(deg_table_hl60[which(deg_table_hl60$logFC <= 1),])
deg_table_UP_kasumi1 <- data.frame(deg_table_kasumi1[which(deg_table_kasumi1$logFC >= 1),])
```

```
deg_table_DOWN_kasumi1 <- data.frame(deg_table_kasumi1[which(deg_table_kasumi1$logFC <= 1),])
deg_table_UP_molm13 <- data.frame(deg_table_molm13[which(deg_table_molm13$logFC >= 1),])
deg_table_DOWN_molm13 <- data.frame(deg_table_molm13[which(deg_table_molm13$logFC <= 1),])
deg_table_UP_monomac6 <- data.frame(deg_table_monomac6[which(deg_table_monomac6$logFC >= 1),])
deg_table_DOWN_monomac6 <- data.frame(deg_table_monomac6[which(deg_table_monomac6$logFC <= 1),])
deg_table_UP_mv411 <- data.frame(deg_table_mv411[which(deg_table_mv411$logFC >= 1),])
deg_table_DOWN_mv411 <- data.frame(deg_table_mv411[which(deg_table_mv411$logFC <= 1),])
deg_table_UP_nb4 <- data.frame(deg_table_nb4[which(deg_table_nb4$logFC >= 1),])
deg_table_DOWN_nb4 <- data.frame(deg_table_nb4[which(deg_table_nb4$logFC <= 1),])
deg_table_UP_nomo1 <- data.frame(deg_table_nomo1[which(deg_table_nomo1$logFC >= 1),])
deg_table_DOWN_nomo1 <- data.frame(deg_table_nomo1[which(deg_table_nomo1$logFC <= 1),])
deg_table_UP_ociaml3 <- data.frame(deg_table_ociaml3[which(deg_table_ociaml3$logFC >= 1),])
deg_table_DOWN_ociaml3 <- data.frame(deg_table_ociaml3[which(deg_table_ociaml3$logFC <= 1),])
deg_table_UP_thp1 <- data.frame(deg_table_thp1[which(deg_table_thp1$logFC >= 1),])
deg_table_DOWN_thp1 <- data.frame(deg_table_thp1[which(deg_table_thp1$logFC <= 1),])


max.len.up = max(length(deg_table_UP_f36p$SYMBOL), length(deg_table_UP_hl60$SYMBOL),
length(deg_table_UP_kasumi1$SYMBOL), length(deg_table_UP_molm13$SYMBOL),
length(deg_table_UP_monomac6$SYMBOL), length(deg_table_UP_mv411$SYMBOL),
length(deg_table_UP_nb4$SYMBOL), length(deg_table_UP_nomo1$SYMBOL),
length(deg_table_UP_ociaml3$SYMBOL), length(deg_table_UP_thp1$SYMBOL))
f36p_UP_genes <- c(deg_table_UP_f36p$SYMBOL, rep(NA, max.len.up -
length(deg_table_UP_f36p$SYMBOL)))
hl60_UP_genes <- c(deg_table_UP_hl60$SYMBOL, rep(NA, max.len.up -
length(deg_table_UP_hl60$SYMBOL)))
kasumi1_UP_genes <- c(deg_table_UP_kasumi1$SYMBOL, rep(NA, max.len.up -
length(deg_table_UP_kasumi1$SYMBOL)))
molm13_UP_genes <- c(deg_table_UP_molm13$SYMBOL, rep(NA, max.len.up -
length(deg_table_UP_molm13$SYMBOL)))
monomac6_UP_genes <- c(deg_table_UP_monomac6$SYMBOL, rep(NA, max.len.up -
length(deg_table_UP_monomac6$SYMBOL)))
mv411_UP_genes <- c(deg_table_UP_mv411$SYMBOL, rep(NA, max.len.up -
length(deg_table_UP_mv411$SYMBOL)))
nb4_UP_genes <- c(deg_table_UP_nb4$SYMBOL, rep(NA, max.len.up - length(deg_table_UP_nb4$SYMBOL)))
nomo1_UP_genes <- c(deg_table_UP_nomo1$SYMBOL, rep(NA, max.len.up -
length(deg_table_UP_nomo1$SYMBOL)))
ociaml3_UP_genes <- c(deg_table_UP_ociaml3$SYMBOL, rep(NA, max.len.up -
length(deg_table_UP_ociaml3$SYMBOL)))
thp1_UP_genes <- c(deg_table_UP_thp1$SYMBOL, rep(NA, max.len.up -
length(deg_table_UP_thp1$SYMBOL)))

max.len.down = max(length(deg_table_DOWN_f36p$SYMBOL), length(deg_table_DOWN_hl60$SYMBOL),
length(deg_table_DOWN_kasumi1$SYMBOL), length(deg_table_DOWN_molm13$SYMBOL),
length(deg_table_DOWN_monomac6$SYMBOL), length(deg_table_DOWN_mv411$SYMBOL),
length(deg_table_DOWN_nb4$SYMBOL), length(deg_table_DOWN_nomo1$SYMBOL),
length(deg_table_DOWN_ociaml3$SYMBOL), length(deg_table_DOWN_thp1$SYMBOL))
f36p_DOWN_genes <- c(deg_table_DOWN_f36p$SYMBOL, rep(NA, max.len.down -
length(deg_table_DOWN_f36p$SYMBOL)))
hl60_DOWN_genes <- c(deg_table_DOWN_hl60$SYMBOL, rep(NA, max.len.down -
length(deg_table_DOWN_hl60$SYMBOL)))
kasumi1_DOWN_genes <- c(deg_table_DOWN_kasumi1$SYMBOL, rep(NA, max.len.down -
length(deg_table_DOWN_kasumi1$SYMBOL)))
molm13_DOWN_genes <- c(deg_table_DOWN_molm13$SYMBOL, rep(NA, max.len.down -
length(deg_table_DOWN_molm13$SYMBOL)))
```

```
monomac6_DOWN_genes <- c(deg_table_DOWN_monomac6$SYMBOL, rep(NA, max.len.down -
length(deg_table_DOWN_monomac6$SYMBOL)))
mv411_DOWN_genes <- c(deg_table_DOWN_mv411$SYMBOL, rep(NA, max.len.down -
length(deg_table_DOWN_mv411$SYMBOL)))
nb4_DOWN_genes <- c(deg_table_DOWN_nb4$SYMBOL, rep(NA, max.len.down -
length(deg_table_DOWN_nb4$SYMBOL)))
nomo1_DOWN_genes <- c(deg_table_DOWN_nomo1$SYMBOL, rep(NA, max.len.down -
length(deg_table_DOWN_nomo1$SYMBOL)))
ociaml3_DOWN_genes <- c(deg_table_DOWN_ociaml3$SYMBOL, rep(NA, max.len.down -
length(deg_table_DOWN_ociaml3$SYMBOL)))
thp1_DOWN_genes <- c(deg_table_DOWN_thp1$SYMBOL, rep(NA, max.len.down -
length(deg_table_DOWN_thp1$SYMBOL)))

deg_table_UP_ALL <- data.frame(F36P = f36p_UP_genes, HL60 = hl60_UP_genes, KASUMI1 =
kasumi1_UP_genes, MOLM13 = molm13_UP_genes, MONOMAC6 = monomac6_UP_genes, MV411 =
mv411_UP_genes, NB4 = nb4_UP_genes, NOMO1 = nomo1_UP_genes, OCIAML3 = ociaml3_UP_genes, THP1 =
thp1_UP_genes)
deg_table_DOWN_ALL <- data.frame(F36P = f36p_DOWN_genes, HL60 = hl60_DOWN_genes, KASUMI1 =
kasumi1_DOWN_genes, MOLM13 = molm13_DOWN_genes, MONOMAC6 = monomac6_DOWN_genes,
MV411 = mv411_DOWN_genes, NB4 = nb4_DOWN_genes, NOMO1 = nomo1_DOWN_genes, OCIAML3 =
ociaml3_DOWN_genes, THP1 = thp1_DOWN_genes)

tab_UP <- table(unlist(deg_table_UP_ALL))
tab_DOWN <- table(unlist(deg_table_DOWN_ALL))

write.table(as.data.frame(tab_UP), "./edgeR_Results/AML_UP_DEG_ALL.txt", sep = "\t", row.names = F)
write.table(as.data.frame(tab_DOWN), "./edgeR_Results/AML_DOWN_DEG_ALL.txt", sep = "\t", row.names = F)

View(as.data.frame(tab[tab > 1]))

sessionInfo()

# Save R session
save.image("./edgeR_Results/AML_RNA-Seq_2017_edgeR.RData")
```

Scientific publication

More P., Goedtel-Armbrust U, Shah V., Mathaes M., Kindler T., Andrade-Navarro M. A., and Wojnowski L. “Drivers of topoisomerase II poisoning mimic and complement cytotoxicity in AML cells.” (submitted)

Congress contributions

More P., Gödtel-Armbrust U., Wojnowski L. “Specific effectors of topoisomerase II poisons contribute to cytotoxicity in AML cell lines.” The FEBS Congress 2018, 9th July 2018, Prague, Czech Republic. (Poster presentation – outstanding poster in molecular oncology award)

More P., Gödtel-Armbrust U., Shah V., Kindler T., Andrade M., and Wojnowski L. “Smart transcriptional effectors of etoposide contribute to cytotoxicity in AML cell lines.” UCT Science Day, 6th September 2018, University Medical Center, Mainz, Germany. (Poster presentation)

More P. “Transcriptional effectors of etoposide contribute to cytotoxicity in AML”. TransMed Christmas Colloquium, 12th December 2018, University Medical Center, Mainz, Germany. (Oral presentation)

More P., Gödtel-Armbrust U., Shah V., Mathaes M, Kindler T., Andrade M., and Wojnowski L. “Transcriptional effectors of etoposide contribute to cytotoxicity in AML cell lines”. 4th German Pharm-Tox Summit: DGPT 2019, 26th February 2019, Stuttgart, Germany. (Oral presentation)